UNIVERSITÁ DEGLI STUDI DELL'INSUBRIA
Dipartimento Di Medicina e Chirurgia

Dottorato di Ricerca in Medicina Sperimentale e Traslazionale
XXXII ciclo

Hyaluronan: a new player in the modulation of adaptive changes to neuromuscular damage in the gastrointestinal tract

Tutor: Dott.ssa Cristina Giaroni

Tesi di Dottorato di:
MICHELA BISTOLETTI
Matricola n. 713348

Anno Accademico: 2018/2019

A Luisa

SUMMARY

Neuronal circuitries within the enteric nervous system (ENS) display a considerable ability to adapt to a changing microenvironment, which comprises several cellular “players” such as neurons, enteric glia, smooth muscle cells, immune cells and the intestinal microbiota (Giaroni et al., 1999). The phenomenon of plasticity plays a fundamental role in the maintenance of gut homeostasis, in physiological conditions. However, remodelling of enteric neuronal circuitries may also occur in pathological conditions, such as during chronic inflammatory states of the gut or during ischemia/reperfusion (I/R) injury. Indeed, inflammatory bowel diseases (IBD) are associated with derangements of the ENS, characterized by increased neuronal excitability (hyperexcitability of primary afferent neurons), synaptic facilitation and reduced inhibitory neuromuscular neurotransmission. Such changes may lead to persistent dysmotility as well as altered visceral pain perception, which represent two of the main IBD symptoms (Vasina et al., 2006). Chronic inflammatory bowel diseases often include episode of ischemia, since the gut is one of most sensitive tissues to ischemic damage in the body (Haglund and Bergqvist, 1999). Intestinal ischemia/reperfusion injury, which is associated with a high morbidity and mortality, may also occur in both surgical and trauma patients (Reinus et al., 1990), as a result of embolism, arterial or venous thrombosis, shock, intestinal transplantation, or necrotising enterocolitis in the human premature newborn (Haglund and Bergqvist 1999; Massberg and Messmer, 1998; Nowicki 2005; Thornton and Solomon, 2002). The I/R insult can seriously affect the structure and function of myenteric neurons (Filpa et al., 2017) resulting in a particularly severe slowing of transit, suggestive of a long-lasting neuropathy (Rivera et al., 2011).

The structural and functional changes occurring in enteric circuitries may be, at least in part, due to the interplay among different cell populations in the enteric microenvironment. In this context, extracellular matrix (ECM) molecules provide an important framework for the enteric microenvironment and may influence the integrity of myenteric neuronal circuitries during both physiological and pathological conditions.

ECM molecules constitute a highly organized environment filling the extracellular space consisting of different types of macromolecules, such as collagens, elastin, fibronectin (FN), laminins, glycoproteins, proteoglycans (PGs) and glycosaminoglycans (GAGs) (Theocharis et al., 2016). Hyaluronan (HA), an unbranched GAG located immediately beneath the epithelial barrier of the gut, is deeply involved in the preservation of homeostasis. HA has also important functions in multiple host-defence mechanisms, promoting leukocyte recruitment in the intestinal

extravascular space during disease states (de la Motte and Kessler, 2015), and acting to decrease inflammation and promote epithelial repair (Zheng et al., 2009). Several reports suggest that HA deposition is dramatically altered during gut inflammation. In experimental animal models of colitis and in the intestine of patients with IBD, accumulation of HA has been observed in the epithelial, submucosal and smooth muscle intestinal layers, and in blood vessels within the submucosal layer (Kessler et al., 2008). In these conditions, degradation of HA into small fragments may promote immune cell activation as well as production of pro-inflammatory cytokines, thus favouring an increased inflammatory response.

Since the majority of studies have focused on the pathophysiological consequences of HA deposition in the submucosal and *muscularis mucosae* layers (de la Motte et al., 2011; Kessler et al., 2008), the aim of this work was to evaluate possible changes of HA homeostasis in the smooth muscle layer (*muscularis propria*), underlying derangement of the gut neuromuscular function during pathological conditions, such as IBD and I/R damage. Functional, morphological and biomolecular investigations were carried out in rat models of pathologies represented, respectively, by 2,4-dinitro-benzene-sulfonic acid (DNBS)-induced colitis and *in vivo* I/R injury, by temporary clamping the superior mesenteric artery. The results obtained, showed that HA contributes to the external architecture of enteric ganglia participating to the formation of a basal lamina surrounding myenteric ganglia. In addition, we were the first to demonstrate that the GAG may form a pericellular coat of condensed matrix surrounding myenteric neurons, similar to the well-organised ECM structures in the central system (CNS), called perineuronal nets (PNNs), which regulate ion homeostasis around active neurons, stabilize synapses and participate to neuronal plasticity (Oohashi et al., 2015; van 't Spijker and Kwok, 2017). Furthermore, the expression of some isoforms of HA synthases, such as HAS1 and HAS2, detected in myenteric neurons, support the hypothesis that myenteric neurons may be a source for HA. After DNBS-induced colitis, HA levels significantly increased in the *muscularis propria* layer and in the myenteric plexus. In particular, the GAG distribution within myenteric ganglia was highly altered, displaying a complete loss of the perineuronal organization. These alterations were associated with an up-regulation of HAS2 in myenteric neurons.

HA levels significantly increased also in rat myenteric ganglia after the *in vivo* I/R. Such enhancement was associated with increased expression of both HAS1 and HAS2 in the myenteric neurons. Interestingly, treatment with an inhibitor of HA synthesis, 4-methylumbelliferone (4-MU), significantly reduced HA levels in myenteric plexus of I/R rats, which was associated with a significant reduction of HAS2 expression. 4-MU-administration in the I/R group was associated with alterations of the myenteric plexus neurochemical coding. From a functional view point, changes in

both excitatory and inhibitory neurotransmission were evidenced, possibly hampering the efficiency of the gastrointestinal transit. Overall, these observations suggest that the I/R-induced neo-synthesis of HA may sustain gastrointestinal motor responses in this pathophysiological condition modulating some neuronal components within myenteric plexus circuitries.

In conclusion, this study provides evidence that HA deposition within myenteric ganglia may have a homeostatic role, contributing to the control of myenteric neuron structure and function. In pathological conditions, such as during I/R, HA sustains the efficiency of the gastrointestinal transit, influencing both the excitatory and inhibitory components of the peristaltic reflex. Hence, modulation of HA deposition within the myenteric ganglia may ameliorate intestinal motility patterns related to these disease states.

INDEX

1 INTRODUCTION

1.1 The Enteric Nervous System

The control of the main digestive functions in gastrointestinal (GI) tract largely depends upon the presence of a complex intrinsic neuronal network, termed enteric nervous system (ENS), that extends from esophagus to the anal sphincter. The ENS has an important role in determining motility patterns, gastric secretion, blood flow, nutrient handling, and the interactions with immune and endocrine systems of the gut, acting in a relative independent mode with respect to the central nervous system (CNS) (Furness et al., 2014). For this reason, it is often referred to as the "second brain" or the "minibrain" (Gershon, 1999; Wood, 2012). However, the ENS is not entirely autonomous, but it works as an integrated system in which afferent signals arising from the lumen are transmitted through enteric, spinal and vagal pathways to CNS, and efferent signals from CNS are driven back to the intestinal wall. This bidirectional communication guarantees the CNS monitoring of a number of gut parameters, from chemical sensing in the lumen, to sensing mechanical stress along the gut wall (Furness, 2000).

The human ENS contains 200-600 million neurons, a number similar to that found in spinal cord, grouped into ganglia which are connected by bundles of nerve processes to form two major plexuses innervating the effector tissues: the myenteric (or Auerbach's) plexus and the submucosal (or Meissner's) plexus (Furness et al., 2012) (Figure 1).

The myenteric plexus lies between the longitudinal and circular muscle layers, extending in the entire length of the gut as a continuous network. It primarily provides motor innervation to the smooth muscle layers and secretomotor innervation to the mucosa. Numerous myenteric neuron projections extend into submucosal ganglia and enteric ganglia of the gallbladder and pancreas (Kirchgessner & Gershon, 1990), and another substantial number into sympathetic ganglia (Goyal & Hirano, 1996). The submucosal plexus is located in the submucosa, between the outer circular muscle layer and the serosal side of the *muscularis mucosae*, where it plays an important part in the control of the secretory function. Large mammals can have two layers of submucosal ganglia, and sometimes a third intermediate layer between them. Submucosal ganglia and connecting fibre bundles form the submucosal plexus, which can be found in the small and large intestine, and rarely in the stomach and esophagus (Furness et al. 2014; Furness, 2012).

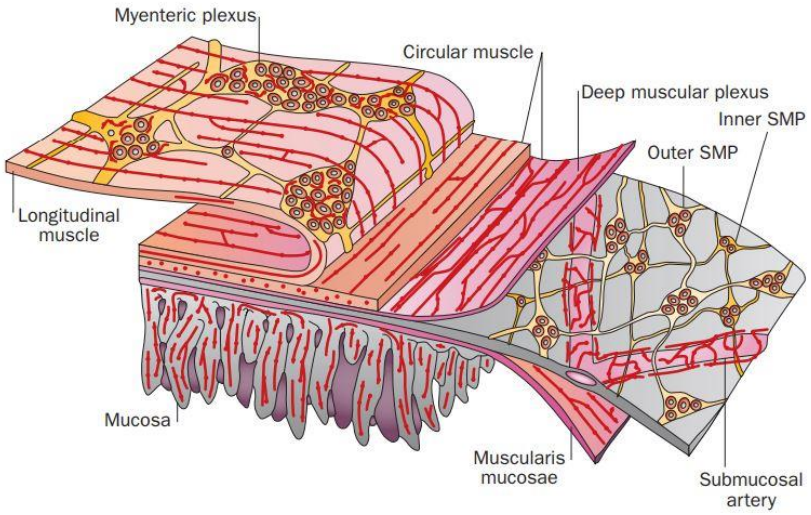

Figure 1. Organisation of the ENS in human small and large intestine. Neurons are confined in ganglia of the myenteric plexus, localized between the longitudinal and circular muscle layers, and in ganglia distributed between the circular muscle and the muscularis mucosa within the submucosa, depicted in the transverse section of the gut wall. The ganglia and fibers in the submucosa form the inner and outer submucosal plexus (SMP). From Furness JB., 2012.

According to the morphology, neurochemical properties, cell physiology, projections to targets and functional roles, approximately 20 distinct types of neurons have been described (Costa et al., 2000), all of which can be mainly grouped into the three major classes of enteric neurons: intrinsic primary afferents neurons (IPANs), interneurons and motor neurons. The myenteric plexus shows a high density of neurons compared to the submucosal plexus with an average ratio of the primary afferents, interneurons and motor neurons of 2:1:1, respectively (Costa et al., 2000; Hansen, 2003). IPANs are sensory neurons, representing the 10-30% of total neurons in the submucosal and myenteric intestinal ganglia, that are able to detect chemical luminal stimuli, mechanical distortion of the mucosa and mechanical forces in the external musculature (e.g. tension of the gut wall) (Furness et al, 2014). IPANs react to these signals to initiate appropriate reflex activity controlling motility, secretion and blood flow (Clerc et al., 2002). IPANs connect with each other, with interneurons and directly with motor neurons (Figure 2). Uni-axonal excitatory and inhibitory motor neurons, which receive prominent fast excitatory synaptic potentials, innervate the longitudinal, circular smooth muscle layers and the *muscularis mucosae* along the entire GI tract (Wood, 2012). The primary neurotransmitters for excitatory motor neurons are acetylcholine (ACh) and tachykinins. Several neurotransmitters have been identified in inhibitory motor neurons, including nitric oxide (NO), vasoactive intestinal peptide (VIP) and ATP-like transmitters, although NO is considered the primary transmitter (Furness et al., 2014). Another important class of enteric neurons is represented by secretomotor and secretomotor/vasodilator neurons regulating electrolyte and water transport across the intestinal mucosa (Vanner and Macnaughton, 2004).

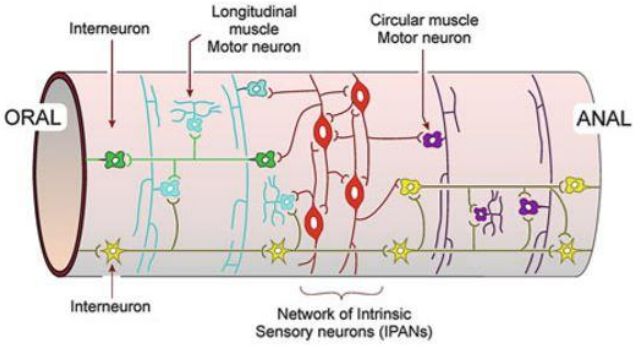

Figure 2. Nerve circuits controlling motility in the small intestine. This simplified circuit diagram shows the major circuitries involved in intrinsic motor reflexes of the small intestine. Intrinsic primary sensory neurons (IPANs, red) detect mechanical distortion and luminal chemistry and connect with excitatory muscle motor neurons (blue) and inhibitory muscle motor neurons (purple) directly and via descending (yellow) and ascending (green) interneurons**.** From Furness et al., 2014.

The next paragraphs will focus on some of these neurotransmitter pathways, which undergo adaptive rearrangements in the different studies carried out in the present thesis.

1.1.1 Cholinergic neurotransmission

Acetylcholine (ACh) is the major excitatory transmission in the ENS, being involved in the regulation of motor, secretory and vascular reflexes, by inducing excitatory potentials in post-synaptic effectors.

ACh is present in the greater population of the enteric neurons and synthesized in nerve terminals from choline and acetyl-CoA by choline acetyltransferase (ChAT). As a classic neurotransmitter, ACh is then translocated into synaptic vesicles by the vesicular acetylcholine transporter (VAChT; Eiden, 1998) and stored in synaptic vesicles until it is released on demand (Wessler et al., 2003).

There are two types of receptors mediating cholinergic transmission within the ENS: the nicotinic (nAChRs) receptors, which are ligand-ion channels, and the muscarinic (mAChRs) G-protein coupled receptors (Caulfield & Birdsall, 1998). Thus, ACh binding generates variable postsynaptic potentials depending on the receptor present on the cell membrane, with nAChRs mediating rapid excitatory transmission and mAChRs mediating slow excitatory transmission (Harrington et al., 2010). At the cholinergic synapse both classes of receptors are present either on effector cells (post- synaptic receptors) or on nerve terminals (pre-synaptic receptors), where they act as autoreceptors regulating release of ACh. nAChR activation is the predominant mechanism for cholinergic neurotransmission in enteric ascending reflex pathways, whilst it retains a minor role in mediating cholinergic transmission within the descending inhibitory reflex (Galligan, 2002). Within the ENS, activation of nAChRs entails rapid reflex propagation, producing fast responses to stimuli. Conversely, activation of mAChRs either induces cell membrane depolarization, resulting in the

initiation of action potential, or cell membrane hyperpolarization, inhibiting additional action potentials by activating second messenger cascades and intracellular signalling pathways (Caulfield & Birdsall, 1998). Owing to different distribution, molecular structure and intracellular signalling of mAChRs and nAChRs, these receptors may differentially influence various intestinal functions, both in physiological and pathologic conditions of the gut. Indeed, several GI disorders are associated with changes in the enteric cholinergic system. Congenital gastrointestinal aganglionosis, such as Hirschsprung's disease, show a completely lack of mAChR3-immunoreactive fibres in smooth-muscle layers and decreased mAChR3 and mAChR2 mRNA levels in the aganglionic segments of the colon, which may be responsible for the typical motility dysfunctions of this pathology (Oue et al., 2000). In addition, abnormal levels of mAChRs expression were correlated with organic GI pathologies, including IBD (Jadcherla, 2002; Oue et al., 2000).

1.1.2 Tachykinergic neurotransmission

Tachykinins are a family of small biologically active peptides that act as a co-neurotransmitter of excitatory enteric neurons. Indeed, tachykinins represent with ACh, the main transmitters of excitatory neurons innervating the muscle, regulating intestinal motility, secretion, and vascular functions. The principal mammalian members of this family are substance P (SP), the first to be discovered in extracts of horse brain and intestine, neurokinin A (NKA) and neurokinin B (NKB) (Holzer and Holzer-Petsche, 1997). These neuropeptides are produced from the cleavage of large precursor proteins in the cell body of the neurons, where they are transported to the varicosities and released after stimulation. Tachykinins bind with high affinity to specific membrane G-protein coupled receptors, namely NK1R, NK2R and NK3R (Holzer and Holzer-Petsche, 1997). Consistent data show that NK1 and NK2 receptors are present on enteric neurons, NK1Rs being expressed also on interstitial Cajal cells (ICC), while NK2 are also highly expressed on smooth muscle cells. Although NK1Rs are considered SP-preferring, NK2Rs NKA-preferring and NK3Rs NKB-preferring receptors, all of these receptors can be fully activated by all tachykinins with moderate selectivity. NK1 and NK2 receptors mediate the transmission from excitatory motor neurons to muscle, whereas NK1 and NK3 participate in slow excitatory transmission at neuro-neuronal synapses in both ascending and descending pathways affecting motility. Moreover, the activation of NK1 and NK2 receptors on mucosal epithelium is involved in fluid secretion (Lecci et al., 2002).

However, tachykinins are not only important for neurotransmission, but they also have effects on tissue growth and differentiation, immunomodulation, tumour growth, and inflammation. In this latter regard, SP, via binding to the NK1Rs, were shown to participate to development of intestinal inflammation by several groups. In the ENS, SP represents a classical sensory neurotransmitter

involved in visceral pain perception associated with inflammation (Foreman, 1987). Several studies have reported altered expression of SP in the ENS of patients with inflammatory and functional GI disorders, such as constipation, diverticulitis, inflammatory bowel disease (IBD) and irritable bowel syndrome (IBS) (Lecci et al., 2006).

1.1.3 Nitrergic neurotransmission

Nitric oxide (NO) is a gaseous messenger molecule, which has numerous molecular targets. It controls regulatory functions such as neurotransmission and vascular tone (Rapoport et al., 1983), gene transcription (Gudi et al., 1999) and mRNA translation (e.g. by binding iron-responsive elements) (Liu et al., 2002) and produces post-translational modifications of proteins (e.g. by ADP-ribosylation) (Brune et al., 1994). The nerves whose transmitter function depend on NO release are called "nitrergic", and such nerves are recognized to play major roles in the control of smooth muscle tone, motility and fluid secretion in the GI tract. In mammals NO can be produced by three different isoforms of the NO synthase enzyme: neuronal NOS (nNOS), inducible NOS (iNOS) and endothelial NOS (eNOS) isoforms. All NOS isoforms utilize as substrate L-arginine and molecular oxygen, and reduced nicotinamide-adenine-dinucleotide phosphate (NADPH) as co-substrates. Flavin adenine dinucleotide (FAD), flavin mononucleotide (FMN) and (6R-)5,6,7,8-tetrahydro-L-biopterin (BH4) are cofactors of all isoenzymes. All NOS proteins are homodimers. NO synthesis is accomplished via two steps. In the first step, NOS hydroxylates L-arginine to Nω-hydroxy-L-arginine, successively NOS oxidizes Nω-hydroxy-L-arginine to L-citrulline and NO (Stuehr et al., 2001). All NOS isoforms bind to the intracellular Ca^{2+}-binding protein, calmodulin. nNOS and eNOS binding to calmodulin is brought about by elevated intracellular Ca^{2+} concentrations (half-maximal activity between 200 and 400 nM), while iNOS binds to calmodulin at extremely low intracellular Ca^{2+} concentrations (below 40nM). (Forstermann and Sessa, 2012).

In the ENS, NO plays a pivotal physiological role in the inhibitory regulation of peristalsis (Furness, 2000). All NOS isoforms have been localized in myenteric neurons of different species (Vannucchi et al., 2002; Talapka et al., 2011). In myenteric neurons, nNOS seems to represent the main source of NO involved in the physiological modulation of non-adrenergic non-cholinergic inhibitory motor responses of the gut (Toda et al., 2005). However, expression of iNOS, but not of nNOS and eNOS, prevails during diseases states, such as intestinal inflammation (Miampamba et al., 1999) and I/R injury (Giaroni et al., 2013). In these conditions, large amounts of NO can cause damages in different cellular populations, such as neurons, by the formation of peroxynitrite and nitrotyrosine (Rivera et al., 2011). This phenomenon reflects a functional plasticity of myenteric neurons that activate

different NOS isoforms depending on either physiological or pathological conditions (Robinson et al., 2011, Giaroni et al., 2013).

1.2 Plasticity in the enteric nervous system: the enteric microenvironment

Plasticity is the ability of the nervous system to rewire its connections, or to adapt its functions in response to alterations of different inputs. In the CNS, the ability of the brain to adapt to changing physiological conditions or traumatic lesions is crucial, due to a lack of a sufficient regeneration potential. The ENS also shows several features that make it a suitable and unique model of plasticity. Enteric ganglia share morphological (e.g., presence of enteric glial cells, resembling CNS astrocytes (Jessen et al., 1985), and absence of collagen fibres) and functional (e.g., growth factors, neurotransmitters) similarities with the CNS, and their complex organization is unmatched in any other section of the peripheral nervous system (Gershon et al., 1994). Second, enteric ganglia maintain integrated functions in the absence of input from the CNS, which has a modulatory role. The ENS undergoes significant changes in physiological conditions during the life span, i.e during development and ageing. Plasticity in the ENS is also evident for clinical (e.g., recovery of motor function after intestinal transplantation) and experimental (e.g., denervation and pharmacological manipulations) observations, which suggest that ENS can react upon microenvironmental changes, maintaining a homeostatic control of the gut functions. Enteric neuronal plasticity may also lead to regeneration of neuronal circuitries and allow the recovery of normal intestinal functions after surgical procedures.

Several ‘‘players’’ are involved when considering adaptive changes in the enteric microenvironment: neurons, enteric glial cells, interstitial cells of Cajal (which are viewed as the intestinal pacemaker cells) (Sanders, 1996) and the gut microbiota. Neuroimmune interactions also play an important role in the ENS homeostasis and plasticity (Bueno et al, 1997, De Winter, 2012). A possible cross-talk between smooth muscle cells and dorsal root ganglion cells has also been demonstrated (Ennes et al, 1997), and this finding may affect the understanding of altered visceral sensitivity and reinforce the concept of a brain–gut axis interaction. In addition, it has already been demonstrated that the gut microbiota play a crucial role in the development of innate and adaptive immunity, and in regulation of gut motility, intestinal barrier homeostasis, nutrient absorption and fat distribution (Bercick et al., 2012; Backhed et al., 2004). In the following paragraphs, some of the major non-neuronal cellular components of the enteric microenvironment will be described.

1.2.1 Enteric glia

Enteric glia cells (EGCs) are an important non-neuronal component of the ENS, similar to CNS astrocytes, which form a cellular and molecular bridge between enteric nerves, enteroendocrine cells, immune cells, and epithelial cells, depending on their location.

During last decades, several studies have clearly shown that this cell population does not play a merely supportive function, serving only as a scaffold for neurons, but EGCs are also actively involved in most gut functions such as mucosal integrity, neuroprotection, adult neurogenesis, neuroimmune interactions, and synaptic transmission (Table 1) (Sharkey, 2015; Gulbransen and Sharkey, 2012).

Table 1. Functional role of enteric glia in the GI tract. Adapted from Sharkey, 2015.

Function	Location of enteric glia	Mediator(s) released/expressed by enteric glia
Epithelial barrier function	Mucosa	S-nitrosoglutathione 15-Deoxy-$\Delta^{12,14}$-prostaglandin J2 TGF-β1 pro-epidermal growth factor
Fluid secretion	Myenteric plexus	NO
Intestinal motility	Myenteric plexus	ATP
Support of enteric neurons and neuronal survival	ENS	L-arginine Glutamine Reduced glutathione Nerve growth factor 15-Deoxy-$\Delta^{12,14}$-prostaglandin J2
Enteric neurotransmission	ENS	ATP
Neurogenesis	ENS	
Immune signalling	ENS	MHC class II, CD80, CD86 IL-1β IL-6 MCP1 Prostaglandin E2 S-100B TLR4

In view of this role in maintaining GI homeostasis, a possible EGC role in the pathophysiology of neurodegenerative or inflammatory disorders has been widely reported (Grubišić et al., 2018; Coelho-Aguiar et al., 2015). Genetic ablation of EGCs results in a fatal haemorrhagic jejuno-ileitis, with enteric plexus disruption and the loss of epithelial layer integrity (Bush et al., 1998), while EGCs destruction by autoimmune mechanism leads to enterocolitis (Cornet et al., 2001). A reduction of the glial network were found in patients with Crohn's disease (CD) and similarly, there is a preferential loss of enteric glia in patients with slow-transit constipation (von Boyen et al., 2011; Cornet et al., 2001). Moreover, loss of neurons and glial cells in myenteric and submucosal plexus is characteristic of necrotizing enterocolitis (NEC), a disease occurring in premature infants (Sigge et al., 1998; Wedel et al., 1998).

1.2.2 Enteric smooth muscle cells

The enteric myocyte can also display phenotype plasticity similar to that of vascular and bronchial smooth muscle cells, whose plasticity has important pathophysiological implications for atherogenesis and airway remodelling, respectively (Johnson et al., 1997). Production of cytokines and/or growth factors by myocytes may alter neuromuscular function and be at the basis of neuromotor dysfunction in patients with IBD (Van Assche et al., 1996). Preclinical studies carried out on rodent gut have shown that enteric myocytes have sensors for inflammatory signals in the gut (Cocks et al., 1999; Giaroni et al., 1999).

1.2.3 Intestinal microbiota

In the human body, the GI tract represents one of the largest interfaces (250–400 m^2) between the host, environmental factors and antigens. The community of commensal microorganisms colonizing in or passing through the GI tract is referred to as the intestinal microbiota (Dethlefsen et al., 2006). The human intestinal tract hosts 3.8 X 10^{13} bacterial cells (Sender et al., 2016), a number ten times greater than human body cells, that belong to 2000 different species and contain nearly 2 million genes (the so-called microbiome) (Qin et al., 2010; Wopereis et al., 2014).

Among the different bacterial phyla detected in the human gut, *Firmicutes* and *Bacteroidetes* are the most representative, whereas other phyla such as *Actinobacteria*, *Proteobacteria*, *Fusobacteria*, and *Verrucomicrobia* are present in smaller quantities (Simrén et al., 2013).

The composition, diversity and abundance of the human gut microbiota vary along the GI tract. The microbial density, increases from 10^1–10^8 microbial cells in the stomach, and small intestine, to 10^{10}–10^{12} cells in the colon and faeces (Booijink et al., 2007; Dethlefsen et al., 2006; Gerritsen et al., 2011), indicating that the greater microbial amount of the human microbiota is located in the large intestine. The composition also differs, with predominance of Gram-positive bacteria in the upper Gl tract and mainly Gram-negative microorganisms and anaerobes in the colon (Jones et al., 2009; Martinez et al., 2010).

The intestinal microbiota coexists in a homoeostatic relationship with the host, contributing to the maturation of the GI tract, metabolism of nutrients, development of the immune host defence and pathogen protection (Figure 3) (Guinane and Cotter, 2013). The saprophytic flora exerts important metabolic activities by extracting energy from otherwise indigestible dietary polysaccharides, such as resistant starch and dietary fibres (Wopereis et al., 2014). These metabolic activities also lead to the production of important nutrients, such as short-chain fatty acids (SCFA), vitamins (e.g. vitamin K, vitamin B12 and folic acid) and amino acids, all essential nutrients for human beings (Albert et al., 1980; Conly et al., 1994). The gut microbiota has a primary role in the development and function

of the innate and adaptive immune responses, and participates in the defence against pathogens by the production of antimicrobial molecules. Moreover, it is essential for normal GI motility, contributing to the regulation of sensory and motor functions and intestinal barrier homeostasis (Parkes et al., 2008; Gerritsen et al., 2011).

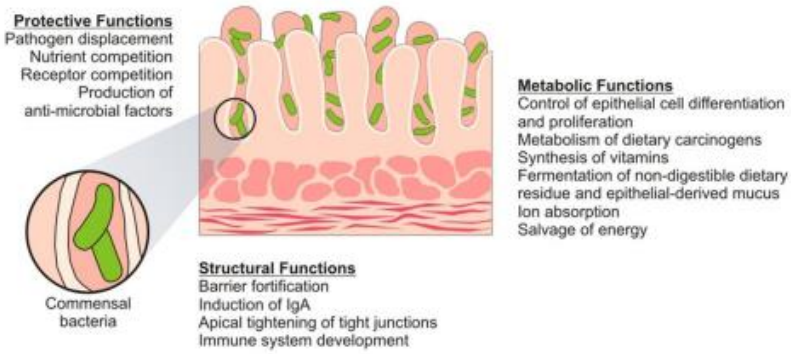

Figure 3. Functions or the intestinal microbiota. Commensal bacteria exert protective, structural and metabolic effects on the intestinal mucosa**.** From Grenham et al., 2011.

The gut microbiota extend its influence beyond the gut, playing a role in the bidirectional communication between the GI tract and CNS (Rhee et al., 2009), the so-called the "microbiota-gut brain axis". This complex network of communication between the gut, the microbiota and the brain includes the CNS, both the sympathetic and parasympathetic branches of the autonomic nervous system (ANS) and the ENS, in addition to the neuroendocrine and neuroimmune systems (Grenham et al. 2011).

It is now evident that our gut microbiome coevolves with us, undergoing an intense process of development throughout the lifespan and establishes its symbiotic relationship with the host early in life (Ley et al. 2008). Maturation of the microbiota occurs in parallel with neurodevelopment and they have similar critical development phases, in which a broad range of different factors may act altering the brain-gut signalling and leading to development of disorders later in life.

Several studies showed that alterations of the gut microbiota composition (dysbiosis) may contribute to the onset of obesity (Ley et al. 2006; Zhang et al. 2009), malnutrition (Kau et al. 2011), diabetes (Qin et al. 2012) and chronic inflammatory diseases such as IBD and IBS (Frank et al. 2007). In the same way, microbiota alterations, through this bidirectional communication, may influence stress reactivity, pain perception neurochemistry, and several other brain-gut disorders (Borre et al., 2014).

1.2.4 Enteric immune system

The human immune system includes the innate immunity, that has a standardized response to all adverse agents, and the adaptive immunity, that specifically recognizes each microorganism and has a specific response and memory. The GI tract represents an important immune organ with a gut-associated lymphoid tissue (GALT), formed by both inductive (Peyer's patches) and effector sites (lamina propria and sub-epithelial cells), representing approximately the 70% of the entire body immune system (Vighi, 2008). Moreover, the GI tract itself structurally forms a vital defensive barrier between externally-derived pathogens and the internal biological environment.

In the GI ecosystem, different factors including the ENS, the gut microbial saprophytic flora and the enteric immune system, interact and influence each other in order to preserve gut homeostasis (Yoo and Mazmanian, 2017). Thus, the resident population of immune cells in the gut is not only involved in the response to deleterious luminal stimuli or pathogens, but takes part also in the maintenance of homeostasis and development of normal intestinal morphology and function (Shea-Donohue and Urban, 2017). Neuroimmune interactions play also a major role in the GI response to stress, inflammation from infection or to disease states, resulting in acute and chronic changes in the GI function that contribute to disease symptoms.

Indeed, a persistent active inflammation in the gut leads to structural and functional remodelling in both neural and immune systems. Higher levels of circulation memory T cells and immunological memory cells in patients with IBD contribute to the disease persistence when the overt inflammation has subsided (Sundin et al., 2014; Takahara et al., 2013). In addition, immunological plasticity is part of the neuronal remodelling in functional bowel disorders, such as IBS. The mechanisms underlying the interplay between enteric neurons and immune cells is complex and involves neuro-, immuno-, and microbe- associated molecules, such as hormones, neuropeptides, cytokines, neurotrophic factors and short chain fatty acids (SCFAs) (Verheijden and Boeckxstaens, 2017). Furthermore, receptors for neurotransmitters are present on immune cells while, receptors for immune mediators are also located on neural structures (Shea-Donohue and Urban, 2017).

Cells involved in innate immunity recognize conserved features of pathogens through pattern recognition receptors (PRR), which include the membrane associated toll-like receptors (TLR), with resulting release of cytokines and chemokines that bind to receptors on immune cells (mast cell, macrophages and Innate lymphoid cells). Mediators released from these resident and recruited cells bind to naïve lymphocytes that develop the appropriate response to the pathogen and initiate a polarized immune response at this level (Figure 4).

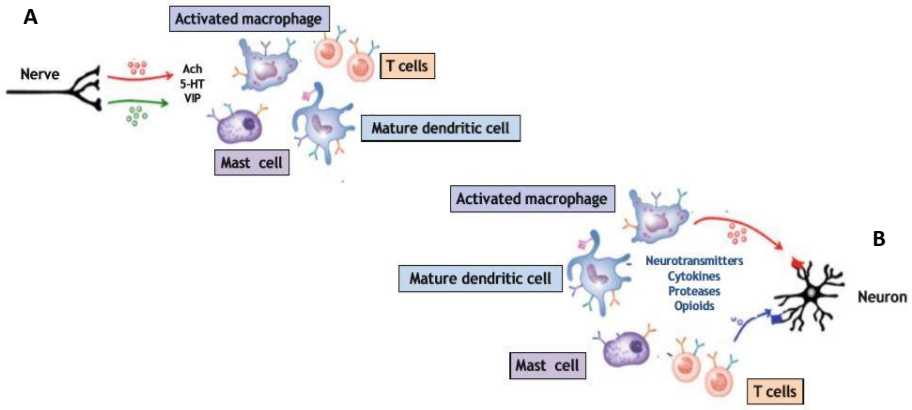

Figure 4. (A) The neuroimmune synapse showing the release of neurotrnsmitters in the proximity of immune cells that induce changes in the phenotype and function of these cells **(B) Resident and recruited immune mediators bind to receptors in nerves.** This may result in changes in neuronal sensitivity. From Shea-Donohue and Urban, 2017.

TLRs are type I transmembrane proteins responsible for the recognition of foreign pathogens referred to as pathogen-associated molecular patterns (PAMPs) (Martin et al., 2010). They play a role in the cross-talk between the intestinal microbiota and the host and protect against pathogenic microorganisms. The expression of TLRs in both the CNS and ENS (Barajon et al., 2009) suggest that TLRs are not only involved in the regulation of the host immune responses but they may also have a role in central aspects of neuroinflammation, neurodevelopment and neuroplasticity (Aravalli et al., 2007; Okun et al., 2011; Brun et al., 2013). Among all TLRs, the most important bacterial sensor proteins are TLR2s and TLR4s. Both these TLRs are expressed by enteric neurons and glia, suggesting that enteric neuronal pathways can directly sense the microbial population (Brun et al., 2013). The importance of TLR2 in the host defence against Gram-positive bacteria has been demonstrated using TLR2-deficient ($TLR2^{-/-}$) mice, which demonstrated a high susceptibility to a challenge with *Staphylococcus aureus* or *Streptococcus pneumoniae* (Takeuchi et al., 2000; Echchannaoui et al., 2002). TLR2s have also a crucial role in host defence against extracellular Gram-positive bacteria exposure (Akira and Takeda, 2004). TLR4s may detect LPS, a major component of Gram-negative bacteria cell wall (Takeda et al., 2003). Recently, TLR2 and TLR4 signalling has been described as fundamental for ensuring intestinal integrity and protecting from harmful injuries, such as inflammation. In fact, changes in TLR2 and TLR4 expression have been reported in both IBS and IBD (Rakoff-Nahoum et al., 2006). The absence of TLR2s seems to increase the susceptibility to intestinal injury and inflammation (Cario et al., 2007). Polymorphisms of TLRs genes as well as a defective immune response appear to be involved in the initiation and perpetuation of chronic inflammation in IBD (Pierik et al., 2006).

1.3 Adaptation to a changing environment: role of the extracellular matrix

As mentioned before, several factors take place in the adaptation to microenvironmental changes in physiological and pathological conditions, both in the CNS and ENS. Some molecular mechanisms that sustain this plasticity are common to both districts. A protein typically correlated to neuronal growth and regeneration, the growth-associated protein-43, is expressed at high levels in the nervous system during development. In adult animals, its expression is lower, but still observable in brain areas showing structural or functional plasticity (Simmons et al., 2008). In the ENS, GAP-43 is strongly expressed in the myenteric and submucosal ganglia at all ages (Stewart et al., 1992), thus giving evidence for a lifelong capability of the ENS to adapt to new challenges (Giaroni et al., 1999). The phenomenon of plasticity has a fundamental role during all the life span, during pre- and post-natal development and aging. During the perinatal period, in the rat myenteric plexus the neuronal number per ganglionic area increases from duodenum to colon (Gabella, 2001; Gabella, 1989). Conversely, the density of enteric neurons decreases with increasing age (Gabella, 2001; Gabella, 1989), and this variation is correlated with changes in motility, mucosal function and changes in specific neuronal phenotypes, such as IPANs (which appear to be the most age-sensitive neurons in the ENS). However, neuronal adaptation in response to changes in their microenvironment occurs even during adult life. As previously described, gut disorders, such as IBD or IBS, can lead to a remodelling of the ENS and to cytokine-induced changes in neurotrophin and neurotransmitter content and release. Inflammation also results in reactive remodeling of EGCs, characterized by an increase in GFAP expression and more “stellate” cell appearance, similar to that seen in reactive astrocytes (Grubišić et al., 2018). In this scenario, extracellular matrix (ECM) molecules provide an important framework for the enteric microenvironment and may influence the integrity of myenteric neuronal circuitries during both physiological and pathological conditions. ECM molecules provide a highly organized environment filling the extracellular space, and consist of different types of macromolecules. The main constituents of ECM are fibrous-forming proteins, such as collagens, elastin, fibronectin (FN), laminins, glycoproteins, proteoglycans (PGs), and glycosaminoglycans (GAGs) (Theocharis et al., 2016).

In the CNS, where the role of ECM has been mostly studied, these molecules are synthetized by neurons, glia and non-neuronal cells, and are secreted into the extracellular space, where then they are associated with cell surface receptors and form heterogeneous aggregates around the neurons, the so-called perineuronal nets (PNNs). The precise composition and specific structures of the PNNs vary from tissue to tissue.

Nevertheless, ECM is not only a mere mesh-like scaffold for the cells. In the CNS, PNN takes part in the regulation of neurogenesis, gliogenesis and circuitry formation during development, and, indeed, substantial changes in its quantity and composition occur in this period (Carulli et al., 2016). Moreover, ECM continues to be essential for synapse stability, neuroprotection and regulation of neuronal plasticity during all the rest of life (De Luca and Papa, 2016).

Synaptic dysfunctions are a critical pathological component of several brain disorders; thus, it has been proposed that ECM and PNN alterations, being involved in processes of plasticity and homeostatic maintenance, may contribute to pathogenesis of neurological and neuropsychiatric disorders (Carulli et al., 2016). In both *in vitro* and *in vivo* models, a strong correlation has been reported between an impairment in ECM molecules expression and the development of Alzheimer's disease, epilepsy, schizophrenia and drug addiction (Dzyubenko et al., 2016; De Luca and Papa, 2016).

Less information, however, are available concerning the role of ECM in the ENS. Some studies show the distribution of several ECM molecules in the basement membranes surrounding enteric ganglions of rat and guinea pig intestines (Bennerman et al., 1986; Laurie et al., 1983). It is now well established that this molecules take part in the regulation of cell migration and differentiation into diverse phenotypes cells, not only during intestinal development but also in adult cell renewal (Rauch and Schäfer, 2003).

Given the presence and the influence of ECM in GI tract, it become particularly interesting to investigate if ECM molecules may participate also to synaptic dysfunction in GI pathological conditions.

1.4 HA and gut homeostasis

1.4.1 Hyaluronan: synthesis, properties and functions

Hyaluronan is a relatively simple component of the extracellular matrix, an unbranched GAG composed of repeating polymeric disaccharides of d-glucuronic acid and N-acetyl-d-glucosamine linked by a glucuronidic β(1→3) bond (McDonald and Camenisch, 2002). The number of repeat disaccharides in a completed HA molecule can reach 10000 or more, with a molecular weight of ∼4000 kDa. Due to its exceptional length and high degree of hydration, hyaluronan makes the ECM an ideal environment in which cells can move and proliferate. Hyaluronan is ubiquitously expressed in the ECM and on cell surfaces of all body fluids and tissues of vertebrates, as well as on surface coats of bacterial species and certain algae (Joy et al., 2018). HA levels are maintained through regulation of the enzymatic activity of HA synthases (HAS) and hyaluronidases, which are

responsible for its synthesis and degradation. HA is produced by a family of three hyaluronan synthase isoenzymes (HAS1, HAS2, and HAS3) that synthetize HA on the inner surface plasma membrane and translocate the final polymer to the extracellular space. In general, HAS2 represents the main HA synthetic enzyme in adult cells and its activity reasonably undergoes fine regulation. However, HAS1 and HAS3 seem to have peculiar roles even if not completely clarified.

In spite of its relative simple structure, HA possesses many physiological roles, regulating different cell behaviors such as cell adhesion, motility, growth and differentiation (Knudson and Knudson., 1993). Several studies have shown that the majority of HA biological effects are size-dependent: HA can exist as large polysaccharides, medium fragments and small oligosaccharides. HA molecules of high molecular weight (HMW) are involved in the maintenance of physiological conditions, whereas fragmented polymers accumulate during tissue injury and function in ways distinct from the native polymer, inducing inflammatory responses and triggering repair processes. (Joy et al., 2018). There is accumulating evidence that free radicals and an enhanced activity of hyaluronidases are responsible for HA fragmentation. The resulting degradation products can stimulate the expression of inflammatory genes by a variety of immune cells at the injury site (Jiang et al., 2007).

It has been suggested that also different HAS isoforms may synthesize HA with different chain length. *In situ*, all three HAS proteins synthesize HA chains of high molecular mass (≥4 × 106 Da). However, *in vitro*, HMW HA (≥4 MDa) is synthesized only by HAS2, while HAS3 and HAS1 synthesize smaller polydisperse chains of an average molecular mass of 800 and 100 kDa, respectively (Heldin et al., 2009). It seems that the difference in size of HA synthesized by the different HAS isoforms may be dependent on (1) the intrinsic enzymatic property, (2) the intracellular environment and (3) additional accessory molecules involved. Interestingly, stimuli such as growth factors and cytokines can regulate the expression of HAS isoforms in vitro, and upregulation of HASs, together with increased accumulation of HA, has been found after tissue damages (Al'Qteishat et al., 2006).

In both physiological and pathological conditions, to accomplish its important functions, HA interacts with specific proteins called hyaladerins, or membrane receptors like CD44 and RHAMM, and toll like receptors (TLRs) such as TLR2 and TLR4 (Vigetti et al., 2014) (Figure 5).

CD44 is considered a primary receptor for HA, existing in at least 10 different isoforms. Its interaction with HA plays an important role in a variety of cell functions like inflammation, development, tumor growth and metastasis. Upon binding with CD44, HMW and LMW HA show distinct inflammatory and angiogenic effects. Native HMW polymers demonstrated anti-inflammatory and anti-angiogenic effects, suppressing cell migration, proliferation and sprout formation. On the other hand, HA oligosaccharides exhibited pro-angiogenic and pro-inflammatory responses, stimulating cell mobility and proliferation (Noble 2002).

HA is also able to induce the expression of inflammatory mediators, such as chemokines and cytokines, through the interaction with TLRs or the TLR adaptor protein MyD88, independently from CD44 activation. The abrogation of TLR2 and 4 as well as MyD88 abolished completely the activation of chemokines in macrophages in *in vitro* models (Jiang et al., 2005). Another study has shown that fragmented HA, via TLR2 and TLR4 signaling, specifically activates dendritic cells in vitro, with subsequent priming of allogeneic T cells. All these data suggest a focus on the role of HA as an immune regulator in both physiological and pathological conditions (Tesar et al., 2006).

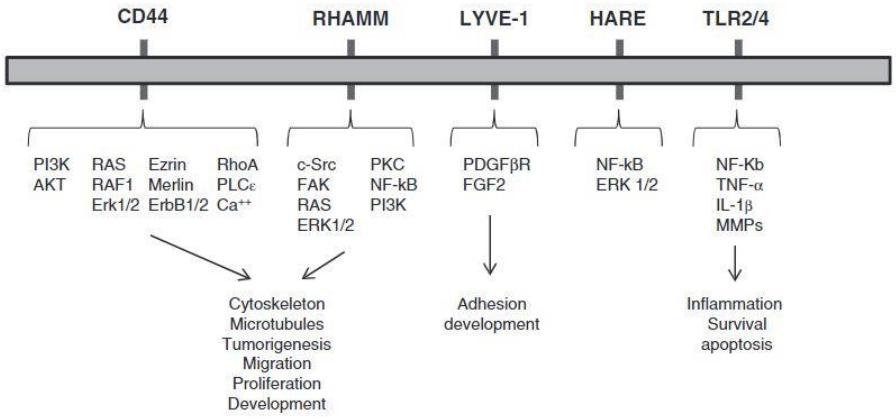

Figure 5. Schematic representation of the signalling cascade of HA receptors and their involvement in cell and tissue functions. From Vigetti et al., 2014.

1.4.2 HA production in health and pathological conditions in the gut

HA is an important extracellular matrix component in the vertebrate intestinal tract, with a concentration four times higher in the colon than in small intestine (Göransson et al., 2002). In both healthy human and mouse guts, HA is prominently located immediately beneath the barrier epithelium, where it is deeply involved in the maintenance of homeostasis. As hydrophilic molecule, it ensnares water and regulates fluid exchange to and from the blood, interacting with lymphatic and blood microvessels that control water and solute transport (de la Motte and Kessler, 2015). As mentioned before, HA have also important functions in multiple host defense mechanisms. HA can participate in innate immune responses in the intestine, promoting leukocyte recruitment in the intestinal extravascular space upon a gut disease or damage, directly or via interaction with the surface receptor CD44 (de la Motte and Kessler, 2015). Interestingly, HA of medium average molecular weight (35 kDa), increased the epithelial expression of a murine orthologue of human β-defensin (HBD2) in mice via TLR4 activation (Hill et al., 2012). HBD2 is a naturally produced antimicrobial peptide with a broad antimicrobial spectrum against bacteria, fungus protozoa, and viruses (Zasloff, 2002). In addition, HBD2 is one of the enteric defensins, which favour the shaping

of the intestinal microflora composition (Salzman et al., 2010), and HBD2 dysregulation has been reported in IBD (Wehkamp et al., 2008).

HA can also act to systemically decrease inflammation and promote epithelial repair. Studies on rodents models have shown that administration of medium molecular weight HA protects from damage during experimentally induced colitis, through the activation of TLR4 receptors that drive COX2 production and promotes recovery (Zheng et al., 2009). In a recent study administration of nanoparticles consisting of medium molecular weight HA complexed with bilirubin, restored the epithelial barrier, reduced the damage score and increased the overall richness and diversity of the saprophytic microbiota in a murine model of colitis (Lee et al., 2019). Several reports have, however, demonstrated that endogenous HA deposition may be highly altered during gut inflammation. In these conditions, small fragments of HA may promote immune cell activation as well as production of pro-inflammatory cytokines, thus favoring an increased inflammatory response. Accumulation of HA in the epithelial, submucosal and smooth muscle intestinal layers and in blood vessels within the submucosal layer has been observed, both in experimental animal models of colitis and in the intestine of patients with IBD (Kessler et al., 2008). These findings are consistent with other data concerning the increased HA deposition in different tissues, such as liver, kidney and lung, during inflammation (Jiang et al., 2011).

The majority of studies have focused on the involvement of HA in the development of fibrotic tissue within the submucosal and *muscularis mucosae* layers (de la Motte et al., 2011; Kessler et al., 2008). However, no information is available on the possible involvement of HA in myenteric neuron derangement in this state. Similarly, given the increasing amount of data concerning the role of HA in inflammatory processes, it could be interesting to investigate its involvement in other pathological conditions affecting the GI tract, such as, for instance, damages derived by an ischemic/reperfusion injury.

1.5 Inflammatory bowel disease (IBD)

IBD is a group of chronic inflammatory bowel disorders, comprising Crohn's disease (CD) and ulcerative colitis (UC) with increasing incidence worldwide (Ng et al., 2017). CD and UC are identified by different inflammation patterns: CD is considered a chronic, segmental inflammation of the GI tract, whereas UC displays inflammation and ulceration restricted to the colon and rectum. Although the exact aetiology is unknown, the inflammation in these two disorders is suggested to develop because of an exaggerated immune response to luminal antigens derived from the gut microbiota or from infecting pathogens, in genetically predisposed individuals (Baj et al., 2019).

Patients with IBD commonly manifest symptoms suggestive of disturbed GI function with sensory, motor and secretory alterations, characterized by periods of exacerbation and remission (Lomax et al., 2005). Long-term changes involving enteric neurons and the smooth muscle layers may lead to persistent dysmotility as well as altered visceral pain perception. Inflammation leads to derangements of enteric neuronal circuitries characterized by increased neuronal excitability (hyperexcitability of primary afferent neurons), synaptic facilitation and reduced inhibitory neuromuscular neurotransmission (Vasina et al., 2006). The interplay among different cell populations in the enteric microenvironment, and infiltrating inflammatory cells may account for the structural and functional changes occurring in enteric circuitries in response to inflammation (Brierly and Linden, 2014). EGC, for example, which represent the most abundant cell population within enteric ganglia, are involved in processes of development and maintenance of afferent sensitization and have the potential to modify visceral perception through interactions with neurons and immune cells during pathological gut states (Morales-Soto and Gulbransen, 2019). Furthermore, neuronal cells in the ENS are located in close proximity to mucosal immunocytes and may regulate one another's functions by releasing a complex set of cytokines, neurotransmitters and hormones. Neuronal activation can lead to degranulation of mast cells and neutrophilic infiltration to the area. Furthermore, neuropeptides, such as SP and VIP, released by enteric nerves, may activate their receptors localized on immune cell membranes, inducing differentiation of immunocytes and inducing IgA production (Aguilera and Melgar, 2016). The enteric microbiota represents a fundamental player in IBD development and plays a central role in inflammation-induced enteric neuron derangement. Indeed, both preclinical and clinical studies suggest that an important player in IBD development is represented by the gut microbiota (Lomax et al., 2005). Evidences show that IBD patients often develop dysbiosis, and that some antibiotics are efficacious in the prevention and treatment of inflammation both in humans and in animal models (Lomax et al., 2005). Metagenomic studies have shown qualitative and quantitative differences in the microbiota composition in IBD patients, which show reduced faecal amounts of the phylum *Firmicutes* (in particular *Faecalibacterium prausnitzii*) and increased levels of the phylum *Proteobacteria*, comprising *E. coli*, with respect to healthy individuals (Marchesi et al., 2016; Hansen et al., 2012). The hypothesis that specific pathobionts, i.e., commensal microorganisms, which in peculiar environmental or genetic conditions, can cause the disease has been put forward, but not yet clear-cut demonstrated, although, biopsies of patients with active CD showed high levels of a particularly invasive adhesive strain of *E. coli* (AIEC) (Aguilera and Melgar, 2016; Buttó et al., 2015). The correlation between dysbiosis and IBD has been demonstrated also in genetically modified mouse models, spontaneously developing the disease. For example, a healthy microbiota is

required in mouse models either overexpressing IL-23 or null for IL-10, which play a pro-inflammatory and anti-inflammatory action via activation of Th17 and Treg lymphocytes, respectively, to spontaneously develop colitis (Lomax et al., 2005; Hoshi et al., 2012). Another important issue, which suggests the crucial role of the gut microbiota in IBD pathogenesis, is represented by the presence of microbial components within the inflammatory lesions (Sekirov et al., 2010; Ni et al., 2017). Genome-wide association studies suggest that TLRs are implicated in IBD pathogenesis (DeJager et al., 2007; Pierik et al., 2006). TLR signalling activation by microbial metabolites is essential for epithelial repair and homeostasis after experimentally-induced colitis. There are data suggesting that TLRs are protective for intestinal epithelium, by promoting epithelial cell survival, inhibiting apoptosis and recruiting stromal and myeloid cells (Malvin et al., 2012). In addition, both TLR2 and TLR4 are also present on neurons in the ENS, and TLR2s may regulate intestinal inflammation by controlling ENS structural and functional integrity (Brun et al., 2013; Caputi et al., 2017). In this scenario, it is particularly important to discover molecules involved in the gut microbiota-neuro-immune axis sustaining neuronal degeneration during pro-inflammatory states, in order to prevent the occurrence of more obvious inflammatory conditions. This opens the opportunity to obtain new molecules displaying high efficacy in the treatment of IBD in association and/or substitution of anti-inflammatory, immunosuppressive and biologic drugs, which represent the conventional therapeutic approach for this gut disorder (Neurath, 2017).

1.6 Ischemia/reperfusion injury

The GI circulation is a highly organized and well-regulated vascular bed, composed by vessels that, via the mesentery, pass through the muscular, submucosa and mucosal compartments of the GI wall. This vascular network provides a high rate blood flow to a large exchange surface area. For this reason, the gut is one of the most ischemia-sensitive tissues in the body (Haglund and Bergqvist, 1999). Intestinal ischemia/reperfusion (I/R) injury is an important clinical problem, associated with a high morbidity and mortality, which may occur as a consequence of embolism, arterial or venous thrombosis, shock, intestinal transplantation, and necrotising enterocolitis in the human premature newborn or in chronic inflammatory diseases (Reinus et al., 1990; Haglund and Bergqvist 1999; Massberg and Messmer, 1998; Nowicki 2005; Thornton and Solomon, 2002). Intra-arterial infusion therapy with smooth-muscle relaxant vasodilators (papaverine), thrombolytic agents (streptokinase and urokinase) and anticoagulants represent possible therapeutic approaches for the acute treatment, although a laparotomy to resect necrotic bowel and local vascular

desobstructive interventions in case of occlusive etiology are more often practiced (MacDonald et al., 2005). I/R injury develops as a consequence of both the hypoxic and the reperfusion components. The interruption of blood supply, occurring with the initial hypoxia, causes severe depletion of tissue energy resources and microscopically detectable damages in the superficial part of the mucosa, which becomes the site for the production of various acute-phase proteins, gut hormones, and cytokines (Zimmerman and Granger, 1992, Carden and Granger, 2000). The exact mechanisms involved in intestinal IR injury are largely unknown, but pro-inflammatory cytokine release, inflammatory cell infiltration, production of reactive oxygen species (ROS), increased expression of nitric oxide (NO), TLR4 signalling and activation of inflammatory transcription factors are certainly involved in these events (Camara-Lemarroy, 2014). Production of such molecules may also harm distant tissues and culminate in multiple organ dysfunctions (Vollmar e Menger, 2010; Kong et al., 1998).

The reperfusion period, although essential to rescue ischemic tissues, paradoxically initiates a cascade of events that may lead to additional cell injury, known as reperfusion injury, exacerbating vascular and tissue damage. (Mallick et al., 2004). The damage, is dramatically magnified by an increased generation of NO, inflammatory mediators and reactive oxygen species (ROS) (Carden and Granger, 2000). In particular, the enhanced net catabolism of ATP during ischemia, resulting in increased hypoxanthine and xanthine concentrations, represents an important mechanism to sustain ROS generation. This pathway is favoured by the conversion of xanthine dehydrogenase to xanthine oxygenase, which generates superoxide free radicals as a by-product of the oxidation of purines to uric acid. The burst of superoxide-generated xanthine oxygenase during reperfusion triggers a free-radical chain reaction that worsen tissue damage by recruiting neutrophils, which may produce additional free-radicals (Haglund and Bergqvist, 1999).

From a structural viewpoint, the I/R insult has severe consequences for the metabolically active intestinal mucosa, which undergoes shedding, barrier dysfunction, and bacterial translocation (Kong et al., 1998). Other enteric cell types, including smooth muscle cells, enteric glial cells and neurons, may also deteriorate. Myenteric neurons are especially sensitive and can be irreversibly compromised (Filpa et al., 2017). Indeed, an I/R injury causes pathological alterations of myenteric ganglia, with dysmotility and a slowing of GI transit, suggestive of a long-lasting neuropathy (Rivera et al., 2011). Among the different enteric neurotransmitter pathways, there is good evidence that energy deprivation in GI tract can preferentially depress cholinergic neuronal pathways involved in intestinal reflexes (Kosterlizt and Robinson, 1959; Mizhorkova et al., 2001). Both spontaneous and electrically evoked endogenous acetylcholine overflow from the guinea pig ileum was altered during glucose and oxygen deprivation, mimicking an *in vitro* ischemic damage (Giuliani et al., 2006;

Mizhorkova et al., 2001; Larson and Martins, 1981). These effects were correlated with a depression of the cholinergic neuro-effector transmission (Corbett and Lees,1997; Mizhorkova et al., 2001). As regards the neuronal component, the sensitivity of enteric cholinergic neurons to I/R damage may be explained considering the strict dependence of neuronal acetylcholine synthesis on the oxidative phosphorylation. Furthermore, the ability of the I/R injury to influence the excitation-contraction coupling at a post-junctional level explains the depression of electrically induced smooth muscle contraction in this condition (Mizhorkova et al., 2001).

Nitrergic inhibitory pathways seem also to play a distinctive role in the development of myenteric neuron derangement during I/R role. In the gut, the three isoforms of NOS, the endothelial NOS (eNOS), the neuronal NOS (nNOS), and the inducible NOS (iNOS), have been identified in different cells, comprising myenteric neurons of different species (Talapka et al., 2011). Nitrergic neurons play a fundamental role in the physiological regulation of peristalsis: nNOS is the predominant NOS in the normal intestine as it is constitutively expressed, whereas iNOS is only expressed in response to cytokines and growth factors. nNOS containing myenteric neurons seem to be selectively targeted by in vivo I/R injury, and damage or loss of function of nNOS-immunopositive neurons may underlie intestinal motility derangement, suggesting that NO produced by nNOS is protective against the metabolic insult (Rivera et al., 2011). Conversely, intestinal I/R damage has been associated with upregulation of iNOS, which may replace nNOS in the synthesis of NO in myenteric neurons (Giaroni et al., 2013).

2 AIMS

Enteric neuronal circuitries display a considerable ability to adapt to a changing microenvironment, which comprises several cellular "players" such as neurons, enteric glia, smooth muscle cells, immune cells and the intestinal microbiota (Giaroni et al., 1999). The phenomenon of plasticity plays a fundamental role in the maintenance of gut homeostasis, in physiological conditions. However, remodelling of enteric neuronal circuitries may also occur in pathological conditions, such as during chronic inflammatory states of the gut or during ischemia/reperfusion (I/R) injury. Indeed, inflammatory bowel diseases (IBD) are associated with derangements of the ENS, characterized by increased neuronal excitability (hyperexcitability of primary afferent neurons), synaptic facilitation and reduced inhibitory neuromuscular neurotransmission. Such changes may lead to persistent dysmotility as well as altered visceral pain perception, which represent two of the main IBD symptoms (Vasina et al., 2006). Intestinal I/R injury, which is associated with a high morbidity and mortality, may result as a consequence of embolism, arterial or venous thrombosis, shock, intestinal transplantation, or necrotising enterocolitis in the human premature newborn, and are also associated with IBD (Haglund and Bergqvist 1999; Massberg and Messmer, 1998; Nowicki 2005; Thornton and Solomon, 2002). The I/R insult, can seriously affect the structure and function of myenteric neurons (Filpa et al., 2017) resulting in a particularly severe slowing of transit, suggestive of a long-lasting neuropathy (Rivera et al., 2011).

In both IBD and I/R conditions, the structural and functional changes occurring in enteric circuitries may be due to, at least in part, to the interplay occurring among different cell populations in the enteric microenvironment. In this context, extracellular matrix (ECM) molecules provide an important framework for the enteric microenvironment and may influence the integrity of myenteric neuronal circuitries during both physiological and pathological conditions. ECM molecules provide a highly organized environment filling the extracellular space, and consists of different types of macromolecules. The main constituents of ECM are fibrous-forming proteins, such as collagens, elastin, fibronectin (FN), laminins, glycoproteins, proteoglycans (PGs), and glycosaminoglycans (GAGs) (Theocharis et al., 2016). Among these components, the unbranched GAG Hyaluronan (HA), which is mainly deposited immediately beneath the epithelial barrier, is deeply involved in the preservation of gut homeostasis. HA can participate in innate immune responses in the intestine, promoting leukocyte recruitment in the intestinal extravascular space in both health and disease states of the gut (de la Motte and Kessler, 2015). Several reports have suggested that HA deposition is drastically altered during gut inflammation. In these conditions, small fragments of HA may promote immune cell activation as well as production of pro-

inflammatory cytokines, thus favouring an increased inflammatory response. Accumulation of HA in the epithelial, submucosal and smooth muscle intestinal layers and in blood vessels within the submucosal layer has been observed, both in experimental animal models of colitis and in the intestine of patients with IBD (Kessler et al., 2008). Nevertheless, the majority of studies have focused on the participation of HA in the development of fibrotic tissue within the submucosal layer during inflammation (de la Motte et al., 2011; Kessler et al., 2008), but no information is available on the possible involvement of HA in the alterations of the neuromuscular function, related to these conditions.

Thus, the first aim of this thesis was to evaluate the role of HA in the adaptive changes of the rat myenteric plexus in an experimental model of IBD induced by intrarectal administration of 2-4-dinitro-benzensulfonic acid (DNBS). In a successive phase, the role of HA in the adaptation of the rat intestinal neuromuscular function was evaluated after in vivo ischemia/reperfusion (I/R) injury, a pathological condition associated with gut inflammation.

Overall, the results obtained in these studies may allow to clarify whether HA participates to the rearrangement of enteric neuronal networks in pathological conditions, associated with important rearrangements of the intestinal neuromuscular function, such as chronic inflammation and I/R injury.

3 MATERIAL AND METHODS

3.1 Animal models

Male Sprague-Dawley or Wistar rats (weight 250-350 g, Envigo, San Pietro al Natisone, Udine, Italy), were housed under controlled environmental conditions (temperature 22±2°C; relative humidity 60-70%) with free access to a standard laboratory chow and tap water, and were maintained at a regular 12/12-h light/dark cycle. Their care and handling were in accordance with the provision of the European Union Council Directive 2010/63, recognized and adopted by the Italian Government (Decree No. 26/2014). Animal Care and Use Ethics Committee of University of Insubria and University of Pavia approved the protocol.

3.1.1 DNBS-induced colitis

Experimental colitis has been induced by administration of a single dose (30 mg) of 2,4-dinitro-benzene-sulfonic acid (DNBS, ICN Biomedicals, CA, USA) dissolved in 0.25 ml of 50% ethanol and administered, under isofluorane anaesthesia, via a polyethylene PE-60 catheter into the colon, 8 cm proximal to the anus. This dose was selected based on a previous study showing that it evoked adequate inflammation without causing unnecessary distress and suffering to the animals, with a mortality rate of 0%. Controls (CTR) were administered 0.25 ml of 50% ethanol (vehicle). DNBS-treated and control rats were kept in separated cages during the study. Animals were euthanized at time of maximal intestinal inflammation, 6 days after the induction of colitis. Distal colon was removed, then opened longitudinally over the mesenteric line and washed with a physiological Tyrode's solution (composition in mM: 137 NaCl; 2.68 KCl; 1.8 CaCl2.2H2O; 2 MgCl2; 0.47 NaH2PO4; 11.9 NaHCO3; 5.6 glucose). DNBS-induced experimental colitis in rats was chosen since the inflammatory response develops rapidly and shares many features with the response observed in human IBDs. Possible physiological and behavioral changes were monitored throughout the treatment period (i.e., changes in body weight, respiration, occurrence of diarrhea, alterations of posture and in the appearance of the coat) to evaluate suffering and distress.

3.1.1.1 Assessment of colonic damage

Colonic damage was evaluated macroscopically and histologically. Macroscopic colonic damage was evaluated according to standard procedures (Sturiale et al., 1999). Briefly, the criteria adopted were the following: presence of adhesions between the colon and other intra-abdominal organs In

particular, the severity of intestinal inflammation was macroscopically evaluated using a gravity score ranging from 0 to 6, according to the following criteria: presence of adhesions between the colon and other intra-abdominal organs (0 = none, 1= mild, 2= major); consistency of colonic fecal material (as an indirect marker of diarrhea) (0 = formed, 1 = loose, 2 = liquid); thickening of the colonic wall, presence and extension of hyperemia and macroscopic mucosal damage [0 = no damage; 1 = hyperemia; 2 = presence of an ulcer; 3 = ulcer + inflammation; 4 = two or more ulcers; 5 = major damage (presence of necrosis < 2 cm); 6 = very severe damage (presence of necrosis >2 cm)]. Ethanol, used as a vehicle, had no effect, per se, on the parameters measured 6 days after induction of colitis. Microscopic evaluation of the damage was histologically investigated on full-thickness samples of distal colon obtained from both DNBS-treated and control rats, which were fixed with 4% formaldehyde in acetate buffer 0.05 M for 24-48 h and successively embedded in paraffin. Hematoxylin and eosin (HE) histological staining was carried out on seven-micron-thick sections and observed under a light microscope (Nikon Eclipse Ni; Nikon, Tokyo, Japan), and data were recorded using a DS-5M-L1 digital camera system (Nikon Corporation, Tokyo, Japan).

3.1.2 Ischemia/reperfusion injury

Rats were anaesthetized with sodium thiopental (100 mg/kg) diluted in sterile phosphate-buffered saline (PBS, composition in mM: 0.14 NaCl, 0.003 KCl, 0.015 Na2HPO4, 0.0015 KH2PO4, pH 7.4), given intraperitoneally. After laparatomy, a loop of the small intestine was exteriorized and the superior mesenteric artery (SMA) was temporarily occluded for 60 min with an atraumatic microvascular clamp. The clip was then gently removed, the abdominal wall was sutured and animals returned to a cage after recovering from anaesthesia. Another group of animals, represented by sham-operated animals, undergoing the same surgical manipulation except SMA occlusion. A last group of normal un-operated rats was used as control (CTR). Animals were euthanized 24 h after reperfusion, when the major histological and functional changes have been evidenced. In addition to these groups, I/R, sham-operated and controls animals were intraperitoneally treated with 4-Methylumbelliferone (4-MU), in order to inhibit hyaluronan synthesis. A single dose of 25 mg/kg 4-MU was administrated 24 h before euthanization. Segments of the small intestine, ~5 cm oral to the ileo-cecal junction, were rapidly excised and rinsed with a physiological ice-cold Tyrode's solution for successive experiments.

3.2 Immunofluorescence and immunohistochemistry

The immunolocalization of hyaluronan (HA) was performed on paraffin-embedded tissue sections, and on longitudinal muscle myenteric plexus (LMMP) whole-mount preparations, using a biotin-

labeled HA-binding protein (HABP, Hokudo Co, Japan). HABP recognizes HA saccharidic sequences and is able to localize HA in tissues by streptavidin conjugation with an appropriate fluorophore. Hyaluronan synthase 1 (HAS1) and 2 (HAS2), Substance P (SP), Choline acetyltransferase (ChAT), neuronal NOS (nNOS) and inducible NOS (iNOS) distributions in myenteric ganglia was also evaluated by immunofluorescence on colonic whole-mount preparations. Details of the primary and secondary antibodies and related optimal dilutions are reported in Table 2.

3.2.1 Ischemia/reperfusion injury

Paraffin cross sections (7-16 μm) from all experimental animal groups were treated for 30 minutes with PBS containing 2% bovine serum albumin (BSA) before biotin-labeled HABP overnight incubation at 4°C. PBS buffer used for washing steps and HABP dilutions contained 2% BSA. After washing, incubation with the suitable streptavidin FITC-conjugated antibody was performed for 60 minutes in a dark humid chamber. Control samples were incubated only with BSA-containing PBS. Coverslips were mounted with Citifluor mounting medium and then observed under a fluorescent microscope (Nikon Instruments).

3.2.2 Whole-mount preparations

Small intestine segments were fixed with 0.2 mol/l PBS containing 4% formaldehyde and 0.2% picric acid for 3 hours, then stored at 4°C in PBS containing 0.05% sodium merthiolate (Thimerosal, Sigma-Aldrich). For the whole-mount preparations, LMMP was gently peeled away from the remainder of the intestinal wall. Nonspecific sites were blocked using PBS added with 1% Triton X-100 and 10% normal horse serum (NHS) (Euroclone, Pero, Italy) for 2 hours, then LMMPs were incubated with optimally diluted antibodies for the staining. Double-labelling was performed during consecutive incubation times: the first primary antibodies were added overnight at 4˚C, followed by incubations with the appropriate secondary antibodies for 2h at room temperature (RT). Washing between antibodies were performed with PBS containing 1% Triton X-100 and 10% NHS. Preparations were mounted onto glass slides, using a mounting medium with DAPI (Vectashield; Vector Lab, Burlingame, CA, USA). Negative controls and interference control staining was evaluated by omitting one or both of the primary antibodies, or one of the secondary antibodies.

Table 2. Primary and secondary antisera and their respective dilutions used for immunofluorescence assay.

Antiserum	Dilution	Source	Hostspecies
Primary antisera			
HABP, biotin	1:100	Hokudo (BC41)	--
HAS1	1:100	Bioss (bs-2946R)	Rabbit
HAS2	1:100	Santa Cruz (sc-34067)	Goat
HUC/D, biotin	1:100	Invitrogen (A-21272)	Mouse
ChAT	1:50	Chemicon (AB144P)	Goat
nNOS	1:50	Santa Cruz (sc-648)	Rabbit
iNOS	1:50	Santa Cruz (sc-8310)	Rabbit
Substance P	1:200	Immunostar (20064)	Rabbit
CD45	1:100	Merck Millipore (MAB079-1)	Mouse
Secondary antisera and streptavidin complexes			
FITC-conjugated streptavidin	1:200	Molecular Probes (SA1001)	--
Cy3-conjugated streptavidin	1:500	Amersham (PA43001)	--
Anti-rabbit Alexa Fluor 488	1:200	Molecular Probes (A21206)	Donkey
Anti-rabbit Alexa Fluor 555	1:500	Cell Signaling (4413)	Goat
Anti-mouse Alexa Fluor 488	1:200	Molecular Probes (A21202)	Donkey
Anti-goat Cy3	1:400	Jackson (705-165-147)	Donkey
$F(ab')_2$ anti-mouse IgG (H+L) biotin	1:300	Caltag Laboratories (M35015)	Goat

3.2.3 Primary cultures of myenteric ganglia

Intestinal segments (20 cm long) were isolated and rinsed with a physiological ice-cold Tyrode's solution. For myenteric ganglia cultures, LMMP segments were minced and enzymatically digested, as described by Bistoletti et al., 2019. After dissociation, 3×10^4 cells per well were seeded on the poly-L-lysine-pre-coated glass coverslips into the 24-well plate and grown in an incubator (37.5 °C, 5% CO2) for six days. Medium was changed every two days. For immunofluorescence staining, cells on coverslips were fixed in PBS containing 4% formaldehyde for 10 min at 37 °C. After blocking non-specific sites with PBS containing 5% normal horse serum (Euroclone) and 0.1% Triton X-100 for 1 h at RT, preparations were double-labelled with HABP and with either an anti-HuC/D antibody. Preparations were mounted on glass slides and analyzed by confocal microscopy. Negative controls were evaluated as described for whole-mounts immunolabelling.

3.2.4 Acquisition and analysis of images

Images were acquired at confocal microscopy using a Leica TCS SP5 confocal laser scanning system (Leica Microsystems GmbH, Wetzlar, Germany). Fluorophores were visualized using a 488 nm excitation filter and 515/530 nm emission filter for Alexa Fluor 488 or fluorescein isothiocyanate (FITC), 543 nm excitation filter and 590/650 nm emission filter for Alexa Fluor 555 or Cy3 dye. All microscope settings were set to collect images below saturation and were kept constant for all images. In intestinal myenteric plexus, the analysis of total neuron population was performed on LMMP preparations, obtained from 5 animals per group, by counting HuC/D$^+$ myenteric cells. The distribution of nitrergic neurons was evaluated by counting HuC/D$^+$/nNOS$^+$ and HuC/D$^+$/iNOS$^+$ neurons. The evaluation of the tachykininergic neuron distribution was performed by counting HuC/D$^+$/SP$^+$ neuronal cells, whereas the distribution of cholinergic neurons was obtained by HuC/D$^+$/ChAT$^+$ neuron count. In the same way the percentage of HAS1 and HAS2 positive neurons was obtained by counting the neurons on the total of HuC/D$^+$ neurons (Stenkamp-Strahm et al., 2013; Robinson et al., 2016). Areas of myenteric ganglia, digitized by capturing 10 fields per preparation at 40X magnification, were measured by tracing boundaries around stained cell somas (HuC/D). In small intestine LMMP whole-mount preparations changes in the immunoreactivity for HA, ChAT and SP were assessed by analysing the density index of labelling per myenteric ganglia area (5 animals per group, 10 fields per preparation at 40X magnification). Images were captured at identical exposure time conditions and thresholded to allow ImageJ software (version 1.48a) to select and measure only stained segments.

3.3 Myeloperoxidase activity

Myeloperoxidase (MPO) was measured in order to assess the development of an inflammatory state caused by neutrophil infiltration. Briefly, mucosa-deprived intestinal samples were suspended in ice-cold potassium phosphate buffer (50 mM, pH 6.0) containing 0.5% hexadecyl trimethylammonium bromide (HTAB) and homogenized (50 mg/ml). After centrifugation (14 000 rpm, 20 minutes, 4°C), an aliquot of the supernatant fraction (34 µl) was mixed with 986 µl of the HTAB-phosphate buffer containing 0.167 mg/ml O-dianisidine dihydrochloride with hydrogen peroxide (0.0005%). Changes in the rate of absorbance were spectrophotometrically recorded at 460 nm. MPO activity was expressed in units (U), defined as the amount of enzyme that degrades 1µmol/min of hydrogen peroxide at 25°C. Experiments were performed four times, and results were expressed in U/mg wet tissue weight.

Alternatively, immunohistochemical analysis of neutrophil infiltration were performed on three-micrometer-thick intestinal paraffin sections, using the avidin-biotin-peroxidase method (Hsu and Raine, 1981) with a polyclonal antibody anti-MPO (Ventana Medical System, Tucson, AZ). Endogenous peroxidase activity was blocked by immersing sections for 10 min in a solution of 3% hydrogen peroxide in water. Primary antibody was incubated overnight at 4°C. Specific biotinylated secondary antibody and avidin-biotin-peroxidase complex were consecutively applied, each for 1 h at room temperature. The immunohistochemical reaction was developed with diaminobenzidine–hydrogen peroxide reaction (Van Noorden et al., 1986). The sections were counterstained with hematoxylin. Neutrophil infiltration was evaluated only in whole well oriented sections of intestine, counting MPO^+ cells in four high-power fields (×400, diameter 0.55 mm) for each mucosal, sottomucosal, muscular, and serosal-sottoserosal layer. MPO value has been reported as the average of MPO^+ cells for field in each layer.

3.4 Quantification of HA levels in the submucosal and *muscularis propria* layers

3.4.1 Chromatographic assay

HA levels were measured in the submucosal and *muscularis propria* layers of DNBS-treated and control animals, following a modified protocol from Raio et al., 2005. 3 cm long colonic segments were cut along the longitudinal axis and opened flat on a sylgard support. After gently removing the mucosa layer, the submucosal layer was separated from the *muscularis propria* under a dissecting microscope. Samples of the submucosal and *muscularis propria* were then lyophilized. HA was purified and digested with hyaluronidase SD in order to obtain Δ disaccharides which were then derivatized with 2-aminoacridone (AMAC) according to Karousou et al., 2014. Separation and analysis of AMAC-derivatives of Δ-disaccharides were done with a Jasco-Borwin chromatograph system with a fluorophore detector (Jasco FP-920, λex = 442 nm and λem = 520 nm). Chromatography was carried out using a reversed phase column (C-18, 4.6 × 150 mm, Bischoff) at room temperature, equilibrated with 0.1 M ammonium acetate, pH 7.0, filtered through a 0.45 µm membrane filter. A gradient elution was done using a binary solvent system composed of 0.1 M ammonium acetate, pH 7.0 (eluent A), and acetonitrile (eluent B). The flow rate was 1 ml/ min, and the following program was used: pre-run of column with 100% eluent A for 20 min, isocratic elution with 100% eluent A for 5 min, gradient elution to 30% eluent B for 30 min and from 30% to 50% for 5 min. Sample peaks were identified and quantified comparing the fluorescence spectra with

standard Δ-disaccharides, using Jasco-Borwin software. Experiments were performed 4 times and HA levels were expressed as ng of HA per mg of dry tissue.

3.4.2 ELISA assay

In control, sham-operated and I/R groups, exposed or not to 4-MU treatment, the level of hyaluronic acid was evaluated in LMMP samples using Hyaluronan Quantikine ELISA Kit (R&D Systems, Minneapolis, MN, US), following the manufacturer's instructions. Before the assay, frozen tissues from 7 rats per group were lyophilized. A solution of PBS and Cell Lysis Buffer 2 (1:1) (R&D) was added and the samples were lysed over night at room temperature, with gentle agitation. The appropriate volumes of Lysis buffer were calculated suspending samples in 500µl of Cell Lysis Buffer 2 each 100 mg of fresh tissue. Debris were then removed by centrifugation and the supernatants were collected for the assay. The absorbance (Abs) values, recorded at the wavelength of 450nm, were corrected subtracting the Abs readings at 570nm. Experiments were performed 4 times and HA levels were expressed as ng of HA per mg of dry tissue.

3.5 Gastrointestinal transit

Gastrointestinal (GI) transit was measured by evaluating the intestinal distribution of orally gavaged fluorescein isothiocyanate (FITC)-labeled dextran (70 kDa, FD70) from the stomach to the colon. FITC-dextran, dissolved in 0.9% saline, were intragastric administered to I/R, sham-operated and CTR animals, and to the relative groups treated with 4-MU (200 µl of 6.25 mg/ml FITC-dextran solution for each rat). Animal were sacrificed 30 minutes after administration, and the entire GI tract was collected, divided into 15 segments: a single stomach segment (sto), 10 equal-length segments of small intestine (S1-S10), a single caecum segment (CEC), and 3 equal-length segments of colon (C1-C3). Luminal contents from each sample (both tissue and fecal content) were collected and clarified by centrifugation (12,000 rpm for 10 minutes). The cleared supernatants were assayed in duplicate for FD70 concentration, with a Krebs solution control and a FITC-dextran control (1:10 part dilution of FITC-dextran and Krebs solution respectively). The fluorescent signal was measured at 492/521 nm using a microplate reader (Infinite 200pro, TECAN). Data were expressed as percentage (%) of fluorescence for each segment and GI transit was calculated as the geometric center (GC) of distribution of the fluorescent marker using the following formula (Wehner et al., 2007):

$$GC = \Sigma \text{ (\% of total fluorescence signal per segment} * \text{segment number)}/100$$

3.6 *In vitro* contractility studies

Intestinal contractility was examined *in vitro* by measuring tension changes of small intestine samples from I/R, sham-operated and CTR animals, using the isolated organ bath technique. 1 cm segments of full-thickness rat small intestine were rapidly excised, washed with Krebs solution (composition in nM: NaCl 118, KCl 4,7, $CaCl_2 \cdot 2H_2O$ 2,5, $MgSO_4 \cdot 7H_2O$ 1,2, K_2HPO_4 1,2, $NaHCO_3$ 25, $C_6H_{12}O_6$ 11), mounted in isolated baths containing 10 ml of continuously oxygenated (95% O2 and 5% CO2) and heated (37°C) Krebs solution. Small intestinal segments were positioned along the longitudinal axis and connected, by means of a silk ligature, to an isometric transducer. Mechanical activity was recorded with a PowerLab acquisition data system (ADInstruments, UK) and elaborated with a LabChart 6.0 program (ADInstruments, UK). An initial load of 1 g was applied to each intestinal specimen. After 45 min equilibration, small intestinal segments were exposed to increasing concentrations (0.01-100 μM) of the muscarinic agonist, carbachol (CCh), to obtain concentration-response curves. Neuronal mediated contractions were obtained by Electric Field Stimulation (EFS, 0-40 Hz; 1-ms pulse duration, 10-s pulse train, 40 V) using platinum bipolar electrodes, attached to an S88 stimulator (Grass Instrument Co., Quincy, MA, USA), which were positioned in parallel to intestinal preparations in the isolated organ baths. Contractile responses were expressed as g tension/g dry tissue weight of small intestine segments. Concentration-response curves to CCh were subjected to a nonlinear regression analysis (fitted to a sigmoidal equation) to calculate the potency (EC50) and the maximum effect (Emax). EFS response curves in the different experimental conditions were analysed by two way ANOVA as described in the Statistical Analysis section. Relaxation responses were measured at the frequency of 10 Hz after an incubation period of 20 min with atropine 1 μM and guanethidine 1 μM, in order to evaluate non-adrenergic non-cholinergic transmission (NANC) neuromuscular responses. To evaluate the nitrergic component of the on-inhibitory NANC-mediated transmission, small intestine samples were incubated in NANC conditions, with 100 μM L-Nω-Nitroarginine methyl ester chloridrate (L-NAME, an non-selective NOS inhibitor), or 10 μM 1400W (a specific iNOS inhibitor), for additional 20 minutes before applying a 10 Hz EFS. Under NANC conditions, EFS induced a primary on-relaxation of small intestine segments that was calculated as the AUC and normalized per g dry tissue weight to allow comparisons between tissue samples.

3.7 RNA isolation and quantitative RT-PCR

Total RNA from LMMPs of small intestine and colon samples was extracted with TRIzol (Invitrogen) and treated with DNase I (DNase Free, Ambion), to remove possible traces of contaminating DNA. 2.5 μg of total RNA were then retrotranscribed using the High Capacity cDNA synthesis kit (Applied

Biosystems, ThermoScientific, Massachusetts, USA). Quantitative RT-PCR (qRT-PCR) was performed with an Abi Prism 7000 real-time thermocyclator (Applied Biosystems). TaqMan® Gene Expression Mastermix (Applied Biosystem) was used to detect HAS1 (Rn00597231_m1), HAS2 (Rn00565774_m1) and the housekeeping gene β-actin (Rn00667869_m1) mRNA levels, following the manufacturer's instructions. To evaluate the expression of HIF1α, TNFα, IL-1β, and IL-6 qRT-PCR was carried out with Power Sybr Green Universal PCR Master Mix (Applied Biosystems), as indicated by manufacturer's instructions. Primers were designed using Primer Express software (Applied Biosystems) on the basis of available sequences deposited in public database. Primer sequences were: HIF1α fw 5'- AAGCACTAGACAAAGCTCACCTG -3', rev 5'- TTGACCATATCGCTGTCCAC -3'; TNFα fw 5'- CCCAGACCCTCACACTCAGAT -3', rev 5'- TTGTCCCTTGAAGAGAACCTG -3'; IL-1β fw 5'- CCCTGCAGCTGGAGAGTGTGG -3', rev 5'- TGTGCTCTGCTTGAGAGGTGCT -3'; IL-6 fw 5'- GTGCAATGGCAATTCTGATTGTA -3', rev 5'- CTAGGGTTTCAGTATTGCTCTGA -3'; β-actin fw 5'- TGACAGGATGCAGAAGGAGA-3', rev 5'- TAGAGCCACCAATCCACACA-3'. Primers were designed to have a similar amplicon size and similar amplification efficiency, and were used at a final concentration of 500 nmol/L for each. The $2^{-\Delta\Delta Ct}$ method was applied to compare the relative gene expression. β-actin was used as housekeeping gene. Experiments were performed at least four times for each different preparation.

3.8 Western immunoblot analysis

To analyse HAS1 and HAS2 protein levels, small intestine LMMPs preparations were homogenized in ice cold isolation buffer [10 mM, Tris-acetate 5 mM, EDTA 1 mM, phenylmethylsulfonyl fluoride (PMSF) 10% protease inhibitor cocktail (Sigma Aldrich, Milan Italy) and 1% phosphatase inhibitor cocktail (Sigma Aldrich, Milan Italy), pH = 7.4]. The crude homogenate was centrifuged at 30 000g for 30 min at 4° C. The supernatant was collected, while the resulting pellet was re-suspended and incubated for 15 min at RT in a second buffer (Tris-HCl 20mM, NaCl 140 mM, pH 7.4, 10% protease inhibitor cocktail and 1% phosphatase inhibitor cocktail). Quantification of protein concentration in the supernatant and in pellet was performed by means of the micromethod of Bradford (1976). After protein quantification samples were diluted in Laemli sample buffer (Tris-HCl 300 mM, pH 6.8, glycerole 10%, SDS 2%, β-mercaptoethanol 0.04%). Sample aliquots were then boiled for 5 min at 95°C to mediate protein denaturation. Protein were separated on 8% SDS-polyacrylamide gel electrophoresis (SDS-PAGE) and electroblotted to PVDF membranes (Merck Millipore, Italy). Membranes were then incubated in a blocking solution consisting of 5% fat-free milk dissolved in PBS-Tween, 2 hours at room temperature in order to saturate aspecific sites. Membranes were incubated with primary antibodies against HAS1 and HAS2 overnight at 4 °C, followed by a second

incubation at room temperature with horseradish peroxidase (HRP)-linked appropriate secondary antibodies. Dilutions and reactivity of primary and secondary antisera are reported in table 3. The antibody/substrate complex was visualized by chemiluminescence (LiteAblot, Euroclone, Milan, Italy). In each membrane β-actin or α-tubulin were used as protein loading controls. Experiments were performed at least four times for each different preparation. Signal intensity was quantified by densitometric analysis using Image J NIH image software.

Table 3. Primary and secondary antisera and their respective dilutions used for western blot analysis.

Antiserum	Dilution	Source	Hosts species
Primary antisera			
HAS1	1:1000	Thermo Scientific (3E10)	Mouse
HAS2	1:1000	Santa Cruz (sc-34067)	Goat
β–actin	1:1000	Cell Signalling Technology (#3700)	Mouse
α–tubulin	1:1000	Cell Signalling Technology (#2125)	Rabbit
Secondary antisera			
Anti-goat IgG HRP-linked	1:20000	Santa Cruz (sc-2020)	Donkey
Anti-rabbit IgG HRP-linked	1: 10000	Santa Cruz (sc-2313)	Donkey
Anti-mouse HRP-linked	1:10000	Santa Cruz (sc-2314)	Donkey

3.9 Statistical analysis

All results are reported as mean ± standard error of the mean (SEM), except for the geometric center, which is presented as median and range (minimum-maximum), of at least 4 experiments. Statistical significance was calculated with the unpaired Student's *t* test (when comparing two groups of data) or, when comparing three or more groups of data, analysis of variance with one-way ANOVA, followed by Tukey's post-hoc test for multiple variables or two-way ANOVA, where appropriate. Differences were considered statistically significant when *P* values were <0.05. GraphPad Prism software (GraphPad 5.03 Software Inc, La Jolla, USA) was used for statistical analysis.

4 RESULTS

4.1 HA and DNBS induced colitis

4.1.1 Assessment of colitis

4.1.1.1 Macroscopic assessment

Six days after intracolonic administration of DNBS, body weight of rats was significantly reduced with respect to non-inflamed controls (Figure 6 A). Bowel of DNBS-treated animals was dilated at intervals and distal colon appeared thickened and ulcerated with evident regions of transmural inflammation. A twenty-fold increase of macroscopic damage score was observed in comparison with controls (Figure 6 B) and adhesions between the colon and other intra-abdominal organs were present (Figure 6 C). Faecal consistency did not significantly change between the two groups (Figure 6 D).

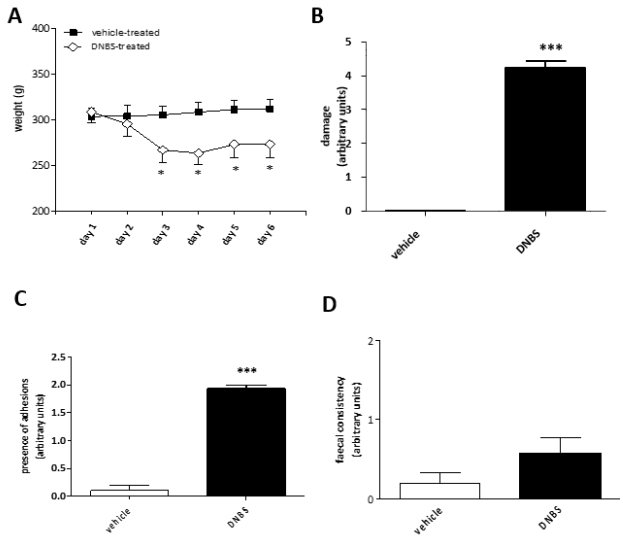

Figure 6. (A) Body weight change in control (vehicle treated) and DNBS-treated animals, **(B)** macroscopic damage expressed in arbitrary units obtained from DNBS-treated (solid bar) and control s (empty bar), **(C)** presence of adhesions in colonic specimens, and **(D)** faecal consistency. Data are expressed as mean ± S.E.M. n=7 rats per group. * P<0.05 by one way ANOVA with Tukey's post hoc test and *** P<0.001 by Student's t test vs control.

4.1.1.2 Histological assessment

Distal colonic cross-sections of control animals showed normal morphology features: a compact epithelium and well-formed crypts, an underlying thin layer composed of smooth muscle cells (the *muscularis mucosae*), a submucosal layer containing vascularized loose connective tissue and ganglia of the submucosal plexus, and a thick external smooth muscle layer of the *muscularis propria* (Figure 7A). Myenteric ganglia between the circular and longitudinal muscle of the

muscularis propria were compact and composed by healthy neurons and glial cells (Figure 7 C). CD45 staining, indicative of inflammatory cell infiltration, was almost negligible in the colon of control cross sections (Figure 7 E).

In contrast, both the colonic mucosa and serosal epithelium of DNBS-treated rats displayed morphological abnormalities (Figure 7 B). The mucosal surface was irregular and the crypt architecture was highly altered. The thickness of submucosa and *muscularis propria* layers increased showing prominent leukocyte infiltration as demonstrated by a significant enhancement of CD45 staining (Figure 7 F). Important degenerative changes were also observed in myenteric ganglia, where dots-like structures in the nucleus, cytoplasmic vacuolization and irregular nuclear and cellular membranes were observed. Large spaces between muscle cells were also evident (Figure 7 D).

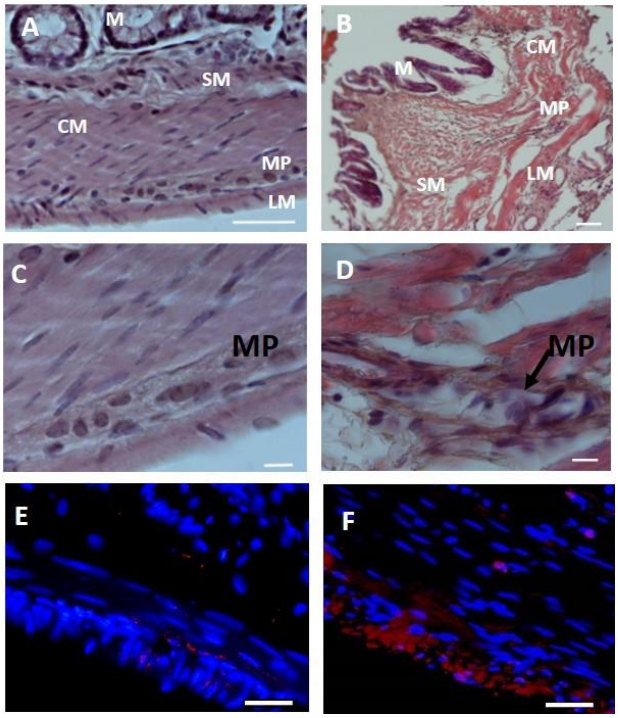

Figure 7. (A-B) Hematoxilin-eosin (HE) staining representing the morphology in (A) control and (B) DNBS-treated cross section preparations (bars 50 µm and 100 µm). **(C-D)** details of the myenteric plexus in a cross-section obtained from (C) control rat colon and (D) DNBS-treated animals (bar 10 µm). Arrow indicates cytoplasmic vacuolization and irregular nuclear and cellular membranes. (**E**) In the distal colon of CTR animals, CD45 staining, as an index of inflammatory infiltrate, was slight, and significantly after DNBS treatment (**F**) (bars: 10 µm). **M**, mucosa; **SM**, submucosa; **CM**, circular muscle; **LM**, longitudinal muscle; **MP**, myenteric plexus.

In agreement with data obtained with cross-sections of DNBS-treated rat colon (Ippolito et al., 2015), in colonic whole-mount preparation, DNBS-induced inflammation was associated with a decrease in the total number of myenteric neurons, which displayed a reduced soma area compared to control samples (Figure 8 A-B). After DNBS treatment, HuC/D immunoreactivity was faint in the cytoplasm of the majority of myenteric neurons, and a number of neurons showed

increased HuC/D staining in the nucleus relative to the cytoplasm (Figure 8 C-D).

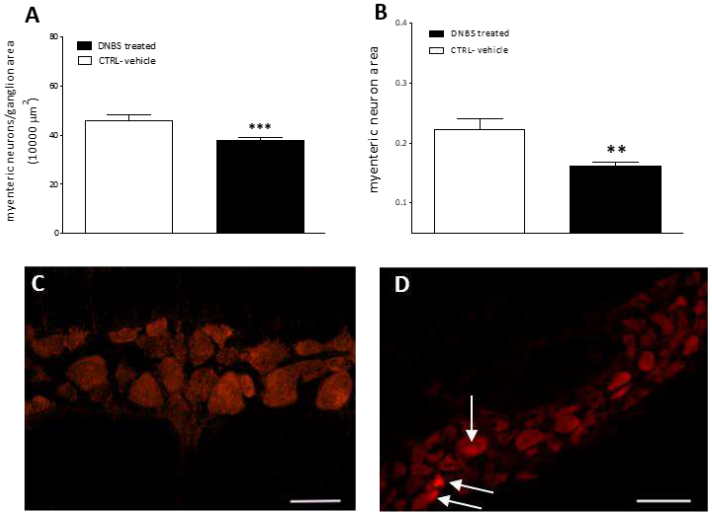

Figure 8. DNBS-treatment induced changes in myenteric neurons. (A) Myenteric neuron number normalized per ganglion area calculated in colonic whole-mounts obtained from DNBS-treated (solid bar) and control animals (empty bar). **(B)** Mean myenteric neuron area calculated in colonic whole-mounts obtained from DNBS-treated (solid bar) and control animals (empty bar). Values are expressed as mean±SEM N=5 rats/group. ***P*<0.01 and ****P*<0.01 *vs* values obtained in vehicle-treated control animals by Student's t test. **(C-D)** HuC/D staining of myenteric neurons in CTR and DNBS-treated colonic whole-mount LMMP preparations. Arrows indicate HuC/D translocation in myenteric neurons after DNBS-induced colitis (bar: 50mm)

4.1.1.3 Biomolecular assessment

In DNBS-treated animals, a significant enhancement in the expression of inflammatory cytokines such as TNFα, IL-1β, and IL-6 was evidenced with respect to control rats (Figure 9 A). Furthermore, myeloperoxidase (MPO) activity significantly increased in mucosa-deprived rat colonic segments from DNBS-treated animals compared to controls, suggesting the occurrence of inflammation-induced massive neutrophil infiltration into the intestinal wall (Figure 9 B).

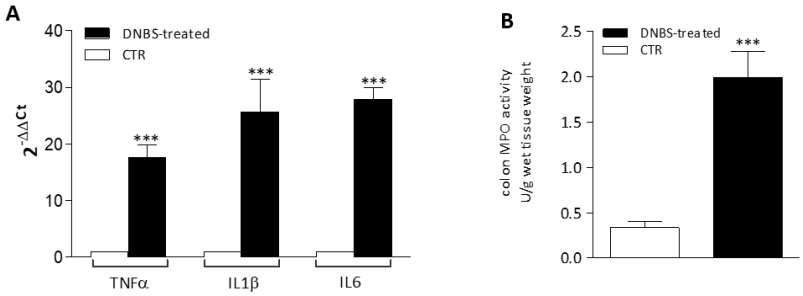

Figure 9. (A). **Expression of inflammatory markers in the rat colon after DNBS-induced colitis. (A)** qRT-PCR quantification of TNFα, IL1-β and IL-6 mRNA levels obtained in the distal colon of control animals (CTR, empty bars) and after DNBS treatment (solid bars). Values are mean±S.E.M. N=5 rats/group. ***p<0.001 vs values obtained in CTR animals; Significance was evaluated by Student's t test. **(B)** Values are mean±S.E.M. N=5 rats/group. ***p<0.001 vs values obtained in CTR animals; Significance was evaluated by Student's t test.

4.1.2 Localization of HA in the rat colon myenteric plexus

Control colonic cross-sections revealed a regular distribution of HA in the epithelial crypts, the underlying submucosal and *muscularis propria* layer with myenteric plexus, as indicated by HA binding protein (HABP) staining (Figure 10 A). In longitudinal muscle myenteric plexus (LMMP) whole mount preparations, HA staining was particularly intense on the surface of myenteric ganglia and along the interconnecting fibre strands (Figure 10 B and 11 A).

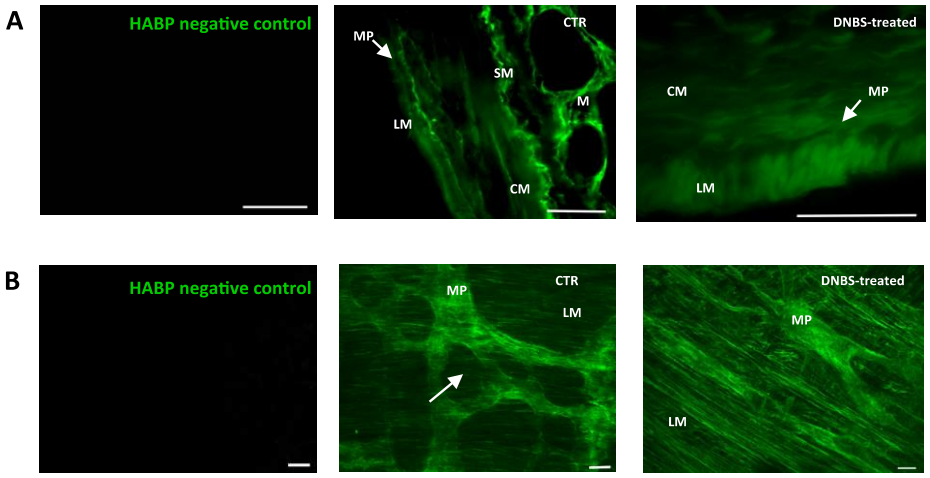

Figure 10. HA staining in rat colon after DNBS treatment. (A) HABP staining in rat colon cross-sections obtained from control (vehicle-treated animals), DNBS-treated animals, and relative negative control (bar 50 µm). **(B)** HABP staining in rat colon LMMP whole-mount preparations from control and DNBS-treated animals and relative negative control, bar 50 µm. **M**, mucosa; **SM**, submucosa; **CM**, circular muscle; **LM**, longitudinal muscle; **MP**, myenteric plexus. HABP staining in myenteric plexus fiber strands (arrow)

In addition, a faint HA labeling was found in myenteric neuron cytoplasm, as demonstrated by co-staining with the neuronal marker HuC/D. A more intense and organised HA signal was detected in the perineuronal space surrounding neurons as well. (Figure 11 A-F). The ability of HABP to label myenteric neurons suggests that, in the myenteric plexus, neuronal cells may represent a source for HA. To evaluate this hypothesis, HABP binding was performed on primary cultures of small intestine myenteric ganglia. As result, the HuC/D co-staining showed an intense HA staining on the soma of some neurons (Figure 11 J-L).

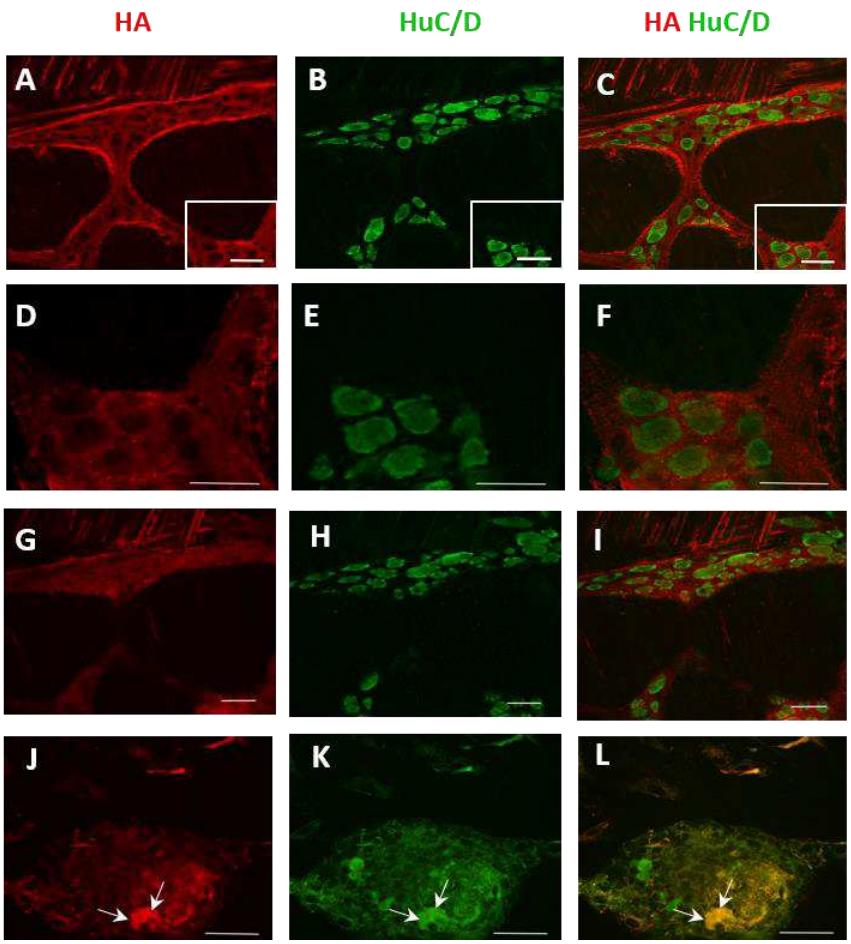

Figure 11. Co-localization of HA in control rat intestine. (A-C) Confocal images showing co-localization of HABP with HuC/D in a colonic whole-mount median section showing a myenteric ganglion. HABP immunofluorescence was prevalently found in neuronal soma and in the perineuronal space (insets, panels D-F). **(G-I)** HABP intensely stained the surface of the same ganglion and (A) interconecting fibers (*). **(J-L)** Confocal image of a rat small intestine myenteric ganglion culture double-stained with HABP and HuC/D. Arrows indicate neurons displaying high HA staining. Bar 50 μm.

4.1.3 HA levels are upregulated after DNBS-induced colitis

After DNBS treatment, HA levels significantly increased in both the *muscularis propria* and submucosal layers versus values obtained in control preparations (Figure 12). Accordingly, an increased HABP staining was observed both in colonic cross-sections and LMMPs compared to controls (Figure 10 A-B).

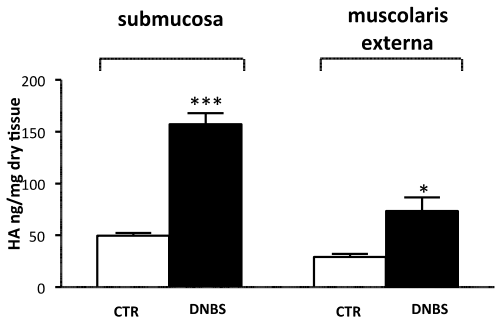

Figure 12. HA levels in rat colon after DNBS treatment. HA levels measured in colonic submucosal and muscularis externa layers from control (empty bars) and DNBS-treated animals (solid bars). Values are expressed as mean±S.E.M. N=5 rats/group. *P<0.05 and ***P<0.001 vs control animals by Student's t test.

In preparations obtained from DNBS-treated animals, the structured HA distribution within myenteric ganglia disappeared, and, in particular, perineuronal HA was less evident. HA labeling remains visible in the cytoplasm of myenteric neurons, on ganglia surface and along interconnecting fibers (Figure 10 A-B, Figure 13 A-H).

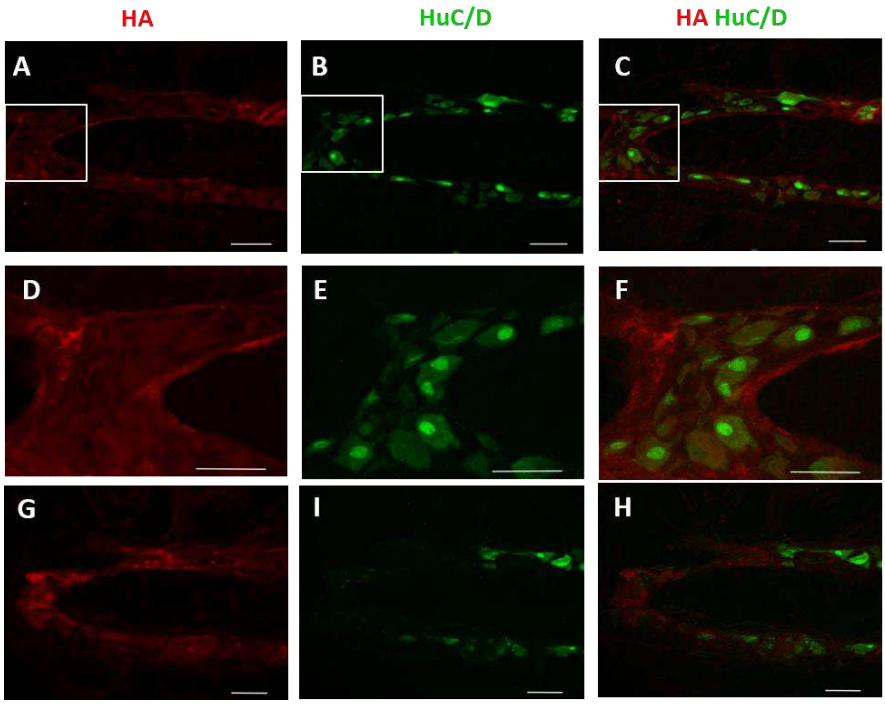

Figure 13. Co-localization of HABP with HuC/D in whole-mount preparations of the rat colon after DNBS-treatment. (**A-C)** Confocal image showing co-localization of HABP with HuC/D in a median section of a myenteric ganglion. HABP immunofluorescence was prevalently present in the soma of myenteric neurons, perineuronal staining was absent (insets, **D-F**). Several neurons displayed a prominent HuC/D staining in the nucleus and faint cytoplasmic HuC/D immunoreactivity. (**G-H**) HABP staining the surface of the same ganglion. Bar 50 μm.

4.1.4 Expression of HAS2 in myenteric neuron after DNBS-induced treatment

Colonic whole-mount preparations of control animals revealed the presence of HAS2 in myenteric plexus. When double labeled with HABP or HuC/D, HAS2 was discontinuously localized in the cytoplasm of a small percentage of myenteric neurons (figure 14 B-D, I-K).

qRT-PCR and western blot investigations confirmed the presence of both transcript and protein of HAS2 in the colon of control rats (Figure 15 B-C).

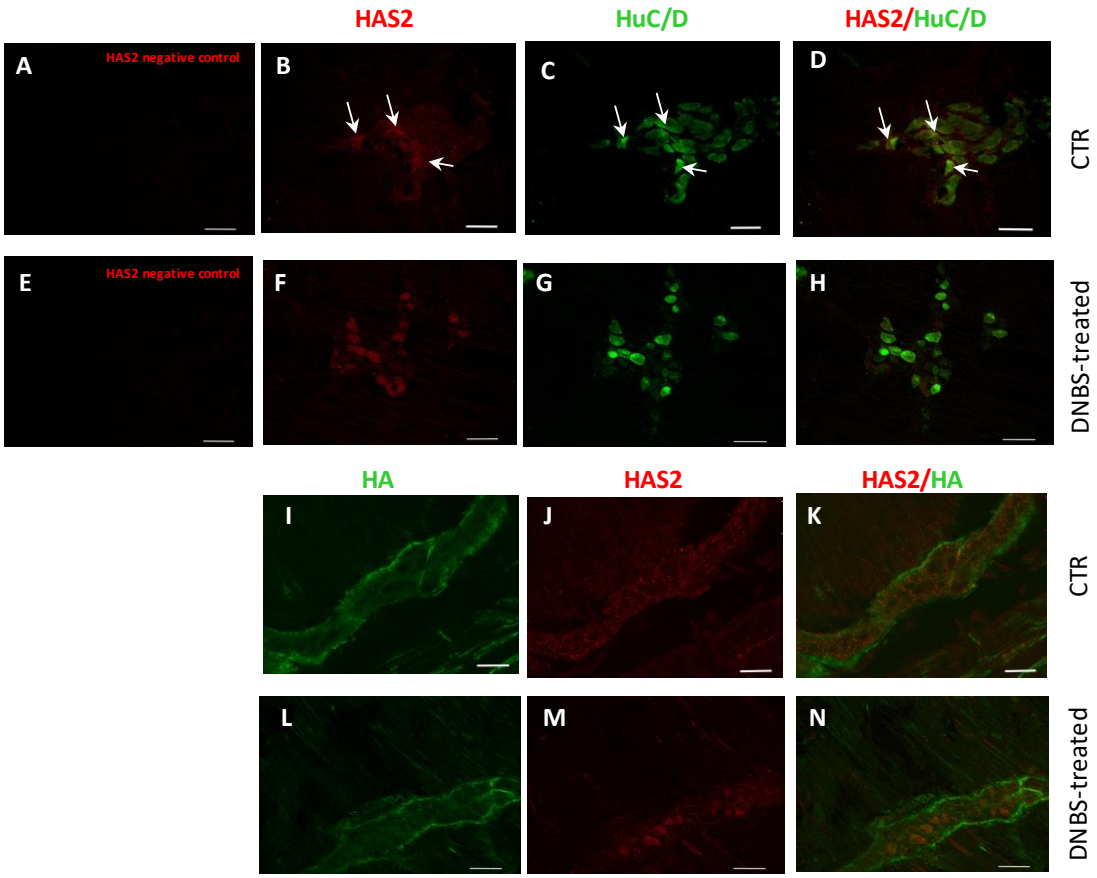

Figure 14. HAS2 and HuC/D co-localization in the rat colon myenteric plexus of control and DNBS-treated animals. (A-H) Confocal images showing co-localization of HAS2 with HuC/D in LMMP whole-mount preparations obtained from in control (vehicle treated) (**B-D**) and after DNBS-treatment (**F-H**). HAS2 and HABP co-localization in the rat colon myenteric plexus of control and DNBS-treated animals. (**I-N**) Co-localization of HAS2 with HABP in LMMP whole-mount preparations of control (**I-K**) and DNBS-treated animals (**L-N**). Panels **A** and **E** show negative controls for HAS2 staining in control and DNBS-treated preparations, respectively. Bar 50 μm.

After DNBS-induced colitis, the number of HAS2 immunopositive myenteric neurons significantly increased in treated animals with respect to control values (Figure 14 F-H; Figure 15 A). In myenteric ganglia obtained from DNBS-treated rats, HAS2 staining around the neuronal profile was less evident than in controls (Figure 14 L-N). In addition, both HAS2 transcript and protein were significantly higher compared to control animals (Figure 15 B-C). In LMMP preparations obtained from control rats, HAS2 specific antibody revealed one band at 63 kDa, while a double band could

be observed at 63 kDa in preparations obtained from DNBS-treated mice, which may result from post-translational modifications of the protein induced by inflammation (Vigetti et al., 2014).

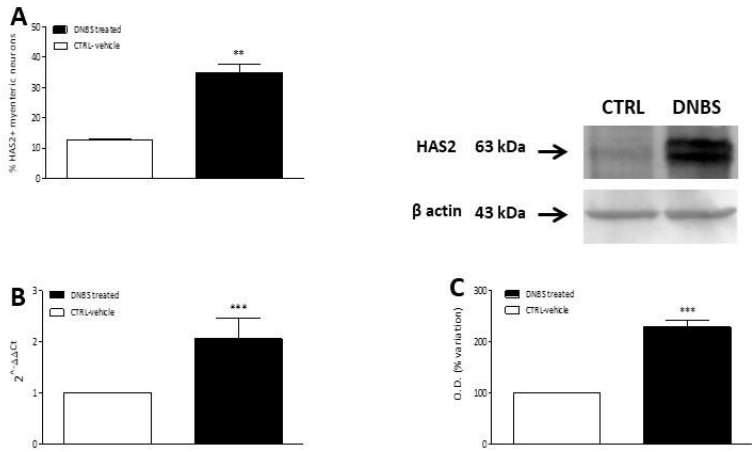

Figure 15. HAS2 expression in myenteric ganglia. **(A)** Percentage of myenteric neurons per mm^2 co-staining for HuC/D and HAS2 from control (empty bars) and DNBS-treated animals (solid bars). Values are expressed as mean±S.E.MN=5 rats/group. **(B)** qRT-PCR quantification of HAS2 transcripts in control and in DNBS-treated animals. Values are mean±S.E.M. N= 5 rats/group. The relative gene expression was determined by comparing $2^{-\Delta\Delta Ct}$ values normalized to β-actin. **(C)** HAS2 protein expression analyzed in LMMPs obtained from control and DNBS-treated animals. Values are expressed as mean±S.E.M. of the percentage variation of the normalized optical density (O.D.). N=5 rats/group. obtained from DNBS-treated preparations with respect to values obtained in control samples. **P<0.01 and ***P<0.001 vs control animals by Student's t test.

4.2 Role of HA in the adaptive changes of the intestinal neuromuscular function after an I/R injury in the rat small intestine

4.2.1 Histological assessment

After occlusion of the terminal branch of the superior mesenteric artery, the corresponding small intestinal segment became purple and returned to a normal pink color after blood flow restoration. Animal recovered uneventfully from anesthesia and once awake were active, ate normally and did not show any sign of distress. A gross visual inspection of the regions subjected to I/R did not reveal any abnormality with respect to sham-operated and un-operated control animals at all times. Administration of 4-MU, 25 mg/kg, did not induce significant gross morphology changes in small intestinal segments obtained from animals subjected to I/R injury, sham-operated and controls, versus the respective untreated groups. However, in all experimental groups, after 4-MU treatment intestinal segments and mesenteric attachments were loser compared to the untreated groups. After 24 hours of reperfusion following ischemia, myenteric neurons both in the submucosal and myenteric plexus showed signs of cellular suffering, displaying swollen soma, cytoplasm vacuolization and ill-defined cellular membrane with respect to control preparations (Figure 16

A,C). Nuclear inclusions were sometimes present. The smooth muscle layer was also altered by the I/R injury, with cytoplasmic vacuolization and spaces between cells in some regions of *muscularis propria* with respect to control preparations (Figure 16 A,C). Mucosa and serosal epithelium did not display prominent histological abnormalities. In sham-operated samples, histological features of neurons or muscle cell cellular suffering were rarely observed. In control and sham-operated groups, 4-MU treatment did not modify the architecture of myenteric neurons. In the I/R group, after 4-MU treatment, cytoplasmic vacuolization and spaces were still visible in some regions of the *muscularis propria* and within the myenteric plexus, in addition, myenteric neurons displayed signs of nuclear suffering and cellular shrinking, although to a minor extent, than in the I/R untreated group. (Figure 16 C,D).

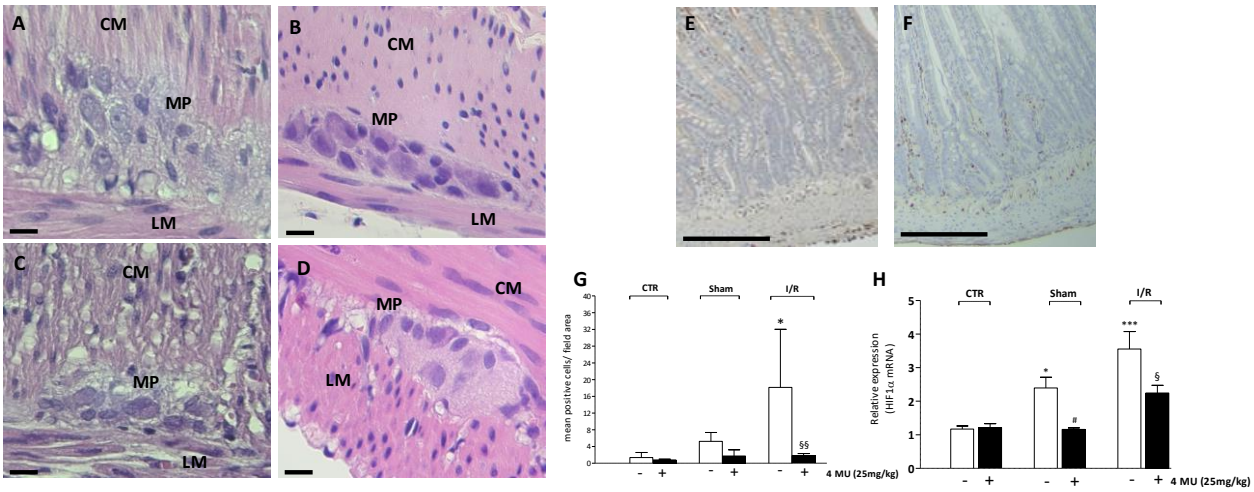

Figure 16. (A-D) smooth muscle cells in the circular (CM) and longitudinal (LM) layers and myenteric plexus (MP) of CTR (A), CTR 4-MU treated (B), I/R (C) and I/R 4-MU treated (D) rat small intestine (HE, original magnification 600x; bar: 0.01mm). **(E,F)** MPO immunohistochemical staining of whole wall rat small intestine obtained from I/R and 4-MU treated I/R animals. Neutrophils are well marked (brown) and their count is easy for all the layers. **(G)** Neutrophil infiltrate in the intestinal wall in the different experimental groups, expressed as number of neutrophils in the rat small intestine *muscularis propria*. Values are expressed as mean±SD of neutrophil count. P<0.05 vs CTR and P<0.01 vs I/R by one way ANOVA followed by Tukey's test. N=5 rats/group. **(H)** RT-PCR quantification of HIF1α in rat small intestine LMMPs in the different experimental groups. Values are expressed as means±SEM. N=5 rats/group. **P*<0.05, ****P*<0.001 by one way ANOVA followed by Tukey's test vs CTR; #P<0.05 vs Sham; §P<0.05 vs I/R. Relative gene expression was determined by comparing $2^{-\Delta\Delta Ct}$ values normalized to β-actin.

4.2.2 Neutrophil infiltration, myeloperoxidase activity and HIF-1α levels

In the *muscularis propria* a significant increase in the number of neutrophil cells per field was observed after 24 hours of reperfusion with respect to control preparations (Figure 16 E-G). Also in the sham-operated group, the number of neutrophils increased, but not significantly, with respect to controls (Fig 16 G). After 4-MU treatment, the number of neutrophils in the *muscularis propria* of the I/R and sham-operated groups was significantly reduced, reaching values not significantly different with respect to controls (Figure 16 G). In small intestine LMMPs obtained from the sham-

operated and I/R groups, the expression of HIF-1α mRNA significantly increased with respect to CTR preparations. After 4-MU treatment, HIF-1α mRNA levels were significantly reduced in both the sham-operated and I/R group, reaching values not significantly different compared to controls (Figure 16 H).

4.2.3 In vivo 4-MU treatment regulates HA levels in rat small intestine LMMPs after I/R injury

In LMMP whole-mount preparations of control animals, HA staining was detected on the surface of myenteric ganglia and along interconnecting fiber strands (Figure 17 A). In addition, a faint HA labeling was found in myenteric neuron cytoplasm and in the perineuronal space, as demonstrated by co-staining with the pan neuronal marker HuC/D (Figure 17 B,D). After 4-MU treatment, HA labelling in myenteric ganglia was fainter, as suggested by a decrease, although not significant, in the density index (Figure 17 M). The intensity and distribution of HA staining in the myenteric plexus of sham-operated animals was not significantly different with respect to control preparations and was only slightly reduced after 4-MU treatment (Figure 17 M). In good agreement with HABP staining, HA levels measured by ELISA assay in LMMP preparations obtained from sham-operated animals were not significantly different from those obtained in control preparations, both with and without 4-MU treatment (Figure 17 N).

After I/R injury, HA density index significantly increased with respect to control and sham-operated groups, as shown in panels E, F and M of Figure 17. Accordingly, ELISA assay revealed a significant increase of the GAG levels in LMMP preparations obtained from the I/R group versus control and sham-operated groups (Figure 17, panel N). After I/R injury HA staining in myenteric neuron cytoplasm and in perineuronal space was conserved and displayed higher intensity with respect to controls (Figure 17 F,H). HA labelling in LMMP preparations obtained from 4-MU-treated rats subjected to I/R injury was faint and the density index was significantly reduced with respect to the I/R group, reaching values not significantly different from those obtained in control and sham-operated animals (Figure 17, I-L, M). HA levels in the I/R 4-MU treated group remained significantly elevated with respect to controls and sham-operated groups, but were reduced with respect to the untreated I/R group (Figure 17 N).

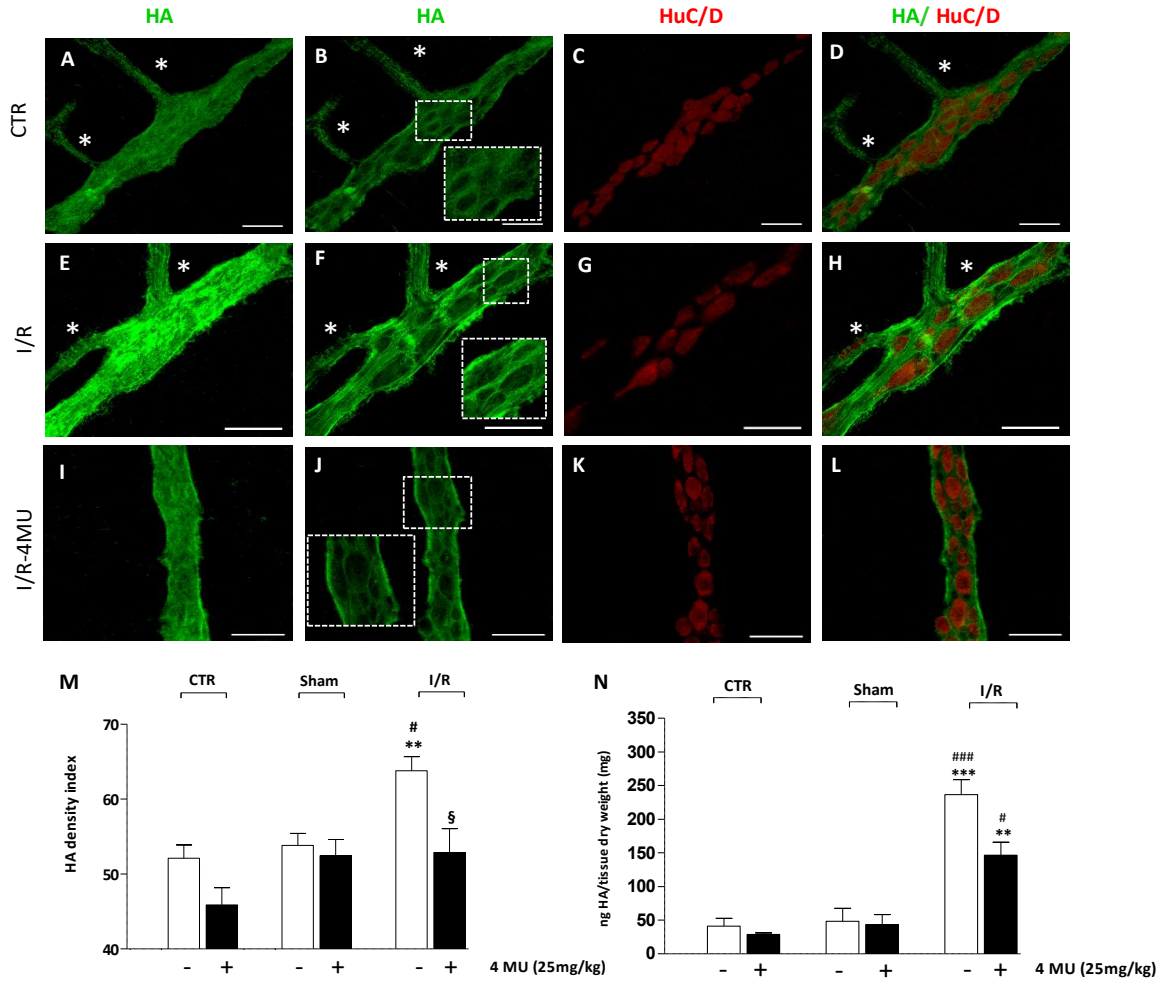

Figure 17. In vivo 4-MU treatment regulates HA levels in rat small intestine LMMPs after I/R injury. (A-L) Representative confocal microphotographs showing HA staining of the rat small intestine myenteric plexus in control conditions (CTR, A-D), after ischemia followed by 24 hours of reperfusion (I/R, E-H) and in the I/R group treated with 4-methylumbelliferone (4-MU, 25 mg/kg, ip) (I-L). In all groups, HA intensely stained the surface of the myenteric ganglia and interconnecting fibers (*) (panels A,E,I) . In confocal median sections of myenteric ganglia, HA immunofluorescence was prevalently found in neuronal soma and in the perineuronal space (insets, panels B,F,J), as demonstrated by double-staining with the pan-neuronal marker, HuC/D. Bar 50 μm. (M) HA density index of HA in LMMP preparations obtained the different experimental groups with and without treatment of 4-MU, as indicated on bottom of bars. Data are reported as mean ± SEM. **P<0.001 vs CTR, P<0.05 vs sham-operated, P<0.05 vs I/R by one-way ANOVA with Tukey's post hoc test, N=5 rat/group. (N) Quantification of HA levels by ELISA assay in small intestine LMMP preparations obtained from the different experimental groups with and without treatment of 4-MU, as indicated on bottom of bars. HA levels are expressed as ng of HA normalized per mg of dry tissue weight. ***P<0.001 and **P<0.01 vs CTR; ###P<0.001 and P<0.05 vs sham-operated by one-way ANOVA with Tukey's post hoc test, N=6 rat/group.

4.2.4 Influence of 4-MU treatment on I/R induced changes of HAS1 and HAS2 expression in rat small intestine myenteric plexus

Immunohistochemical experiments revealed the presence of HAS1 in rat small intestine myenteric ganglia and along interconnecting fibers (Figure 18 A-F). HAS1 staining was detected in the cytoplasm and cytosolic membrane of with large-, medium- and small-sized ovoid neurons. Intense HAS1 labelling was also found in enteric glial cells surrounding myenteric ganglia (Figure 18 A,C). In

LMMP preparations obtained from the I/R group, the number of HAS1^{+} myenteric neurons was significantly higher than in the control and sham-operated groups (Figure 18 G). Such enhancement was reduced after 4-MU treatment as, in this condition, the number of HAS1^{+} myenteric neurons diminished with respect to the I/R group, remaining significantly higher versus controls but not versus sham-operated animals (Figure 18 G). In the sham-operated and I/R groups, HAS1 mRNA levels significantly increased with respect to control preparations (Figure 18 H). In the I/R group, HAS1 mRNA levels were also significantly higher than in preparations obtained from sham-operated animals. In the sham-operated group after 4-MU treatment, HAS1 mRNA levels were still significantly higher with respect to controls and similar to those obtained in the respective untreated groups. In the I/R group after 4-MU treatment, HAS1 mRNA levels were significantly higher with respect to controls, but not versus the sham-operated group, and were slightly, but not significantly, reduced with respect to the I/R untreated group (Figure 18 H).

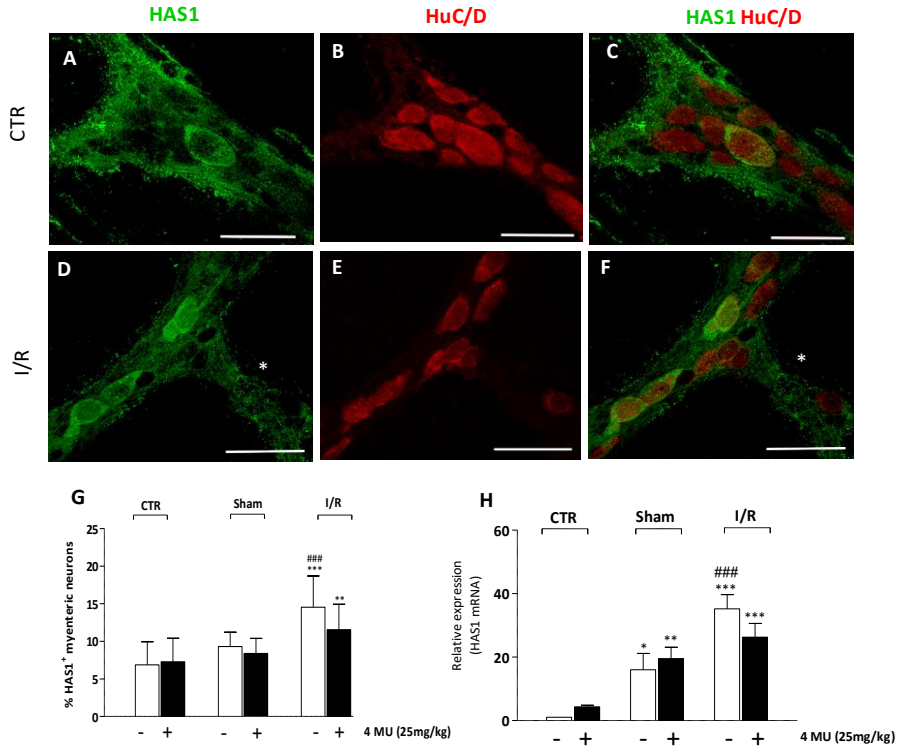

Figure 18. Enhancement of HAS1 expression in the rat small intestine myenteric plexus is regulated by 4-MU treatment. (A-F) Confocal images showing co-localization of HAS1 with the pan neuronal marker HuC/D in myenteric neurons of CTR animals (A-C) and after I/R injury (D-F). HAS1 stained the soma and cytoplasmic membranes of ovoid myenteric neurons, interconnecting fibers (*) and enteric glial cells (arrow). Panel **G** shows the percentage of myenteric neurons co-staining for HuC/D and HAS1. Bar 50 μm. **P<0.01, ***P<0.001 vs CTR, ###P<0.001 vs sham-operated by one-way ANOVA with Tukey's post hoc test. N=5 rat/group **(H)** HAS1 mRNA levels in LMMP preparations obtained from the different experimental groups. Histograms show HAS1 relative gene expression determined by comparing $2^{-\Delta\Delta Ct}$ values normalized to β-actin. *P<0.05, **P<0.01, ***P<0.001 vs CTR, ###P<0.001 vs sham-operated by one-way ANOVA with Tukey's post hoc test. N=5 rat/group.

HAS2 immunoreactivity was immunohistochemically found in the cytoplasm, nuclear and cytosolic membranes of few medium-sized ovoid neurons of control rat small intestine myenteric plexus

(Figure 19 A-C). The number of HAS2^{+} myenteric neurons significantly increased with respect to sham-operated and control animals after ischemia followed by 24 hours of reperfusion (Figure 19 D-F,G). In this latter condition, 4-MU treatment induced a reduction of the number of HAS2^{+} myenteric neurons, which, however, remained significantly higher than in controls and sham-operated animals (Figure 19 G). In LMMP preparations obtained from animals undergoing I/R, HAS2 mRNA levels significantly increased with respect to both control and sham-operated preparations (Figure 19 H). 4-MU treatment did not modify HAS2 mRNA expression in both control and sham-operated preparations. In the I/R group, 4-MU treatment significantly reduced I/R-induced enhancement of HAS2 transcripts with respect to the untreated animals, reaching values not significantly different versus those obtained in control and sham-operated rats (Figure 19 H). HAS3 mRNA levels were not measurable by qRT-PCR in LMMPs of all experimental groups.

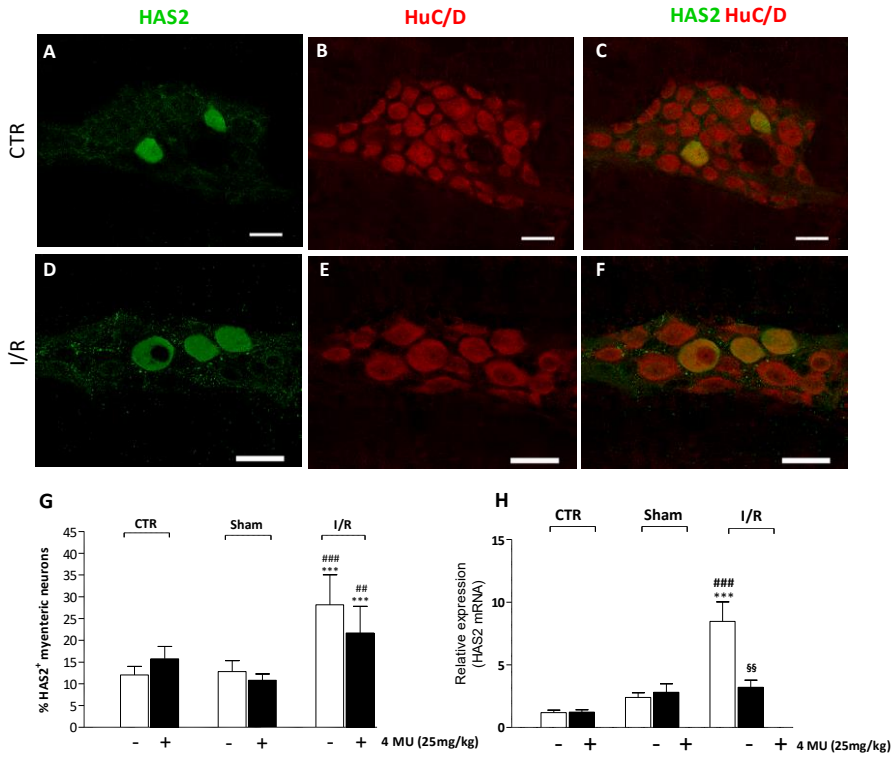

Figure 19. Enhancement of HAS2 expression in the rat small intestine myenteric plexus is regulated by 4-MU treatment. (A-F) Confocal images showing co-localization of HAS2 with HuC/D in myenteric neurons of CTR animals (A-C) and after I/R injury (D-F). HAS2 stained the soma of ovoid myenteric neurons. Panel G shows the percentage of myenteric neurons co-staining for HuC/D and HAS2. Bar 50 μm. ***P<0.001 vs CTR, ###P<0.001 vs sham-operated by one-way ANOVA with Tukey's post hoc test. N= 5 rat/group. (H) mRNA levels of HAS2 in LMMP preparations obtained from the different experimental groups. Histograms show HAS2 relative gene expression determined by comparing $2^{-\Delta\Delta Ct}$ values normalized to β-actin. ***P<0.001 vs CTR, ###P<0.001 vs sham-operated, §§P<0,01 vs I/R by one-way ANOVA with Tukey's post hoc test. N=5 rat/group.

4.2.5 Efficiency of the gastrointestinal transit after I/R injury with and without 4-MU treatment

After 24h I/R injury, the GI transit significantly decreased, as shown by the higher content of non-absorbable FITC-labelled dextran in the upper part of the GI tract (Figure 20 A). Accordingly, I/R injury induced a significant reduction of the geometric center (GC) compared with that of control and sham-operated animals. In sham-operated animals, the GC was not significantly different from the value obtained in control animals. 4-MU treatment did not significantly modify both the efficiency of the GI transit and the value of the GC in control and sham-operated groups. In the I/R group, treatment with 4-MU, induced a significant reduction of the GC with respect to both control and sham-operated untreated animals (Figure 20 B). In addition, in the I/R, 4-MU treatment induced a significant delay in gastric emptying with respect to both control and sham-operated untreated groups (Figure 20 C).

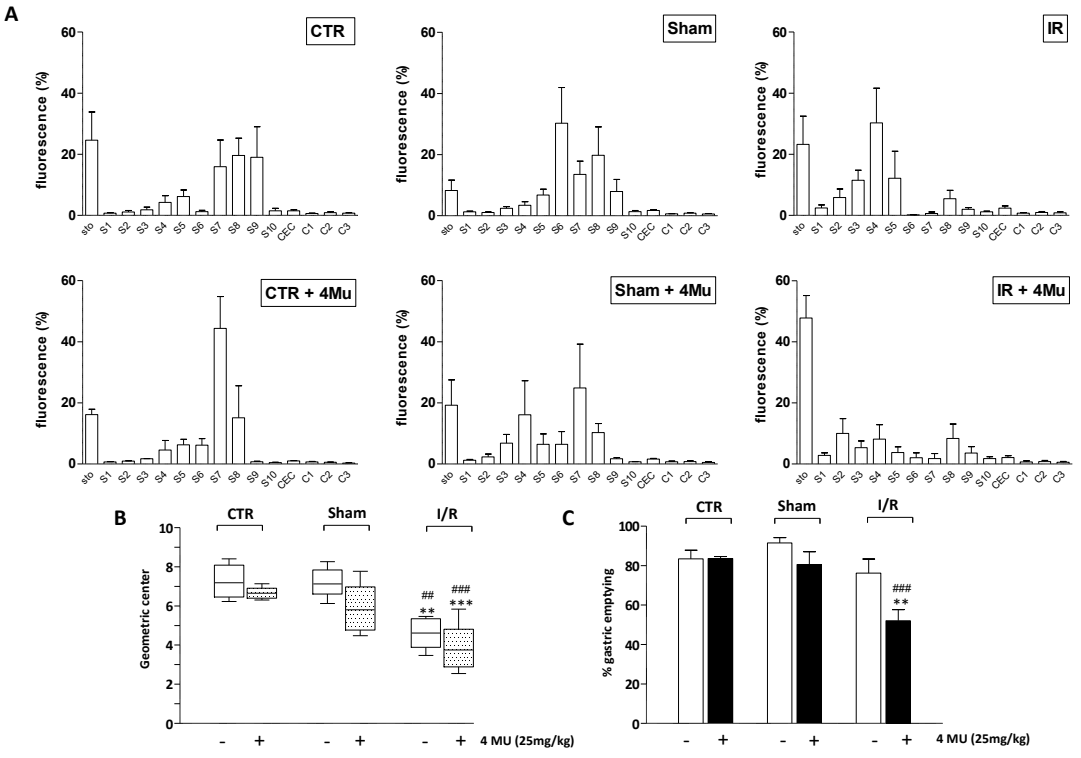

Fig 20. 4-MU treatment affects G/I transit and gastric emptying after I/R injury in the rat. (A) Percentage of non-absorbable FITC-dextran distribution along the gastrointestinal (GI) consisting of stomach (Sto), small bowel (Sb 1–10), caecum (Cec) and colon (C 1–3); **(B)** geometric centre (GC) of non-absorbable FITC-dextran distribution; **(C)** Percentage of gastric emptying in the different experimental groups. Data are reported as mean ± SEM for panels (A) and (C) and as median, minimum, maximum, upper and lower quartiles for panel (B). **P< 0.01 and ***P<0.001 vs CTR, ##P<0.01 and ###P<0.001 vs sham-operated and by one-way ANOVA with Tukey's post hoc test. N=5 rat/group.

4.2.6 I/R injury alters excitatory neuromuscular contractility: effect of 4-MU treatment

The effects of I/R injury on the rat small intestine neuromuscular function were examined *in vitro* by measuring tension changes of the longitudinal muscle contractile activity, which underlies the preparative phase of the peristaltic reflex and is synchronous with circular muscle contraction during peristalsis, thus influencing the whole propulsive bowel activity (Smith and Robertson, 1998). In all experimental groups, small intestine segments displayed spontaneous contractile activity consisting of phasic contractions, displaying a significantly reduced amplitude (tension) in the sham-operated and I/R groups with respect to control animals (Table 4). In all experimental groups, 4-MU treatment did not modify the amplitude of spontaneous contractions, which remained significantly lower in the sham-operated and I/R treated groups with respect to the control untreated group (Table 4). The frequency of spontaneous basal contraction was similar in all experimental groups (Table 4).

Table 4. Basal spontaneous contractile activity of small intestine from all experimental groups (*P<0.05 and **P<0.01 vs CTR by one way ANOVA with Tukey's post hoc test).

Experimental group	***Frequency (cicle/min)***	***Basal Tension (g)***
CTR	17,79 ± 0,408	10,43 ± 0,920
CTR 4-MU	17 ± 0,564	10,47 ± 1,305
sham	16,75 ± 0,509	7,09 ± 0,740 **
sham 4-MU	16,83 0,458	7,13 ± 0,592 **
I/R	18,45 ±0,511	7,56 ± 0,834 *
I/R 4-MU	17,71 ± 0,45	6,67 ± 0,774 **

To evaluate changes in the excitatory neuromuscular response, cumulative concentration–response curves to the non-selective cholinergic agonist, carbachol (CCh), were performed on the longitudinally oriented small intestine segments from all experimental groups. I/R induced a significant downward shift of the concentration–response curve to CCh with a decrease in maximum response (Emax) with respect to values obtained in control and sham-operated. In the sham-operated group the contractile response curve to CCh was superimposable with the response observed in the control group (Figure 21, A). In the control group, 4-MU treatment induced a significant increase in the Emax with respect to the value obtained in untreated controls (Figure 21 A). The concentration-response curves to CCh were not significantly modified both in the sham-operated and in the I/R group after 4-MU treatment (Figure 21 A). The potency of CCh in inducing concentration-dependent contractile responses in the control group was [0.17 (0.10-0.28) µM, n=5)], and was not significantly different from those observed in the other experimental groups [CTR-4MU: 0.34 (0.25-0.46) µM, n=5; sham-operated: 0.20 (0.15-0.27) µM, n=5; sham-operated-

4MU: 0.15 (0.11-0.20) µM, n=5; I/R: 0.11 (0.036-0.32) µM, n=5; I/R-4MU: 0.15 (0.06-0.36) µM, n=5]. To further investigate potential changes in the excitatory contractile function, the effect of EFS was evaluated at increasing frequencies of stimulation on small intestine preparations. In the I/R and sham-operated groups, EFS-elicited contractions were significantly reduced with respect to controls (Figure 21 B). In the control and sham-operated groups, 4-MU treatment did not modify the responses to EFS compared to those observed in the respective untreated groups. EFS-induced contractions in the 4-MU treated sham-operated group remained significantly lower than in controls. In the I/R group after 4-MU treatment, EFS-evoked responses of the small intestine longitudinal muscle were higher with respect to those obtained in the respective untreated group, remaining lower compared to those obtained in control group. EFS-mediated responses were of neuronal origin, since in all groups addition of the neuronal blocker tetrodotoxin (1µM) totally abolished the EFS-induced responses. In small intestine myenteric plexus, distribution of ChAT immunoreactivity was similar in all experimental groups as demonstrated by the unchanged density index (Figure 21 panels C, D).

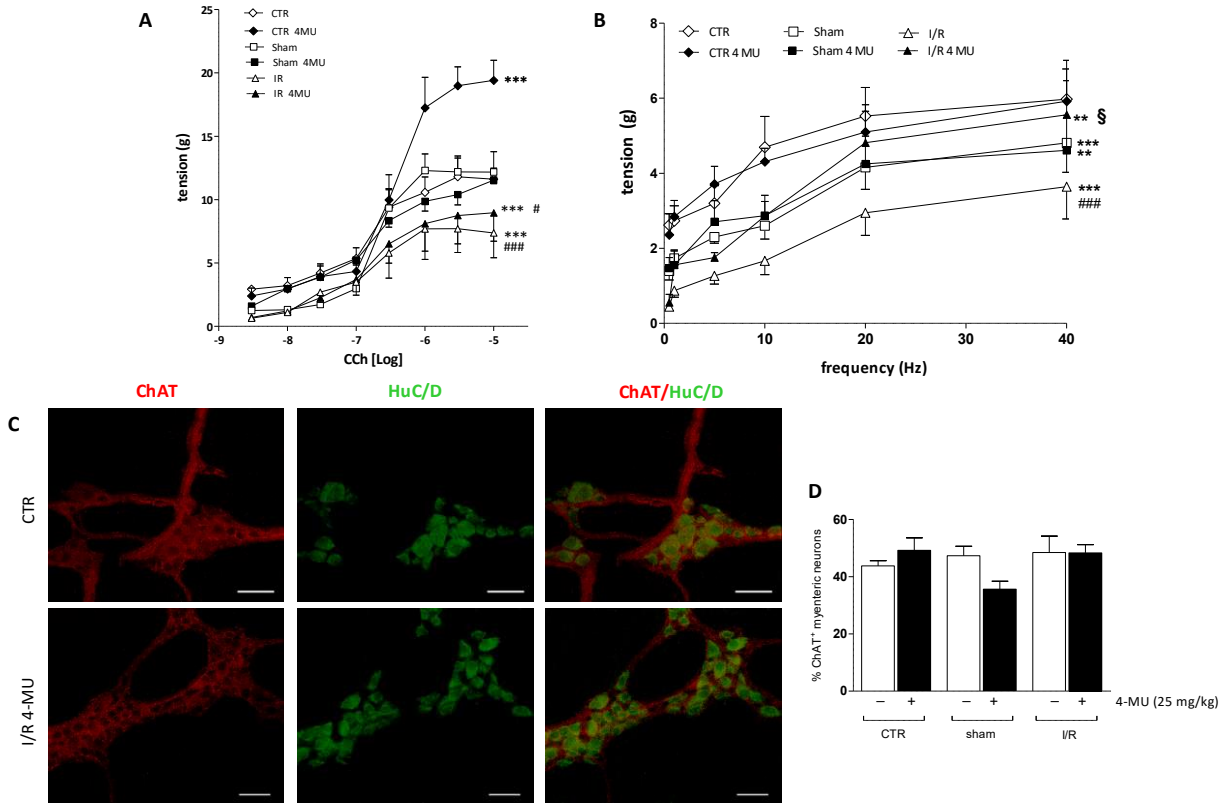

Figure 21. 4-MU treatment influences excitatory contractility in the rat small intestine. (A) Concentration–response curves to carbachol (CCh) of isolated rat small intestine segments in the different experimental groups (N=5 rats per group). **(B)** Neuromuscular excitatory responses induced by EFS (0.5–40 Hz) in isolated small intestine preparations obtained from the different experimental groups N=5 rat/group. **(C)** Representative confocal photomicrographs showing the distribution of ChAT (red, marker for cholinergic neurons) and HuC/D (green, pan-neuronal marker) and **(D)** ChAT density index in LMMP preparations obtained from all experimental groups (N=5 rat/group). Data are shown as mean ± SEM. (A-B) statistical significance: **P < 0.01, ***P < 0.001 vs; ###P<0.001 vs sham-operated; §P<0.05 vs I/R by Two way ANOVA (A-B).

4.2.7 I/R injury influences the inhibitory neuromuscular response: effect of 4-MU treatment

Non-adrenergic non-cholinergic induced responses to 10 Hz transmural stimulation were evaluated in the small intestine of all groups in the presence of guanethidine and atropine. In these conditions, control and sham-operated segments displayed similar inhibitory relaxation responses with or without 4-MU treatment (Figure 22 A). In I/R and 4-MU-treated I/R groups, NANC relaxation responses were significantly reduced with respect to control and 4-MU treated control groups (Figure 22 A). In all groups, the inhibitory responses were mediated by NO, as demonstrated by the ability of the non-selective NOS inhibitor, L-NAME, to significantly reduce NANC-evoked relaxations at 10 Hz stimulation frequency by 50% the respective experimental groups in the absence of the inhibitor (Figure 22 A). In the control and 4-MU-treated control groups, 10 Hz EFS-induced on-relaxations in NANC conditions were not influenced by pretreatment with 1400 W, a selective iNOS inhibitor (Figure 22 A). In sham-operated group, addition of 1400W significantly reduced NANC on-relaxations, while in the 4-MU-treated sham-operated group the relaxation response was only slightly reduced with respect to values obtained in the absence of the inhibitor. In the I/R group, addition of 1400W reduced NANC on-relaxations with respect to the control group in the presence of 1400W and, although not significantly, with respect to the I/R group in the absence of the inhibitor (Figure 22 A). In the 4-MU treated I/R group, 1400W was not able to significantly reduce NANC relaxations neither with respect to the I/R group nor to the control group in the presence of the inhibitor (Figure 22 A). To further investigate the possible effects of 4-MU treatment on I/R-induced alterations of the enteric nitrergic neurotransmission, we evaluated the distribution of nNOS and iNOS neurons in the myenteric plexus in the different experimental conditions. In particular, immunohistochemical co-localization with the pan neuronal marker HuC/D showed that the number of $nNOS^+$ myenteric neurons was similar in all the experimental groups (Figure 22 B, C). $nNOS^+$ neurons displayed morphological changes in both I/R and 4-MU treated I/R groups as demonstrated by the significantly enhanced area/soma ratio and total area with respect to control and sham-operated groups (Figure 22 D, E). The number of $iNOS^+$ neurons significantly increased in the small intestine of the I/R group with respect to control and sham-operated animals (Figure 22 panels F,G). After 4-MU treatment, the number of $iNOS^+$ neurons were significantly reduced with respect to the I/R group displaying values similar to those obtained in the control and sham-operated groups (Figure 22 F, G).

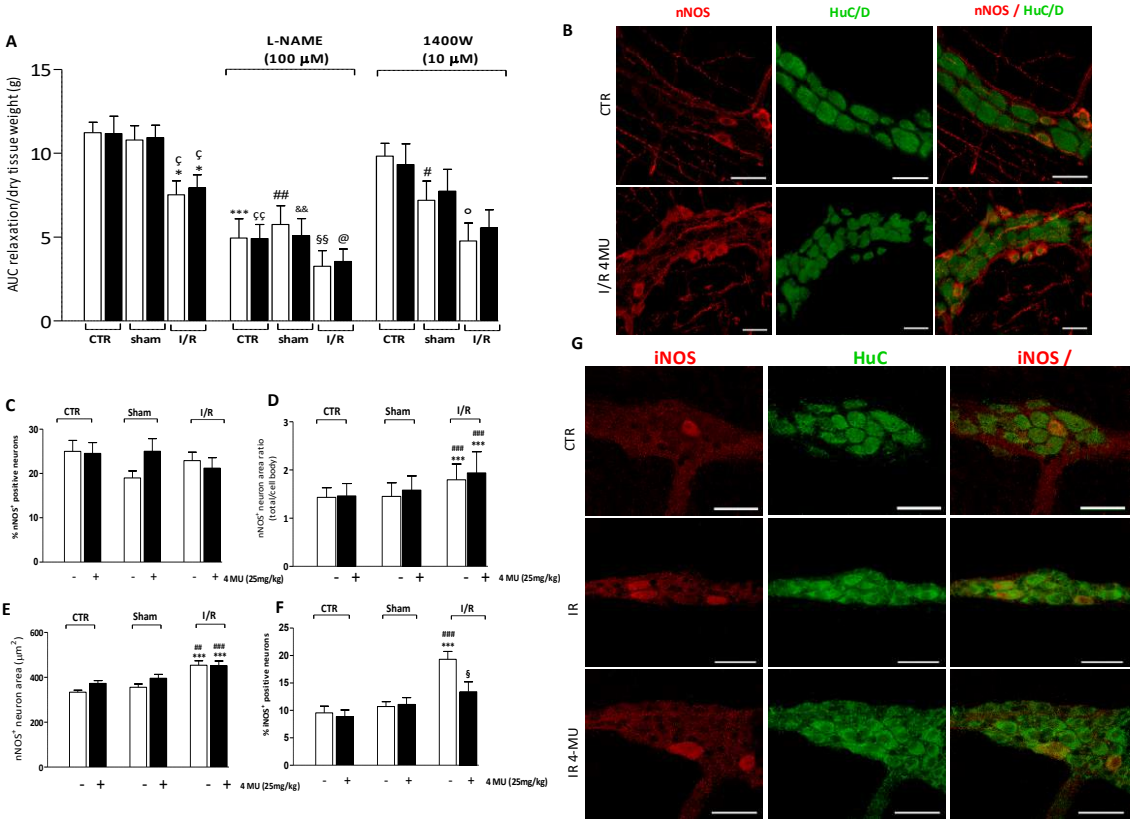

Figure 22. Effect of 4-MU treatment on inhibitory neurotransmission in the rat small intestine. (A) 10 Hz EFS-evoked NANC on-relaxation responses in the different experimental groups in the absence and presence L-NAME and 1400W, (N=5 rats per group). Data are reported as mean ± SEM. Statistical significance: *P< 0.05, ***P<0.001 vs CTR; ᶜP<0.05, ᶜᶜP<0.01 vs CTR 4-MU; ##P<0.01 vs sham-operated; &&P<0.01 vs sham-operated 4-MU; §§P<0.01 vs I/R; @P<0.05 vs I/R 4-MU; °P<0.05 vs CTR 1400W by one-way ANOVA followed by Tukey's post hoc test. (B) Representative confocal photomicrographs showing the distribution of nNOS immunoreactive myenteric neurons (red) and their co-localization with pan neuronal marker HuC/D (green). (C) percentage of HuC/D$^+$-nNOS$^+$ neurons with respect to total HuC/D$^+$ neurons in ileal LMMP whole-mount preparations in the different experimental groups, (N = 5 rats per group). (D,E) Morphological analyses of nNOS immunoreactive myenteric neurons in rat small intestine of the different experimental groups. (D) Ratios of total cell areas, including dendrites, to cell body area and (E) nNOS$^+$ cell profile total areas, including dendrites. Values are expressed as means±SEM. ***P<0.001 vs control ,##P<0.01 and ###P<0.001 vs sham-operated by one way ANOVA followed by Tukey's test. (F) Percentage of HuC/D$^+$-iNOS$^+$ neurons with respect to total HuC/D$^+$ neurons in ileal LMMP whole-mount preparations in the different experimental groups, (N = 5 rats per group). Values are expressed as means±SEM. ***P<0.001 vs. control, ###P<0.001 vs sham-operated and §P<0.05 vs I/R by one way ANOVA followed by Tukey's test. (G) Representative confocal photomicrographs showing the distribution of iNOS immunoreactive myenteric neurons (red) and their co-localization with pan neuronal marker HuC/D (green).

4.2.8 I/R injury influences NANC small intestine SP excitatory neurotransmission: effect of 4-MU treatment

In small intestine whole-mount preparations from all experimental groups, immunoreactivity of SP, a neuropeptide member of the tachykinin family with higher affinity for NK1 than for NK2 or NK3 receptors (Lecci et al., 2006), was generally faint in the soma of myenteric neurons and more intense in nerve varicose fibers within myenteric ganglia and in interconnecting trunks along the

longitudinal muscle (Figure 23 A). In control and 4-MU-treated control preparations, the percentage of SP^+ myenteric neurons staining and the relevant density index were similar (Figure 23 B, C). The number of SP^+ myenteric neurons in the sham-operated group as well the density index was slightly, but not significantly, higher than in controls; after 4-MU treatment both values decreased (Figure 23 B, C). In the I/R group, the number of SP^+ myenteric neurons as well as the density index significantly increased. Both enhancements were significantly reduced by 4-MU treatment (Figure 23 B, C). To assess the contribution of non-cholinergic excitatory neurotransmitters to the small intestine motor function, post-stimulus excitatory off-responses were evaluated under NANC conditions in the presence of L-NAME, to unmask tachykininergic nerve-evoked contractions (Lecci et al., 2006). The tachykinin-mediated response was not significantly different in control, 4-MU-treated control, sham-operated and 4-MU-treated sham-operated groups (Figure 23 D). After I/R, tachykinin-mediated contractions were significantly reduced with respect to both control and

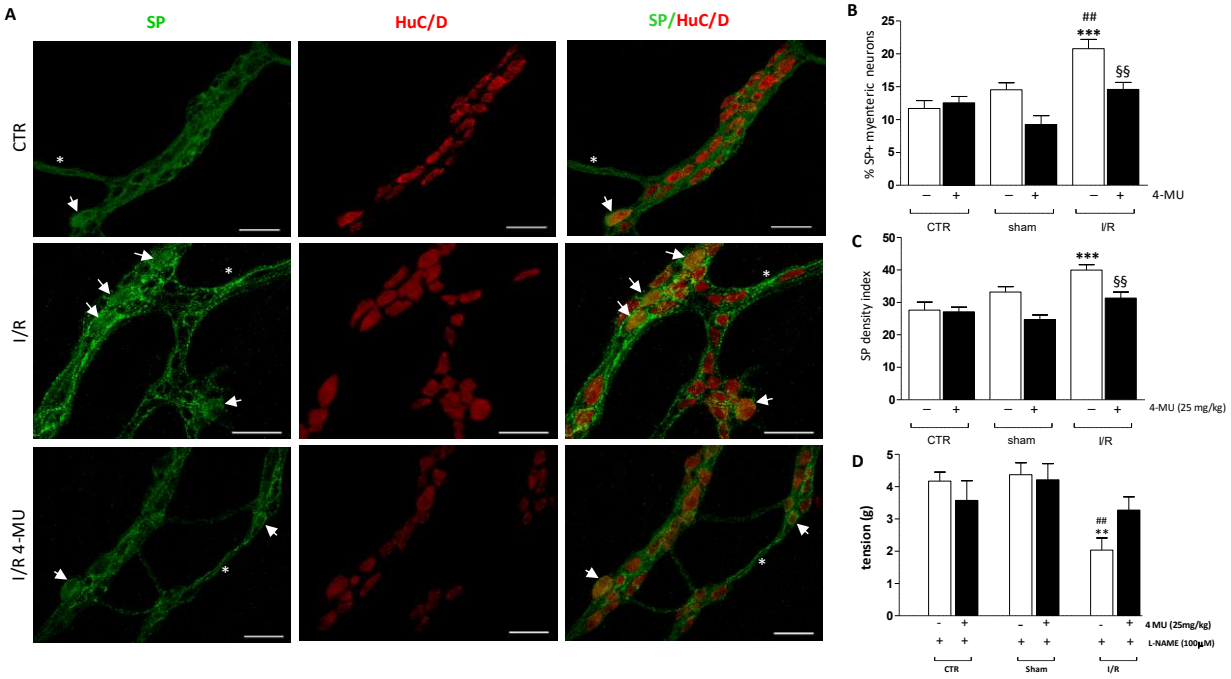

Figure 23. 4-MU modulation of tackykinergic neurotransmission in the rat small intestine after I/R injury. (A) Representative confocal microphotographs showing the distribution of SP (green) and HuC/D (red) in rat myenteric plexus obtained from CTR, I/R and I/R-4MU groups (N = 5 rats per group). Scale bars = 50 µm. Arrows indicate SP^+-HuC/D^+ neurons, asterisk interconnecting fibers. (B) Percentage of SP^+-HuC/D^+ neurons with respect to total HuC/D^+ neurons and (C) density index of SP immunoreactivity in small intestine LMMP whole-mount preparations in the different experimental groups (N = 5 rats per group). (D) Tachykininergic-mediated contractions evoked by 10 Hz EFS in small intestine segments in the different experimental groups (N = 5 rats per group), under NANC conditions, in absence or presence of L-NAME. Data are reported as mean ± SEM. Difference significance: **P < 0.01, ***P < 0.001 vs CTR; $^{\#\#}$P<0.01 vs sham-operated; §§P<0.01 vs I/R.

sham-operated animals and returned to control values after 4-MU treatment (Figure 23 D).

5 DISCUSSION

The present project aimed to evaluate the role of Hyaluronan (HA) in adaptive changes of the gut neuromuscular function, in experimental models of inflammatory bowel disease (IBD) and after intestinal ischemia/reperfusion (I/R) injury. In both studies important changes in HA homeostasis have been demonstrated within the myenteric plexus, suggesting a role for the glycosaminoglycan (GAG), which is a fundamental component of the extracellular matrix (ECM), in the rearrangement of enteric neuronal networks in pathophysiological conditions, eventually underlying participation to changes in the gut motor functions.

5.1 HA involvement in myenteric plexus derangement after DNBS-induced colitis in rats

In the first part of the study, morphological investigations and biomolecular data provided evidence that HA, produced by myenteric neurons, is abundantly present in myenteric ganglia. These findings represent the first demonstration that the GAG may be involved in the formation of a pericellular coat of condensed matrix surrounding myenteric neurons, similar to the mesh-like structure called perineuronal net (PNN), that is associated with some classes of neurons in the central nervous system (CNS) (van 't Spijker and Kwok, 2017). The existence of a PNN in the CNS has been for the first time proposed by Golgi and consists of a soft and well-organized structure of ECM molecules, which occupies a large part of the neuronal tissue (Suttkus et al., 2016). Chondroitin sulfate proteoglycans, HA and its link proteins HAPLN1 and HAPLN4, as well as the large glycoprotein tenascin-R, are the main components of the PNN, whose main functions are the regulation of ion homeostasis around active neurons, stabilization of synapses and participation to neuronal plasticity (Oohashi et al., 2015; van 't Spijker and Kwok, 2017). Immunohistochemical reports have previously demonstrated that ECM molecules, such as laminin, type IV collagen, nidogen, heparin sulfate proteoglycans and fibronectin, are present in or nearby the basement membrane that surrounds myenteric ganglia (Bannerman et al., 1986). In accordance, whole-mount preparations from our samples showed a strong HA labeling on the myenteric ganglia surface, indicating that HA may contribute to the external architecture of enteric ganglia. However, in contrast with previous reports, that were not able to detect ECM molecules within myenteric ganglia (Bannerman et al., 1986), HA staining was also visible in the perineuronal space surrounding myenteric neurons. In both colonic whole-mount preparations and in primary cultures of myenteric ganglia, neurons co-expressed HA and the neuronal marker HuC/D, suggesting that the source for GAG is represented

by colonic myenteric neurons. However, although a strong HA staining was found in the soma of myenteric neurons in culture, only a faint labeling was evidenced in the cytosol of myenteric neurons from whole-mount preparations. This discrepancy may be due to the presence of trophic factors in the culture medium used to grow isolated myenteric ganglia, which may favor a higher HA turnover (Jacobson et al., 2000; Li et al., 2007). HA may sustain the accumulation of the PNN surrounding myenteric neurons through the binding with its receptors on neuronal surface, such as CD44 or RHAMM-l, or, directly, via one of the three transmembrane HA synthases (HAS1-3), which can retain HA on cell surface (Carulli et al., 2006). In the present study myenteric neurons were shown to express HAS2, the main isoform of the three HASs in adult cells (Vigetti et al., 2014), supporting the hypothesis that colonic myenteric neurons may be a source for HA. Interestingly, the presence of HAS2 mRNA and protein has recently been demonstrated in developing rat cortical neurons, consolidating the hypothesis that neurons are able to synthesize HA (Fowke et al., 2017).

After DNBS-induced colitis, HA deposition in the whole wall of the rat colon was significantly altered with respect to control preparations, in analogy with data obtained in human colon biopsies obtained from IBD patients and in murine dextran sodium sulfate (DSS)-induced colitis (Kessler et al., 2008; de la Motte et al., 2003). In the present study a rearrangement of HA distribution occurred in DNBS-treated colonic specimens, changing from a well-defined matrix to a dense deposit in all the intestinal layers, as observed in the DSS-treated mouse colon (Kessler et al., 2008). A peculiar feature of the inflamed colon, observed also in this study, is submucosal and smooth muscle thickening with increased deposition of connective ECM components (Ippolito et al., 2015; Zhu et al., 2012). Thus, increased HA levels in both layers during inflammation may take part in the fibrotic process, as suggested in other peripheral organs and in vascular smooth muscle cells (de la Motte et al., 2011; Moretto et al., 2015).

In addition to previous data describing deposition of HA in the epithelial and submucosal layer, the results obtained in this thesis indicate that inflammation may induce considerable changes in HA distribution also in myenteric ganglia. At this level, the perineuronal HA envelope was significantly reduced, while HA staining in neuronal cytoplasm and ganglia surface was still visible. We cannot exclude that this altered deposition is caused by a fragmentation of the GAG, after the inflammatory injury. Evidences, obtained in both humans and experimental animal models, suggest that the PNN retains a neuroprotective role against neurotoxic molecules, preventing, for example, amyloid-β toxicity deposition or oxidative stress, in selective vulnerable neuron types (Suttkus et al., 2016). In agreement with previous reports, in this study DNBS treatment induced significant alterations in myenteric ganglia, including a drastic reduction of HuC/D positive neurons, the presence of nuclear aggregates, cytosolic vacuolization, smaller area and changes in HuC/D

immunoreactivity distribution (Ippolito et al., 2015). Enhancement of HuC/D nuclear staining with respect to the cytoplasm is indicative of myenteric neuron damage, which may occur in different pathological conditions (Tacker et al., 2011; Giaroni et al., 2013). We cannot exclude that the degradation of a perineuronal HA sheath participates to alterations of myenteric neuron function, as observed after degradation of the PNN in cortical mouse slices (Shah and Lodge, 2013). A recent study, carried out on HAS3 deficient mice, showed a reduction of HA deposition in the CA1 striatum pyramidale of the hippocampus that was associated with a lower extracellular space volume and increased epileptogenic activity (Arranz et al., 2014). Furthermore, in the hippocampus, enhanced neuronal activity during episodes of status epilepticus, were correlated with synaptic reorganization caused by PNN loss (McRae et al., 2012). Hence, we cannot exclude that alterations in perineuronal HA deposition may contribute to changes in myenteric neuron structure and function during an inflammatory challenge. In particular, similarly to hippocampal neurons during status epilepticus, inflammation-induced removal of the PNN in the intestine may contribute, at least in part, to the development of neuronal hyper-excitability and synaptic facilitation observed during inflammation (Brierley and Linden, 2014).

Alteration of HA distribution after experimentally-induced colitis was associated with up-regulation of HAS2 expression in myenteric neurons. Accordingly, expression of HA synthetic enzymes, such as HAS2 and HAS3, are increased in mouse colon epithelium after DSS-induced colitis (Zheng et al., 2009), as well as in intestinal microvessel endothelial cells and submucosal smooth muscle cells from IBD patients (Kessler et al., 2008). We cannot exclude that HAS2 increased expression in myenteric neurons during DNBS-induced colitis serves to retain inflammatory cells in the proximity of myenteric ganglia, since we observed a prominent leukocyte infiltration and increase of MPO activity in the *muscularis propria*. In addition in agreement with previous reports, at this level, pro-inflammatory cytokines, such as TNFα, IL-1β and IL-6, were up-regulated, (Barada et al., 2006; Bakirtzi et al., 2014).The interplay between myenteric neurons and immunocytes may be fundamental in the remodeling of the neuronal network in response to a neuromuscular damage during gut inflammation. Both myenteric neurons and immunocytes may regulate one another's functions by releasing a complex set of cytokines, neurotransmitters and hormones. Neuronal activation can lead to degranulation of mast cells and recruitment of neutrophils to the area (Lakhan and Kirchgessner, 2010). HA produced by HAS2 in myenteric neurons, may therefore take a part in recruiting immunocytes nearby myenteric ganglia during intestinal inflammation. This hypothesis is supported by the ability of myenteric ganglia in culture to produce HA “cable-like” structures, which confer to HA the ability to attach serum components, such as the heavy chain of inter-alpha trypsin inhibitor, which are known to increase the adhesiveness of HA to leukocytes (de

la Motte and Kessler, 2015). In microvessel endothelial cells and submucosal smooth muscle cells obtained from IBD patients HA cable-like structures, deriving from medium molecular weight HA, were shown to recruit mononuclear leukocytes via CD44 receptors (de la Motte, 2011). Further fragmentation of HA may sustain the inflammatory response by stimulating inflammatory cytokine production by monocytes (de la Motte et al., 2009).

In conclusion, in this study we provide evidence that myenteric neurons may produce HA which retains a homeostatic role by contributing to the formation of an extracellular matrix basal membrane enveloping the surface of myenteric ganglia as well as a perineuronal net surrounding myenteric neurons. After DNBS-induced colitis this well-organized HA structure is highly altered, especially within myenteric ganglia. This alteration is associated with increased neuronal HAS2 expression and may participate to myenteric neuron derangement underlying changes in motor function. We cannot exclude that modulation of HA production during intestinal inflammation may ameliorate intestinal motility patterns which represent a remarkable cause of IBD symptoms

5.2 HA is a modulator of the rat small intestine neuromuscular function after in vivo I/R injury

In the second part of this study, functional, morphological and biomolecular analyses demonstrated that HA may also influence the neurochemical coding and function of the myenteric neurons after an in vivo I/R injury in rats. Several investigations suggest that an intestinal I/R injury has detrimental consequences on the ENS structure and function. However, the effects of I/R on enteric neurons remain largely to be discovered. The result obtained in this study evidenced that, after I/R injury, HA levels within the small intestine *muscularis propria* significantly increased with respect to both controls and sham-operated animals. This change was associated with an increased deposition of the GAG both on the surface and in the perineuronal space. Overall, these observations are in good agreement with previous reports on the accumulation of HA after reperfusion following interruption of blood flow, both in the periphery and in the CNS, suggesting that the GAG may have a role in the pathophysiology of the I/R injury (Colombaro et al., 2013; Al'Qteishat et al., 2006). Analogously to data obtained in post mortem tissues of patients after an ischemic stroke and in the mouse brain after an I/R injury (Lindwall et al., 2013; Al Qteishat et al., 2006), increased HA deposition in the myenteric plexus of the ischemic/reperfused rat small intestine may depend upon an up-regulation of HA synthases, HAS1 and HAS2. This is suggested by the increased number of $HAS1^{+}$ and $HAS2^{+}$ myenteric neurons as well as by the increased mRNA

levels for both proteins in longitudinal muscle myenteric plexus (LMMP) preparations. Increased HAS1 mRNA levels in LMMP obtained from sham-operated animals was not reflected by an increase in $HAS1^+$ myenteric neurons, possibly owing to the enzyme overexpression in enteric glial cells. This hypothesis is in line with the mild inflammatory state, observed in this experimental group. In vivo treatment with the HA synthesis inhibitor, 4-methylumbelliferone (4-MU), reduced HA density index and HA levels in LMMP preparations more efficaciously in the I/R group than in the control and sham-operated groups, suggesting that the I/R-induced HA *de novo* synthesis was principally influenced by administration of the drug. This observation may reflect the ability of 4-MU to downregulate HA synthases in I/R conditions (Kultti et al., 2009), as suggested also by the reduction of $HAS1^+$ and $HAS2^+$ myenteric neurons and mRNAs.

In the rat small intestine myenteric plexus, changes of HA deposition after I/R may be associated with alterations of the intestinal neuromuscular function. In agreement with previous reports, the I/R injury induced a significant slowing of the gastrointestinal transit (Filpa et al., 2017; Ballabeni et al., 2002). Treatment with 4-MU aggravated I/R-induced gastrointestinal transit slowing and significantly reduced gastric emptying, suggesting that the I/R-induced HA neo-synthesis may sustain gastrointestinal motor responses in this pathophysiological condition. Indeed, in the I/R group, but not in control neither in the sham-operated group, 4-MU administration was associated with alterations in both excitatory and inhibitory NANC transmission, concomitantly with alterations of the myenteric plexus neurochemical coding. Such changes do not apparently depend upon changes in the inflammatory infiltrate or in the activation of I/R-induced molecular pathways, as suggested by the reduced levels of both MPO stained neutrophils and HIF1α mRNA in the I/R treated with 4-MU group (Filpa et al., 2017; Kannan et al., 2011). Data obtained on both spontaneous and carbachol-induced contractions are in good agreement with previous studies showing that, in rats, a transitory occlusion of the superior mesenteric artery followed by 24 hours of reperfusion downregulates muscarinic post-junctional contractile responses (Hierholzer et al., 1999; Ballabeni et al., 2002). The I/R-induced impairment of both basal and pharmacologically-stimulated longitudinal muscle contractions was unchanged after 4-MU treatment, suggesting that HA deposition does not influence post-junctional cholinergic excitatory responses. In the control group, 4-MU treatment was associated with an increased contractile efficacy of carbachol, as suggested by the significant enhancement of the Emax in the relevant concentration-response curve. This data may suggest that modulation of HA synthesis in the small intestine *muscularis propria* may favor either muscarinic receptor recruitment, or may enhance receptor coupling with effector systems in smooth muscle cells. Both in the sham-operated and I/R group, TTX-sensitive, contractions evoked by increasing EFS frequencies, were significantly lower than in control

specimens, indicating that the neuronal component of the excitatory contractile response was impaired in both conditions. However, in segments obtained from sham-operated animals, 4-MU treatment did not influence the contractile responses to EFS, whereas the drug significantly enhanced the response in the I/R group. In this regard, HA may modulate the efficiency of excitatory neuronal pathways only in specific pathophysiological conditions, i.e after interruption of blood flow followed by reperfusion and not under conditions of mild inflammation, occurring in the sham-operated group. Several studies suggest that excitatory cholinergic neurons may be particularly vulnerable to hypoxic/ischemic insults and there are evidences that hypoxia may preferentially depress cholinergic neuronal pathways involved in the intestinal reflexes (Corbett and Lees, 1997; Giuliani et al., 2006; Larson and Martins, 1981). In this study the density index of ChAT staining in myenteric ganglia was similar in the different experimental groups. However, we cannot exclude that functional changes of myenteric cholinergic neurons, i.e alterations of ACh release, may underlie changes of EFS excitatory responses with or without 4-MU treatment (Corbett and Lees, 1997; Giuliani et al., 2006). Modifications of non-cholinergic excitatory neurotransmitter pathways may also be involved in the modulation of the EFS response in the different experimental groups. Indeed, in the I/R group, the off-contractions observed in NANC conditions, which is mediated by tachykinins, such as substance P, was significantly reduced after I/R injury, and was re-established to control values after 4-MU treatment. These data strongly support the hypothesis that, in I/R conditions, inhibition of HA synthesis by 4-MU may enhance excitatory non-cholinergic contractions. 4-MU modulation of the off-NANC contractions during I/R is apparently in contrast with the ability of the drug to reduce the I/R-induced enhancement of SP^+ myenteric neurons and density index. Accordingly, SP release enhances following acute brain ischemia and is critically involved in the development of vasogenic edema and neuronal injury (Corrigan et al., 2015; Richter et al., 2018). In this study, we cannot exclude that HA contributes to increase SP synthesis and expression in myenteric neurons during I/R. Such enhancement may be followed by downregulation of NK1 receptors, underlying reduced contractile NANC responses. All these effects on the enteric tackykininergic transmission are reversed by 4-MU treatment.

Intestinal I/R injury is associated with impairment of the NANC inhibitory transmission (Filpa et al., 2017; Giaroni et al., 2013; Rivera et al., 2011). Accordingly, in this study, a significant reduction of rat small intestine NANC-mediated relaxations was observed after in vivo I/R, but not in the sham-operated group. The on-relaxation in I/R conditions was not influenced by 4-MU treatment, remaining downregulated after blockade of HA synthesis. In all experimental groups, sensitivity of the NANC relaxation to the non-selective nitric oxide inhibitor, L-NAME, suggests that NO represents a major component of the inhibitory response. Indeed, nitrergic neurons seem to be

selectively involved in an I/R gut injury and previous studies indicate that both nNOS and iNOS expressing myenteric neurons may undergo important changes (Filpa et al., 2017; Filpa et al., 2015; Rivera et al., 2009). In small intestine segments obtained from control animals with and without 4-MU treatment, NANC on-relaxations were insensitive to the iNOS inhibitor, 1400W, reflecting the low number of constitutively iNOS expressing myenteric neurons in both groups. A mild inflammatory state may account for the enhanced sensitivity to 1400W in sham-operated animals with/without 4-MU treatment. In the I/R group, NANC relaxations were significantly reduced by 1400W, suggesting that iNOS is the main isoform involved in the inhibitory response in this condition (Filpa et al., 2017). Accordingly, the number of $iNOS^+$ neurons increased in the rat myenteric plexus after I/R, as already demonstrated (Filpa et al., 2017; Giaroni et al., 2013). In the I/R group, after 4-MU treatment, the number of $iNOS^+$ myenteric neurons returned to values not different from those obtained in controls, suggesting that blockade of HA synthesis may influence iNOS expression/activity. These observations are in good agreement with reports on the ability of HA to induce iNOS mRNA (Campo et al., 2012). The number of $nNOS^+$ myenteric neurons was similar in all experimental group. However, as previously described, important morphological alterations were observed in $nNOS^+$ neurons, with increased total neuron area, which persisted after 4-MU treatment. These functional and morphological data, suggest that during and I/R injury, HA may sustain nitrergic relaxations, mainly via iNOS, but not nNOS, regulation. In addition, alternative inhibitory neurotransmitter pathways, comprising purines and peptides may sustain the on-relaxation during I/R (Furness et al., 2014). In view of its vasodilatory, neuroprotective and antioxidant properties, one of these neurotransmitters may be represented by vasoactive intestinal peptide (VIP), which is involved in the rearrangement of myenteric neurons during I/R injury (Borges 2016; de Silva de Souza, 2015).

In conclusion, these data suggest that HA sustains the efficiency of the gastrointestinal transit during an I/R injury influencing both the excitatory and inhibitory components of the peristaltic reflex. In this condition, after blockade of HA synthesis excitatory neuronal pathways, mainly tachykinergic, are up-regulated, while inhibitory responses remain downregulated, overall deteriorating transit efficiency. The beneficial effects of HA may depend upon the ability of the I/R-induced neoformed GAG to maintain the neuronal structure and function of myenteric neuronal pathways in these pathological conditions.

6 REFERENCES

Aguilera M, Melgar S. Microbial neuro-immune interactions and the pathophysiology of IBD. In New Insights into Inflammatory Bowel Disease; Huber, S., Ed.; Intechopen: London, UK, 2016; pp. 181–215.

Akira S, Takeda K. Toll-like receptor signalling. Nat Immunol. 2004; 4: 499–511.

Al'Qteishat A, Gaffney J, Krupinski J, Rubio F, West D, et al. 2006. Changes in hyaluronan production and metabolism following ischaemic stroke in man. Brain 129:2158–76.

Albert MJ, Mathan VI, Baker SJ. Vitamin B12 synthesis by human small intestinal bacteria. Nature. 1980; 283(5749):781-2.

Aravalli RN, Peterson PK, Lokensgard JR. Toll-like receptors in defense and damage of the central nervous system. J Neuroimmune Pharmacol. 2007; 2(4):297-312.

Arranz AM, Perkins KL, Irie F, Lewis DP, Hrabe J, Xiao F, Itano N, Kimata K, Hrabetova S, Yamaguchi Y. Hyaluronan deficiency due to Has3 knock-out causes altered neuronal activity and seizures via reduction in brain extracellular space. J Neurosci. 2014 Apr 30;34(18):6164-76.

Backhed F, Ding H, Wang T, Hooper LV, Koh GY, Nagy A, Semenkovich CF, Gordon JI: The gut microbiota as an environmental factor that regulates fat storage. Proc Natl Acad Sci U S A 2004; 101(44):15718-15723.

Baj A, Moro E, Bistoletti M, Orlandi V, Crema F, Giaroni C. Glutamatergic Signaling Along The Microbiota-Gut-Brain Axis. Int J Mol Sci. 2019 Mar 25;20(6).

Ballabeni V, Barocelli E, Bertoni S, Impicciatore M. Alterations of intestinal motor responsiveness in a model of mild mesenteric ischemia/reperfusion in rats. Life Sci. 2002 Sep 13;71(17):2025-35.

Bannerman PG, Mirsky R, Jessen KR, Timpl R, Duance VC. Light microscopic immunolocalization of laminin, type IV collagen, nidogen, heparan sulphate proteoglycan and fibronectin in the enteric nervous system of rat and guinea pig. J Neurocytol. 1986 Dec;15(6):733-43.

Barajon I, Serrao G, Arnaboldi F, Opizzi E, Ripamonti G, Balsari A, Rumio C. Tolllike receptors 3, 4, and 7 are expressed in the enteric nervous system and dorsal root ganglia. J Histochem Cytochem. 2009; 57(11):1013-23.

Bercik P, Collins SM, Verdu EF: Microbes and the gut-brain axis. Neurogastroenterol Motil 2012; 24(5):405-413.

Bistoletti M, Moretto P, Giaroni C. Method for Detecting Hyaluronan in Isolated Myenteric Plexus Ganglia of Adult Rat Small Intestine. Methods Mol Biol. 2019;1952:117-125.

Booijink CC, Zoetendal EG, Kleerebezem M, de Vos WM. Microbial communities in the human small intestine: coupling diversity to metagenomics. Future Microbiol. 2007; 2(3):285-95.

Borges SC, da Silva de Souza AC, Beraldi EJ, Schneider LC, Buttow NC. Resveratrol promotes myenteric neuroprotection in the ileum of rats after ischemia-reperfusion injury. Life Sci. 2016 Dec 1;166:54-59.

Borre YE, O'Keeffe GW, Clarke G, Stanton C, Dinan TG, Cryan JF. Microbiota and neurodevelopmental windows: implications for brain disorders. Trends Mol Med. 2014 Sep;20(9):509-18.

Brierley SM, Linden DR. Neuroplasticity and dysfunction after gastrointestinal inflammation. Nat. Rev. Gastroenterol. Hepatol. 2014; 11:611–627.

Brun P, Giron MC, Qesari M, Porzionato A, Caputi V, Zoppellaro C, Banzato S, Grillo AR, Spagnol L, De Caro R, Pizzuti D, Barbieri V, Rosato A, Sturniolo GC, Martines D, Zaninotto G, Palù G, Castagliuolo I. Toll-like receptor 2 regulates intestinal inflammation by controlling integrity of the enteric nervous system. Gastroenterology. 2013;145(6):1323-33.

Brune B, Dimmeler S, Molina y Vedia L, Lapetina EG. Nitric oxide: a signal for ADP-ribosylation of proteins. Life Sci 1994;54:61–70.

Bueno L, Fioramonti J, Delvaux M, Frexinos J. Mediators and pharmacology of visceral sensitivity: from basic to clinical investigations. Gastroenterology. 1997;112:1714–43.

Bush TG, Savidge TC, Freeman TC, Cox HJ, Campbell EA, Mucke L, Johnson MH, Sofroniew MV. Fulminant jejuno-ileitis following ablation of enteric glia in adult transgenic mice. Cell. 1998; 93:189–201.

Buttó, LF, Schaubeck M, Haller D. Mechanisms of microbe-host interaction in Crohn's disease: Dysbiosis vs. Pathobiont Selection. Front. Immunol. 2015; 6, 555.

Camara-Lemarroy CR, Ibarra-Yruegas BE, Gongora-Rivera F. Gastrointestinal complications after ischemic stroke. J Neurol Sci. 2014 Nov 15;346(1-2):20-5.

Campo GM, Avenoso A, D'Ascola A, Scuruchi M, Prestipino V, Nastasi G, Calatroni A, Campo S. The inhibition of hyaluronan degradation reduced pro-inflammatory cytokines in mouse synovial fibroblasts subjected to collagen-induced arthritis. J Cell Biochem. 2012 Jun;113(6):1852-67.

Caputi V, Marsilio I, Cerantola S, Roozfarakh M, Lante I, Galuppini F, Rugge M, Napoli E, Giulivi C, Orso G, Giron MC. Toll-Like Receptor 4 Modulates Small Intestine Neuromuscular Function through Nitrergic and Purinergic Pathways. Front Pharmacol. 2017 Jun 8;8:350.

Carden DL, Granger DN. Pathophysiology of ischaemia-reperfusion injury. J Pathol. 2000 Feb;190(3):255-66.

Cario E, Gerken G, Podolsky DK. Toll-like receptor 2 controls mucosal inflammation by regulating epithelial barrier function. Gastroenterology. 2007; 132(4):1359-74.

Carulli D, Kwok JC, Pizzorusso T. Perineuronal Nets and CNS Plasticity and Repair. Neural Plast. 2016; 2016:4327082.

Carulli D, Rhodes KE, Brown DJ, Bonnert TP, Pollack SJ, Oliver K, Strata P, Fawcett JW. Composition of perineuronal nets in the adult rat cerebellum and the cellular origin of their components. J Comp Neurol. 2006 Feb 1;494(4):559-77.

Caulfield MP, Birdsall NJ. International Union of Pharmacology. XVII. Classification of muscarinic acetylcholine receptors. Pharmacol Rev. 1998 Jun;50(2):279-90.

Clerc N, Gola M, Vogalis F, Furness JB. Controlling the excitability of IPANs: a possible route to therapeutics. Curr Opin Pharmacol. 2002 Dec;2(6):657-64.

Cocks TM, Sozzi V, Moffatt JD, Selemidis S. Protease-activated receptors mediate apamin-sensitive relaxation of mouse and guinea pig gastrointestinal smooth muscle. Gastroenterology. 1999;116:586–92.

Coelho-Aguiar Jde M, Bon-Frauches AC, Gomes AL, Veríssimo CP, Aguiar DP, Matias D, Thomasi BB, Gomes AS, Brito GA, Moura-Neto V. The enteric glia: identity and functions. Glia. 2015 Jun;63(6):921-35.

Colombaro V, Declèves AE, Jadot I, Voisin V, Giordano L, Habsch I, Nonclercq D, Flamion B, Caron N. Inhibition of hyaluronan is protective against renal ischaemia-reperfusion injury. Nephrol Dial Transplant. 2013 Oct;28(10):2484-93.

Conly JM, Stein K, Worobetz L, Rutledge-Harding S. The contribution of vitamin K2 (menaquinones) produced by the intestinal microflora to human nutritional requirements for vitamin K. Am J Gastroenterol. 1994; 89(6):915-23.

Corbett AD, Lees GM. Depressant effects of hypoxia and hypoglycaemia on neuro-effector transmission of guinea-pig intestine studied in vitro with a pharmacological model. Br J Pharmacol. 1997 Jan;120(1):107-15.

Cornet A, Savidge TC, Cabarrocas J, Deng WL, Colombel JF, Lassmann H, Desreumaux P, Liblau RS. Enterocolitis induced by autoimmune targeting of enteric glial cells: a possible mechanism in Crohn's disease? Proc Natl Acad Sci U S A. 2001; 98:13306–13311.

Corrigan F, Vink R, Turner RJ. Inflammation in acute CNS injury: a focus on the role of substance P. Br J Pharmacol. 2016 Feb;173(4):703-15.

Costa M, Brookes SJ, Hennig GW. Anatomy and physiology of the enteric nervous system. Gut. 2000; 47 Suppl 4: iv15-9; discussion iv26.

da Silva de Souza AC, Borges SC, Beraldi EJ, de Sá-Nakanishi AB, Comar JF, Bracht A, Natali MR, Buttow NC. Resveratrol Reduces Morphologic Changes in the Myenteric Plexus and Oxidative Stress in the Ileum in Rats withIschemia/Reperfusion Injury. Dig Dis Sci. 2015 Nov;60(11):3252-63.

De Jager PL, Franchimont D, Waliszewska A, Bitton A, Cohen A, Langelier D, Belaiche J, Vermeire S, Farwell L, Goris A, Libioulle C, Jani N, Dassopoulos T, Bromfield GP, Dubois B, Cho JH, Brant SR, Duerr RH, Yang H, Rotter JI,Silverberg MS, Steinhart AH, Daly MJ, Podolsky DK, Louis E, Hafler DA, Rioux JD; Quebec IBD Genetics Consortium; NIDDK IBD Genetics Consortium. The role of the Toll receptor pathway in susceptibility to inflammatory bowel diseases. Genes Immun. 2007; 8 (5):387-97.

de la Motte C, Nigro J, Vasanji A, Rho H, Kessler S, Bandyopadhyay S, Danese S, Fiocchi C, Stern R. Platelet-derived hyaluronidase 2 cleaves hyaluronan into fragments that trigger monocyte-mediated production of proinflammatory cytokines. Am J Pathol. 2009 Jun;174(6):2254-64.

de la Motte CA, Hascall VC, Drazba J, Bandyopadhyay SK, Strong SA. Mononuclear leukocytes bind to specific hyaluronan structures on colon mucosal smooth muscle cells treated with polyinosinic acid:polycytidilic acid. Am J Pathol. 2003; 163, 121–133.

de la Motte CA, Kessler SP. The role of hyaluronan in innate defense responses of the intestine. Int J Cell Biol. 2015;2015:481301. Epub 2015 Mar 30.

de la Motte CA. Hyaluronan in intestinal homeostasis and inflammation: implications for fibrosis. Am J Physiol Gastrointest Liver Physiol. 2011; 301(6):G945-9.

De Luca C, Papa M. Looking Inside the Matrix: Perineuronal Nets in Plasticity, Maladaptive Plasticity and Neurological Disorders. Neurochem Res. 2016 Jul;41(7):1507-15.

De Winter BY, Van Den Wijngaard RM, De Jonge WJ. Intestinal mast cells in gut inflammation and motility disturbances. Biochim Biophys Acta. 2012; 1822(1):66-73.

DeJager PL, Franchimont D, Waliszewska A, Bitton A, Cohen A, Langelier D, Belaiche J, Vermeire S, Farwell L, Goris A, et al. The role of the Toll receptor pathway in susceptibility to inflammatory bowel diseases. Genes Immun. 2007, 8, 387–397.

Dethlefsen L, Eckburg PB, Bik EM, Relman DA. Assembly of the human intestinal microbiota. Trends Ecol Evol. 2006; 21(9):517-23.

Dzyubenko E, Gottschling C, Faissner A. Neuron-Glia Interactions in Neural Plasticity: Contributions of Neural Extracellular Matrix and Perineuronal Nets. Neural Plast. 2016;2016:5214961.

Echchannaoui H, Frei K, Schnell C, Leib SL, Zimmerli W, Landmann R. Toll-like receptor 2-deficient mice are highly susceptible to Streptococcus pneumonia meningitis because of reduced bacterial clearing and enhanced inflammation. J Infect Dis. 2002; 186(6):798-806.

Eiden LE. The cholinergic gene locus. J Neurochem. 1998 Jun;70(6):2227-40.

Ennes HS, Young SH, Raybould HE, Mayer EA. Intercellular communication between dorsal root ganglion cells and colonic smooth muscle cells in vitro. NeuroReport 1997;8:733–37.

Filpa V, Carpanese E, Marchet S, Pirrone C, Conti A, Rainero A, Moro E, Chiaravalli AM, Zucchi I, Moriondo A, Negrini D, Crema F, Frigo G, Giaroni C, Porta G. Nitric oxide regulates homeoprotein OTX1 and OTX2 expression in the rat myenteric plexus after intestinal ischemia-reperfusion injury. Am J Physiol Gastrointest Liver Physiol. 2017 Apr 1;312(4):G374-G389.

Foreman JC. Peptides and neurogenic inflammation. Br Med Bull. 1987 Apr;43(2):386-400.

Förstermann U, Sessa WC. Nitric oxide synthases: regulation and function. Eur Heart J. 2012;33(7):829-37.

Fowke TM, Karunasinghe RN, Bai JZ, Jordan S, Gunn AJ, Dean JM. Hyaluronan synthesis by developing cortical neurons in vitro. Sci Rep. 2017 Mar 13;7:44135.

Frank D, St Amand A, Feldman R, Boedeker E, Harpaz N and Pace N. (2007) Molecularphylogenetic characterization of microbial community imbalances in human inflammatory bowel diseases. Proc Natl Acad Sci USA 104: 13780–13785.

Furness JB, Callaghan BP, Rivera LR, Cho HJ. The enteric nervous system and gastrointestinal innervation: integrated local and central control. Adv Exp Med Biol. 2014; 817:39-71.

Furness JB. The enteric nervous system and neurogastroenterology. Nat. Rev. Gastroenterol. Hepatol. 2012; 9: 286-94

Furness JB. Types of neurons in the enteric nervous system. J Auton Nerv Syst. 2000; 81(1-3):87-96.

Gabella G. Development and ageing of intestinal musculature and nerves: the guinea-pig taenia coli. J Neurocytol. 2001 Sep-Oct;30(9-10):733-66.

Gabella G. Fall in the number of myenteric neurons in aging guinea pigs. Gastroenterology. 1989 Jun;96(6):1487-93. Erratum in: Gastroenterology 1989 Oct;94(4):1072.

Galligan JJ. Nicotinic acetylcholine and P2X receptors in the enteric nervous system. Proc West Pharmacol Soc. 2002; 45:231-4.

Gastroenterology and Hepatology 14(5):269-278.Ng, S.C.; Shi, H.Y.; Hamidi, N.; Underwood, F.E.; Tang, W.; Benchimol, E.I.; Panaccione, R.; Ghosh, S.; Wu, J.C.Y.; Chan, F.K.L.; et al. Worldwide incidence and prevalence of inflammatory bowel disease in the 21st century: A systematic review of population-based studies. Lancet 2017; 390, 2769–2778.

Gerritsen J, Smidt H, Rijkers GT, de Vos WM. Intestinal microbiota in human health and disease: the impact of probiotics. Genes Nutr. 2011; 6(3):209-40.

Gershon MD, Kirchgessner AL, Wade PR. Functional anatomy of the enteric nervous system. In: Johnson LR, ed. Physiology of the gastrointestinal tract. New York: Raven, 1994:381–422.

Gershon MD. The enteric nervous system: a second brain. Hosp Pract. 1999;34(7):31-2, 35-8, 41-2 passim. Review.

Giaroni C, De Ponti F, Cosentino M, Lecchini S, Frigo G. Plasticity in the enteric nervous system. Gastroenterology. 1999;117(6):1438-58.

Giaroni C, Marchet S, Carpanese E, Prandoni V, Oldrini R, Bartolini B, Moro E, Vigetti D, Crema F, Lecchini S, Frigo G. Role of neuronal and inducible nitric oxide synthases in the guinea pig small intestine myenteric plexus during in vitro ischemia and reperfusion. Neurogastroenterol Motil. 2013;25(2):e114-26.

Giuliani D, Giaroni C, Zanetti E, Canciani L, Borroni P, Lecchini S, Frigo G. Involvement of glutamate receptors of the NMDA type in the modulation of acetylcholine and glutamate overflow from the guinea pig ileum during in vitro hypoxia and hypoglycaemia. Neurochem Int. 2006 Feb;48(3):191-200.

Goransson V, Johnsson C, Nylander O, and Hansell P, “Renomedullary and intestinal hyaluronan content during body water excess: a study in rats and gerbils,” The Journal of Physiology,vol.542,no.1,pp.315–322,2002.

Goyal RK, Hirano I. The enteric nervous system. N Engl J Med., 1996; 25;334(17):1106-15.

Grenham S, Clarke G, Cryan JF, Dinan TG. Brain-gut-microbe communication in health and disease. Front Physiol. 2011 Dec 7;2:94.

Grubišić V, Verkhratsky A, Zorec R, Parpura V. Enteric glia regulate gut motility in health and disease. Brain Res Bull. 2018 Jan;136:109-117.

Grubišić V, Verkhratsky A, Zorec R, Parpura V. Enteric glia regulate gut motility in health and disease. Brain Res Bull. 2018 Jan;136:109-117.

Gudi T, Hong GK, Vaandrager AB, Lohmann SM, Pilz RB. Nitric oxide and cGMP regulate gene expression in neuronal and glial cells by activating type II cGMP-dependent protein kinase. FASEB J 1999;13:2143–52.

Guinane CM, Cotter PD. Role of the gut microbiota in health and chronic gastrointestinal disease: understanding a hidden metabolic organ. Therap Adv Gastroenterol. 2013 Jul;6(4):295-308.

Gulbransen BD, Sharkey KA. Novel functional roles for enteric glia in the gastrointestinal tract. Nat Rev Gastroenterol Hepatol. 2012 Nov;9(11):625-32.

Haglund U, Bergqvist D. Intestinal ischemia – the basics Langenbeck's. Arch Surg 1999; 384: 233–8.

Hansen MB. The enteric nervous system I: organisation and classification. Pharmacol Toxicol. 2003; 92(3):105-13.

Hansen, R.; Russell, R.K.; Reiff, C.; Louis, P.; McIntosh, F.; Berry, S.H.; Mukhopadhya, I.; Bisset, W.M.; Barclay, A.R.; Bishop, J.; et al. Microbiota of de-novo pediatric IBD: Increased *faecalibacterium prausnitzii* and reduced bacterial diversity in Crohn's but not in ulcerative colitis. Am. J. Gastroenterol. 2012; 107, 1913–1922.

Harrington AM, Hutson JM, Southwell BR. Cholinergic neurotransmission and muscarinic receptors in the enteric nervous system. Prog Histochem Cytochem. 2010; 44(4):173-202.

Heldin P, Karousou E, Skandalis SS. Growth factor regulation of hyaluronan deposition in malignancies. Hyaluronan in cancer biology: Elsevier, 2009:37–50.

Hierholzer C, Kalff JC, Audolfsson G, Billiar TR, Tweardy DJ, Bauer AJ. Molecular and functional contractile sequelae of rat intestinal ischemia/reperfusion injury. Transplantation. 1999 Nov 15;68(9):1244-54.
Hill DR, Kessler SP, Rho HK, Cowman MK, de la Motte CA. Specific-sized hyaluronan fragments promote expression of human β-defensin 2 in intestinal epithelium. J Biol Chem. 2012 Aug 31;287(36):30610-24

Holzer P, Holzer-Petsche U. Tachykinins in the gut. Part II. Roles in neural excitation, secretion and inflammation. Pharmacol Ther. 1997;73(3):219-63.

Hoshi N, Schenten D, Nish SA, Walther Z, Gagliani N, Flavell RA, Reizis B, Shen Z, Fox JG, Iwasaki A, Medzhitov R. MyD88 signalling in colonic mononuclear phagocytes drives colitis in IL-10-deficient mice. Nat Commun. 2012;3:1120.

Hoshi N, Schenten D, Nish SA, Walther Z, Gagliani N, Flavell RA, Reizis B, Shen Z, Fox JG, Iwasaki A, Medzhitov R. MyD88 signalling in colonic mononuclear phagocytes drives colitis in IL-10-deficient mice. Nat. Commun. 2012, 3, 1120.

Hsu SM, Raine L. Protein A, avidin, and biotin in immunohistochemistry. J Histochem Cytochem. 1981; 29: 1349 –1353.

Ippolito C, Segnani C, Errede M, Virgintino D, Colucci R, Fornai M, Antonioli L, Blandizzi C, Dolfi A, Bernardini N. An integrated assessment of histopathological changes of the enteric neuromuscular compartment in experimental colitis. J Cell Mol Med. 2015; 19(2):485-500

Jacobson A, Brinck J, Briskin MJ, Spicer AP, Heldin P. Expression of human hyaluronan synthases in response to external stimuli. Biochem. 2000; J 348, 29–35.

Jadcherla SR. Inflammation inhibits muscarinic signaling in in vivo canine colonic circular smooth muscle cells. Pediatr Res. 2002; 52(5):756-62.

Jessen KR, Mirsky R. Glial fibrillary acidic polypeptides in peripheral glia. Molecular weight, heterogeneity and distribution. J Neuroimmunol. 1985; 8:377–393.

Jiang D, Liang J, Fan J, Yu S, Chen S, Luo Y, Prestwich GD, Mascarenhas MM, Garg HG, Quinn DA, Homer RJ, Goldstein DR, Bucala R, Lee PJ, Medzhitov R, NoblePW. Regulation of lung injury and repair by Toll-like receptors and hyaluronan. Nat Med. 2005 Nov;11(11):1173-9.

Jiang D, Liang J, Noble PW. Hyaluronan in tissue injury and repair. Annu Rev Cell Dev Biol. 2007;23:435-61.

Jiang D, Liang J,and Noble PW. Hyaluronan as an immune regulator in human diseases. Physiological Reviews. 2011; vol.91,no. 1,pp.221–264.

Johnson SR, Knox AJ. Synthetic functions of airway smooth muscle in asthma. Trends Pharmacol Sci. 1997;18:288–92.

Jones WJ, Roe BA, Affourtit JP, Egholm M, Henrissat B, Heath AC, Knight R, Gordon JI. A core gut microbiome in obese and lean twins. Nature. 2009; 457(7228):480-4.

Joy RA, Vikkath N, Ariyannur PS. Metabolism and mechanisms of action of hyaluronan in human biology. Drug Metab Pers Ther. 2018 Mar 28;33(1):15-32.

Kannan KB, Colorado I, Reino D, Palange D, Lu Q, Qin X, Abungu B, Watkins A, Caputo FJ, Xu DZ, Semenza GL, Deitch EA, Feinman R. Hypoxia-inducible factor plays a gut-injurious role in intestinal ischemia reperfusion injury. Am J Physiol Gastrointest Liver Physiol. 2011 May;300(5):G853-61.

Karousou E, Asimakopoulou A, Monti L, Zafeiropoulou V, Afratis N, Gartaganis P, Rossi A, Passi A, Karamanos NK. FACE analysis as a fast and reliable methodology to monitor the sulfation and total amount of chondroitin sulfate in biological samples of clinical importance. Molecules. 2014 Jun 12; 19(6):7959-80.

Kau A, Ahern P, Griffin N, Goodman A and Gordon J. Human nutrition, the gut microbiome and the immune system. Nature. 2011; 474: 327–336.

Kessler S, Rho H, West G, Fiocchi C, Drazba J, and de LaMotte C,“Hyaluronan (HA) deposition precedes and promotes leukocyte recruitment in intestinal inflammation,” Clinical and Translational Science. 2008; vol.1,no.1,pp.57–61,.

Kirchgessner AL, Gershon MD. Innervation of the pancreas by neurons in the gut. J Neurosci 1990; 10:1626-42.

Knudson CB, Knudson W. Hyaluronan-binding proteins in development, tissue homeostasis, and disease. FASEB J 1993;7:1233–41.

Kong SE, Blennerhassett LR, Heel KA, McCauley RD, Hall JC. Ischaemia-reperfusion injury to the intestine. Aust N Z J Surg. 1998 Aug;68(8):554-61.

Kosterlitz HW, Robinson JA. Reflex contractions of the longitudinal muscle coat of the isolated guinea-pig ileum. J Physiol. 1959 May 19;146(2):369-79.

Kultti A, Pasonen-Seppänen S, Jauhiainen M, Rilla KJ, Kärnä R, Pyöriä E, Tammi RH, Tammi MI. 4-Methylumbelliferone inhibits hyaluronan synthesis by depletion of cellular UDP-glucuronic acid and downregulation of hyaluronan synthase 2 and 3. Exp Cell Res. 2009 Jul 1;315(11):1914-23.

Lakhan SE, Kirchgessner A. Neuroinfammation in infammatory bowel disease. J Neuroinfammation. 2010; 7, 37.

Larson RE, Martins HR. Early effect of glucose and oxygen deprivation on the spontaneous acetylcholine release from the myenteric plexus of the guinea pig ileum. Can J Physiol Pharmacol. 1981 Jun;59(6):555-61.

Laurie GW, Leblond CP, Martin GR. Light microscopic immunolocalization of type IV collagen, laminin, heparan sulfate proteoglycan, and fibronectin in the basement membranes of a variety of rat organs. Am J Anat. 1983 May;167(1):71-82.

Lecci A, Capriati A, Altamura M, Maggi CA. Tachykinins and tachykinin receptors in the gut, with special reference to NK2 receptors in human. Auton Neurosci. 2006 Jun 30;126-127:232-49.

Lecci A, Santicioli P, Maggi CA. Pharmacology of transmission to gastrointestinal muscle. Curr Opin Pharmacol. 2002 Dec;2(6):630-41.

Lee Y, Sugihara K, Gillilland MG 3rd, Jon S, Kamada N, Moon JJ. Hyaluronic acid-bilirubin nanomedicine for targeted modulation of dysregulated intestinal barrier, microbiome and immune responses in colitis. Nat Mater. 2019

Lefer AM, Lefer DJ. Nitric oxide. II. Nitric oxide protects in intestinal inflammation. Am J Physiol. 1999 Mar;276(3):G572-5.

Ley R, Turnbaugh P, Klein S and Gordon J. Microbial ecology: human gut microbes associated with obesity. Nature. 2006; 444: 1022–1023.

Ley RE, Lozupone CA, Hamady M, Knight R, Gordon JI. Worlds within worlds: evolution of the vertebrate gut microbiota. Nat Rev Microbiol. 2008 Oct;6(10):776-88.

Li, L., Asteriou T, Bernert B, Heldin C, Heldin P. Growth factor regulation of hyaluronan synthesis and degradation in human demal fbroblasts: importance of hyaluronan for the mitogenic response of PDGF-BB. Biochem J. 2007; 404, 327–336.

Lindeström LM, Ekblad E. Structural and neuronal changes in rat small intestine after ischemia with reperfusion. Dig Dis Sci. 2004 Aug;49(7-8):1212-22.

Lindwall C, Olsson M, Osman AM, Kuhn HG, Curtis MA. Selective expression of hyaluronan and receptor for hyaluronan mediated motility (Rhamm) in the adult mouse subventricular zone and rostral migratory stream and in ischemic cortex. Brain Res. 2013 Mar 29;1503:62-77.

Liu XB, Hill P, Haile DJ. Role of the ferroportin iron-responsive element in iron and nitric oxide dependent gene regulation. Blood Cells Mol Dis 2002;29: 315–26.

Lomax, A.E.; Fernández, E.; Sharkey, K.A. Plasticity of the enteric nervous system during intestinal inflammation. Neurogastroenterol. Motil. 2005, 17, 4–15.

MacDonald PH, Beck IT, Hurlbut D. Ischemic Disease of the Intestine. First Principles of Gastroenterology. 5th edition Thomas & Shaffer 2005

Mallick IH, Yang W, Winslet MC, Seifalian AM. Ischemia-reperfusion injury of the intestine and protective strategies against injury. Dig Dis Sci. 2004; 49 (9):1359-77.

Malvin NP, Seno H, Stappenbeck TS. Colonic epithelial response to injury requires Myd88 signaling in myeloid cells. Mucosal Immunol. 2012; 5, 194–206.

Malvin NP, Seno H, Stappenbeck TS. Colonic epithelial response to injury requires Myd88 signalling in myeloid cells. Mucosal Immunol. 2012; 5, 194–206.

Marchesi JR, Adams DH, Fava F, Hermes GD, Hirschfield GM, Hold G, Quraishi MN, Kinross J, Smidt H, Tuohy KM, Thomas LV, Zoetendal EG, Hart A. The gut microbiota and host health: a new clinical frontier. Gut. 2016 Feb;65(2):330-9.

Marchesi JR, Adams DH, Fava F, Hermes GDA, Hirschfield GM, Hold G, Quraishi MN, Kinross J, Smidt H, Tuohy KM, Thomas LV, Zoetendal EG, Hart A. The gut microbiota and host health: A new clinical frontier. Gut 2016, 65, 330–339.

Martin R, Nauta AJ, Ben Amor K, Knippels LM, Knol J, Garssen J. Early life: gut microbiota and immune development in infancy. Benef Microbes. 2010; 1(4):367-82.

Martínez I, Kim J, Duffy PR, Schlegel VL, Walter J. Resistant starches types 2 and 4 have differential effects on the composition of the fecal microbiota in human subjects. PLoS One. 2010 Nov 29;5(11).

Massberg S, Messmer K. The nature of ischemia/reperfusion injury. Transplant Proc. 1998; 30: 4217–23 3.

McDonald JA, Camenisch TD. Hyaluronan: genetic insights into the complex biology of a simple polysaccharide. Glycoconj J. 2002 May-Jun;19(4-5):331-9.

McRae PA, Baranov E, Rogers SL, Porter BE. Persistent decrease in multiple components of the perineuronal net following status epilepticus. Eur J Neurosci. 2012 Dec;36(11):3471-82.

Miampamba M, Sharkey KA. Temporal distribution of neuronal and inducible nitric oxide synthase and nitrotyrosine during colitis in rats. Neurogastroenterol Motil 1999; 11: 193–206.

Mizhorkova Z, Batova M, Milusheva EA. Participation of endogenous nitric oxide in the effect of hypoxia in vitro on neuro-effector transmission in guinea-pig ileum. Brain Res Bull. 2001 Jul 1;55(4):453-8.

Morales-Soto W, Gulbransen BD. Enteric Glia: A New Player in Abdominal Pain. Cell Mol Gastroenterol Hepatol. 2019;7(2):433-445.

Moretto P, Karousou E, Viola M, Caon I, D'Angelo ML, De Luca G, Passi A, Vigetti D. Regulation of hyaluronan synthesis in vascular diseases and diabetes. J Diabetes Res. 2015;2015:167283.

Neurath, M. Current and emerging therapeutic targets for IBD. Nat Rev Gastroenterol Hepatol 14, 269–278; 2017.

Ni J, Shen TD, Chen EZ, Bittinger K, Bailey A, Roggiani M, Sirota-Madi A, Friedman ES, Chau L, Lin A, Nissim I, Scott J, Lauder A, Hoffmann C, Rivas G, Albenberg L, Baldassano RN, Braun J, Xavier RJ, Clish CB, Yudkoff M, Li H, Goulian M, Bushman FD, Lewis JD, Wu GD. A role for bacterial urease in gut dysbiosis and Crohn's disease. Sci Transl Med. 2017 Nov 15;9(416).

Ni J, Wu GD, Albenberg L, Tomov VT. Gut microbiota and IBD: Causation or correlation? Nat. Rev. Gastroenterol. Hepatol. 2017; 14, 573–584.

Noble PW. Hyaluronan and its catabolic products in tissue injury and repair. Matrix Biol. 2002 Jan;21(1):25-9.

Nowicki PT. Ischemia and necrotizing enterocolitis: where, when, and how. Semin Pediatr Surg 2005; 14: 152–8.

Okun E, Griffioen KJ, Mattson MP. Toll-like receptors signaling in neural plasticity and disease. Trends in Neurosci. 2011; 34: 1-13.

Oohashi, T., Edamatsu, M., Bekku, Y. & Carulli, D. The hyaluronan and proteoglycan link proteins: Organizers of the brain extracellular matrix and key molecules for neuronal function and plasticity. Exp Neurol 274, 134–144 (2015).

Oue T, Yoneda A, Shima H, Puri P. Muscarinic acetylcholine receptor expression in aganglionic bowel. Pediatr Surg Int. 2000;16(4):267-71.

Parkes GC, Brostoff J, Whelan K, Sanderson JD. Gastrointestinal microbiota in irritable bowel syndrome: their role in its pathogenesis and treatment. Am J Gastroenterol. 2008; 103(6):1557-67.

Pierik M, Joossens S, Van Steen K, Van Schuerbeek N, Vlietinck R, Rutgeerts P, Vermeire S. Toll-like receptor-1,-2, and -6 polymorphisms influence disease extension in inflammatory bowel diseases. Inflamm. Bowel Dis. 2006, 12, 1–8.

Pierik M, Joossens S, Van Steen K, Van Schuerbeek N, Vlietinck R, Rutgeerts P, Vermeire S. Toll-like receptor-1, -2, and -6 polymorphisms influence disease extension in inflammatory bowel diseases. Inflamm Bowel Dis. 2006; 12(1):1-8.

Pierik M, Joossens S, Van Steen K, Van Schuerbeek N, Vlietinck R, Rutgeerts P, Vermeire S. Toll-like receptor-1,-2, and -6 polymorphisms influence disease extension in inflammatory bowel diseases. Inflamm. Bowel Dis. 2006; 12, 1–8.

Qin J, Li R, Raes J, et al. A human gut microbial gene catalogue established by metagenomic sequencing. Nature. 2010: 464: 59–65.

Qin J, Li Y, Cai Z, Li S, Zhu J, Zhang F, Liang S, Zhang W, Guan Y, Shen D, Peng Y, Zhang D, Jie Z, Wu W, Qin Y, Xue W, Li J, Han L, Lu D, Wu P, Dai Y, Sun X, Li Z, Tang A, Zhong S, Li X, Chen W, Xu R, Wang M, Feng Q, Gong M, Yu J, Zhang Y, Zhang M, Hansen T, Sanchez G, Raes J, Falony G, Okuda S, Almeida M, LeChatelier E, Renault P, Pons N, Batto JM, Zhang Z, Chen H, Yang R, Zheng W, Li S, Yang H, Wang J, Ehrlich SD, Nielsen R, Pedersen O, Kristiansen K, Wang J. A metagenome-wide association study of gut microbiota in type 2 diabetes. Nature. 2012; 490(7418):55-60.

Raio L, Cromi A, Ghezzi F, Passi A, Karousou E, Viola M, Vigetti D, De Luca G, Bolis P. Hyaluronan content of Wharton's jelly in healthy and Down syndrome fetuses. Matrix Biol. 2005; 24 (2):166-74.

Rakoff-Nahoum S, Hao L, Medzhitov R. Role of toll-like receptors in spontaneous commensal-dependent colitis. Immunity. 2006 Aug;25(2):319-29.

Rapoport RM, Draznin MB, Murad F. Endothelium-dependent relaxation in rat aorta may be mediated through cyclic GMP-dependent protein phosphorylation. Nature 1983;306:174–76.

Rauch U, Schäfer KH. The extracellular matrix and its role in cell migration and development of the enteric nervous system. Eur J Pediatr Surg. 2003 Jun;13(3):158-62.

Reinus JF, Brandt LJ, Boley SJ. Ischemic diseases of the bowel. Gastroenterol Clin North Am. 1990 Jun;19(2):319-43.

Rhee SH, Pothoulakis C, Mayer EA. Principles and clinical implications of the brain-gut-enteric microbiota axis. Nat Rev Gastroenterol Hepatol. 2009; 6(5):306-14.

Richter F, Eitner A, Leuchtweis J, Bauer R, Ebersberger A, Lehmenkühler A, Schaible HG. The potential of substance P to initiate and perpetuate cortical spreading depression (CSD) in rat in vivo. Sci Rep. 2018 Dec 5;8(1):17656.

Rivera LR, Thacker M, Pontell L, Cho HJ, Furness JB. Deleterious effects of intestinal ischemia/reperfusion injury in the mouse enteric nervous system are associated with protein nitrosylation. Cell Tissue Res 2011; 344: 111–23.

Robinson AM, Stojanovska V, Rahman AA, McQuade RM, Senior PV, Nurgali K. Effects of oxaliplatin treatment on the enteric glial cells and neurons in the mouse small intestine. J Histochem Cytochem. 2016; 64: 530–545.

Robinson MA, Baumgardner JE, Otto CM. Oxygen-dependent regulation of nitric oxide production by inducible nitric oxide synthase. Free Radic Biol Med 2011; 51: 1952–65.

Salzman NH, Hung K, Haribhai D, Chu H, Karlsson-Sjöberg J, Amir E, Teggatz P, Barman M, Hayward M, Eastwood D, Stoel M, Zhou Y, Sodergren E, Weinstock GM, Bevins CL, Williams CB, Bos NA. Enteric defensins are essential regulators of intestinal microbial ecology. Nat Immunol. 2010 Jan;11(1):76-83.

Sanders KM. A case for interstitial cells of Cajal as pacemakers and mediators of neurotransmission in the gastrointestinal tract. Gastroenterology 1996;111:492–515.

Sekirov I, Russell SL, Caetano M, Antunes L, Finlay BB. Gut microbiota in health and disease. Physiol. Rev. 2010; 90, 859–904.

Sekirov I; Russell SL; Caetano M; Antunes L; Finlay BB. Gut microbiota in health and disease. Physiol. Rev. 2010, 90, 859–904.

Sender R, Fuchs S, Milo R. Revised Estimates for the Number of Human and Bacteria Cells in the Body. PLoS Biol. 2016; 14(8)

Shah A, Lodge DJ. A loss of hippocampal perineuronal nets produces defcits in dopamine system function: relevance to the positive symptoms of schizophrenia. Transl Psychiatry. 2013; 3, e215.

Sharkey KA. Emerging roles for enteric glia in gastrointestinal disorders. J Clin Invest. 2015;125(3):918-25.

Shea-Donohue T, Urban JF Jr. Neuroimmune Modulation of Gut Function. Handb Exp Pharmacol. 2017; 239:247-267.

Sigge W, Wedel T, Kuhnel W, Krammer HJ. Morphologic alterations of the enteric nervous system and deficiency of non-adrenergic non-cholinergic inhibitory innervation in neonatal necrotizing enterocolitis. Eur J Pediatr Surg. 1998; 8:87–94.

Simmons AM, Tanyu LH, Horowitz SS, Chapman JA, Brown RA. Developmental and regional patterns of GAP-43 immunoreactivity in a metamorphosing brain. Brain Behav Evol. 2008;71(4):247-62.

Simrén M, Barbara G, Flint HJ, Spiegel BM, Spiller RC, Vanner S, Verdu EF, Whorwell PJ, Zoetendal EG; Rome Foundation Committee. Intestinal microbiota in functional bowel disorders: a Rome foundation report. Gut. 2013; 62(1):159-76.

Smith TK, Robertson WJ. Synchronous movements of the longitudinal and circular muscle during peristalsis in the isolated guinea-pig distal colon. J Physiol. 1998 Jan 15;506 (Pt 2):563-77.

Stenkamp-Strahm CM, Kappmeyer AJ, Schmalz JT, Gericke M, Balemba O. High-fat diet ingestion correlates with neuropathy in the duodenum myenteric plexus of obese mice with symptoms of type 2 diabetes. Cell Tissue Res. 2013; 354: 381–394.

Stewart HJ, Jessen KR, Curtis R, Mirsky R. Schwann cells, neurons and GAP-43. Perspect Dev Neurobiol. 1992; 1(1):45-52. Review.

Stuehr D, Pou S, Rosen GM. Oxygen reduction by nitric-oxide synthases. J Biol Chem 2001;276:14533–36.

Sturiale S, *et al.* Neutral endopeptidase (EC 3.4.24.11) terminates colitis by degrading substance P. *Proc Natl Acad Sci* USA 96, 11653-11658 (1999).

Sundin J, Rangel I, Kumawat AK, Hultgren-Hörnquist E, Brummer RJ. Aberrant mucosal lymphocyte number and subsets in the colon of post-infectious irritable bowel syndrome patients. Scand J Gastroenterol. 2014 Sep;49(9):1068-75.

Suttkus A, Morawski M, Arendt T. Protective properties of neural extracellular matrix. Mol Neurobiol. 2016; 53, 73–82.

Tacker M, Rivera LR, Cho HJ, Furness JB. The relationship between glial distortion and neuronal changes following intestinal ischemia and reperfusion. Neurogastroenterol Motil. 2011; 23, e500–9.

Takahara M, Nemoto Y, Oshima S, Matsuzawa Y, Kanai T, Okamoto R, Tsuchiya K, Nakamura T, Yamamoto K, Watanabe M. IL-7 promotes long-term in vitro survival of unique long-lived memory subset generated from mucosal effector memory CD4+ T cells in chronic colitis mice. Immunol Lett. 2013 Nov-Dec;156(1-2):82-93.

Takeda K, Kaisho T, Akira S. Toll-like receptors. Annu Rev Immunol. 2003; 21:335-76.

Takeuchi O, Hoshino K, Akira S. Cutting edge: TLR2-deficient and MyD88deficient mice are highly susceptible to Staphylococcus aureus infection. J Immunol. 2000 Nov 15;165(10):5392-6.

Talapka P, Bo´ di N, Battonyai I, Fekete E, Bagya´nszki M. Subcellular distribution of nitric oxide synthase isoforms in the rat duodenum. World J Gastroenterol 2011; 17: 1026–9.

Talapka P, Bódi N, Battonyai I, Fekete E, Bagyánszki M. Subcellular distribution of nitric oxide synthase isoforms in the rat duodenum. World J Gastroenterol 17: 1026–1029, 2011.

Tesar BM, Jiang D, Liang J, Palmer SM, Noble PW, Goldstein DR. The role of hyaluronan degradation products as innate alloimmune agonists. Am J Transplant. 2006 Nov;6(11):2622-35.

Theocharis AD, Skandalis SS, Gialeli C, Karamanos NK. Extracellular matrix structure. Adv Drug Deliv Rev. 2016 Feb 1;97:4-27.

Thornton M, Solomon MJ. Crohn's disease: in defense of a microvascular aetiology. Int J Colorectal Dis. 2002; 17: 287–97.

Toda N, Herman AG. Gastrointestinal function regulation by nitrergic efferent nerves. Pharmacol Rev 2005; 57: 315–38.

Van Assche G, Collins SM. Leukemia inhibitory factor mediates cytokine-induced suppression of myenteric neurotransmitter release from rat intestine. Gastroenterology. 1996;111:674– 81.

Van Noorden S, Stuart MC, Cheung A, Adams EF, Polak JM. Localization of human pituitary hormones by multiple immunoenzyme staining procedures using monoclonal and polyclonal antibodies. J Histochem Cytochem. 1986; 34: 287–292.

van 't Spijker HM, Kwok JCF. A Sweet Talk: The Molecular Systems of Perineuronal Nets in Controlling Neuronal Communication. Front Integr Neurosci. 2017 Dec 1;11:33.

Vanner S, Macnaughton WK. Submucosal secretomotor and vasodilator reflexes. Neurogastroenterol Motil. 2004 Apr;16 Suppl 1:39-43.

Vannucchi MG, Corsani L, Bani D, Faussone-Pellegrini MS. Myenteric neurons and interstitial cells of Cajal of mouse colon express several nitric oxide synthase isoforms. Neurosci Lett 2002; 326: 191–5.

Vasina, V.; Barbara, G.; Talamonti, L.; Stanghellini, V.; Corinaldesi, R.; Tonini, M.; De Ponti, F.; De Giorgio, R. Enteric neuroplasticity evoked by inflammation. Auton. Neurosci. 2006, 126–127, 264–272.

Verheijden S, Boeckxstaens GE. Neuroimmune interaction and the regulation of intestinal immune homeostasis. Am J Physiol Gastrointest Liver Physiol. 2018 Jan 1;314(1):G75-G80.

Vigetti D, Karousou E, Viola M, Deleonibus S, De Luca G, Passi A. Hyaluronan: biosynthesis and signaling. Biochim Biophys Acta. 2014; 1840(8):2452-9

Vighi G, Marcucci F, Sensi L, Di Cara G, Frati F. Allergy and the gastrointestinal system. Clin Exp Immunol. 2008 Sep;153 Suppl 1:3-6.

Vollmar B, Menger MD. Intestinal ischemia/reperfusion: microcirculatory pathology and functional consequences. Langenbecks Arch Surg. 2011 Jan;396(1):13-29. doi: 10.1007/s00423-010-0727-x. Epub 2010 Nov 19.

von Boyen G, Steinkamp M. The role of enteric glia in gut inflammation. Neuron Glia Biol. 2010; 6:231–236

Wedel T, Krammer HJ, Kuhnel W, Sigge W. Alterations of the enteric nervous system in neonatal necrotizing enterocolitis revealed by wholemount immunohistochemistry. Pediatr Pathol Lab Med. 1998; 18:57–70.

Wehkamp J, Koslowski M, Wang G, Stange EF. Barrier dysfunction due to distinct defensin deficiencies in small intestinal and colonic Crohn's disease. Mucosal Immunol. 2008 Suppl 1:S67-74.

Wehner S, Behrendt FF, Lyutenski BN, Lysson M, Bauer AJ, Hirner A, Kalff JC. Inhibition of macrophage function prevents intestinal inflammation and postoperative ileus in rodents. Gut. 2007 Feb;56(2):176-85.

Wessler I, Kilbinger H, Bittinger F, Unger R, Kirkpatrick CJ. The non-neuronal cholinergic system in humans: expression, function and pathophysiology. Life Sci. 2003 Mar 28;72(18-19):2055-61.

Wood JD. Cellular neurophysiology of enteric neurons. In: Johnson, L.R., Kaunitz, J.D., Ghishan, F.K., Merchant, J.L., Said, H.M., Wood, J.D. (Eds.), Physiology of the Gastrointestinal Tract, V Edition. Elsevier, San Diego, 2012: 629-69.

Wopereis H, Oozeer R, Knipping K, Belzer C, Knol J. The first thousand days - intestinal microbiology of early life: establishing a symbiosis. Pediatr Allergy Immunol. 2014; 25(5):428-38.

Yoo BB, Mazmanian SK. The Enteric Network: Interactions between the Immune and Nervous Systems of the Gut. Immunity. 2017 Jun 20;46(6):910-926.

Yugandhar NM, Kiran Babu U, Raju CAI, Jaya Raju K, Sri Rami Reddy D. Optimization of glutamic acid production by brevibacterium roseum. Res. J. Microbiol. 2010; 5, 1150–1154.

Zasloff M. Antimicrobial Peptides of Multicellular Organisms: My Perspective. Adv Exp Med Biol. 2019;1117:3-6. doi: 10.1007/978-981-13-3588-4_1

Zhang H, DiBaise JK, Zuccolo A, Kudrna D, Braidotti M, Yu Y, Parameswaran P, Crowell MD, Wing R, Rittmann BE, Krajmalnik-Brown R. Human gut microbiota in obesity and after gastric bypass. Proc Natl Acad Sci U S A. 2009; 106(7):2365-70.

Zheng L, Riehl TE, and Stenson WF. “Regulation of colonic epithelial repair in mice by Toll-like receptors and hyaluronic acid,”Gastroenterology,vol.137,no.6,pp.2041–2051,2009.

Zhu MY, Lu YM, Ou YX, Zhang HZ, Chen WX. Dynamic progress of 2,4,6-trinitrobenzene sulfonic acid induced chronic colitis and fbrosis in rat model. J Dig Dis. 2012; 13, 421–429.

Zimmerman BJ, Granger DN. Reperfusion injury. Surg Clin North Am. 1992 Feb;72(1):65-83.

MICHELA BISTOLETTI

PUBBLICAZIONI

Baj A., Bistoletti M., Bosi A., Moro E., Giaroni C., Crema F. “Marine Toxins and Nociception: Potential Therapeutic Use in the Treatment of Visceral Pain Associated with Gastrointestinal Disorders”. Toxins (Basel). 2019 Jul 31;11(8).

Caloni F., Sambuy Y., Antonini M., Guidali ML., Bistoletti M., Meloni M., Bertero A., Papa E., Giaroni C. “Science and alternative methods: Integrated approaches”. ALTEX.2019;36(2):331-332.

Baj A., Moro E., Bistoletti M., Orlandi V., Crema F., Giaroni C. “Glutamatergic signaling along the microbiota-gut-brain axis”. Int J Mol Sci. 2019 Mar 25;20(6).

Bistoletti M., Moretto P., Giaroni C. “Method for detecting Hyaluronan in isolated myenteric plexus ganglia of adult rat small intestine”. Methods Mol Biol.2019; 1952:117-125.

Bistoletti M., Caputi V., Baranzini N., Marchesi N., Filpa V., Marsilio I., Cerantola S., Terova G., Baj A., Grimaldi A., Pascale A., Frigo G., Crema F., Giron MC., Giaroni C. “Antibiotic treatment-induced dysbiosis differently affects BDNF and TrkB expression in the brain and in the gut of juvenile mice” PLoS One. 2018 Feb 22;14(2).

Bin A., Caputi V., Bistoletti M., Montopoli M., Colucci R., Antonioli L., De Martin S., Castagliuolo I., Orso G., Giaroni C., Debetto P., Giron M.C. “The ecto-enzymes CD73 and adenosine deaminase modulate 5'-AMP-derived adenosine in myofibroblasts of the rat small intestine”. Purinergic Signal. 2018 Sep 29.

Ceccotti C., Giaroni C., Bistoletti M., Viola M., Crema F., Terova G. “Neurochemical characterization of myenteric neurons in the juvenile gilthead sea bream (Sparus aurata) intestine.” PLoS One. 2018 Aug 3;13(8).

Filpa V., Bistoletti M., Caon I., Moro E., Grimaldi A., Moretto P., Baj A., Giron MC., Karousou E., Viola M., Crema F., Frigo G., Passi A., Giaroni C., Vigetti D. “Changes in hyaluronan deposition in the rat myenteric plexus after experimentally-induced colitis”. Scientific Reports 2017, 7(1):17644.

Caputi V., Marsilio I., Filpa V., Cerantola S., Orso G., Bistoletti M., Paccagnella N., De Martin S., Montopoli M., Dall'Acqua S., Crema F., Di Gangi IM., Galuppini F., Lante I., Bogialli S., Rugge M., Debetto P., Giaroni C., Giron MC. “Antibiotic-induced microbiota dysbiosis impairs neuromuscular function in juvenile mice”. British Journal of Pharmacology 2017 174: 3623-3639.

Bolognese F., Bistoletti M., Barbieri P., Orlandi VT. “Honey-sensitive Pseudomonas aeruginosa mutants are impaired in catalase A” Microbiology 2016 162(9):1554-1562.

ABSTRACT A CONGRESSI

Bistoletti M, Caon I, Bosi A, Moro E, Viola M, Baj A, Vigetti D, Crema F, Passi A, Giaroni C. Hyaluronan involvement in neuromuscular adaptation to intestinal ischemia/reperfusion injury. Atti del 39° Congresso Nazionale della Società Italiana di Farmacologia, Firenze, Italy, 20-23 November 2019.

Bosi A, Bistoletti M, Micheloni G, Moro E, Baj A, Crema F, Porta G, Giaroni C. Homeobox transcription factors OTX1 and OTX2 involvement in rat myenteric plexus plasticity after DNBS-induced colitis. Atti del 39° Congresso Nazionale della Società Italiana di Farmacologia, Firenze, Italy, 20-23 November 2019.

Marsilio I, Caputi V, Cerantola S, Bistoletti M, Giaroni C, Zusso M, Giron MC. Effect of high-fat diet and Toll-like receptor 4 on the integrity of mouse enteric and central nervous systems. Atti del 39° Congresso Nazionale della Società Italiana di Farmacologia, Firenze, Italy, 20-23 November 2019.

Cerantola S, Marsilio I, Caputi V, Bistoletti M, Bertazzo A, Giaroni C, Giron MC. Interaction between Toll-like receptor 4 and serotonin signaling in a mouse model of high-fat diet. XXII SIF seminar, Firenze, Italy, 19-20 November 2019.

Bistoletti M, Bosi A, Caon I, Genoni A, Moro E, Karousou E, Viola M, Crema F, Passi A, Griron MC, Baj A, Vigetti D, Giaroni C. Hyaluronan, a new neuroimmune modulator of the microbitoa-immune-gut-axis. 7th World Congress of Targeting Microbiota, Krakow, Poland, 10-11 October 2019.

Solari, E; Marcozzi, C; Giaroni, C; Baj, A; Bistoletti, M; Negrini, D; Moriondo, A. TRPV4 channels involvement in the response of lymphatic vessels intrinsic contractility to temperature. FEPS-SIF Joint Meeting 2019, Bologna, Italy, 10-13 September 2019.

Cerantola S; Marsilio I; Caputi V; Bistoletti M; Bertazzo A; Giaroni C; Giron Mc “Small intestine neuromuscular dysfunctions in a mouse model of high-fat diet-induced obesity: involvement of Tolllike receptor 4 and serotonin” NeuroGastro 2019,Lisbon, Portugal, 5-7 September 2019

Cerantola S; Marsilio I; Caputi V; Salviato E; Ridolfi M; Zuanetti S; Bistoletti M; Giaroni C; Antonella B; Giron Mc “Small intestine neuromuscular dysfunction in a mouse model of dextran sulafte sodium-induced colitis: involvement of toll-like receptor-4” NeuroGastro 2019, Lisbon, Portugal, 5-7 September 2019.

Marsilio I; Caputi V; Cerantola S; Bistoletti M; Giaroni C; Zusso M; Giron Mc “Impact of high-fat diet and Toll-like receptor 4 signaling on the integrity of mouse enteric and central nervous systems” NeuroGastro 2019,Lisbon, Portugal, 5-7 September 2019

Giaroni C. Bistoletti M., Caon I., Bosi, A., Karousou, E., Viola, M., Crema F., Baj A., Vigetti D., Passi A. “Hyaluronan: a new player in the adaptive changes of the intestinal neuromuscular function to ischemia/reperfusion injury” 7Th FEBS Advanced lecture Course FEBS-MPST 2019, Porto Heli, Greece, 2-7 May 2019.

Solari E., Marcozzi C., Bistoletti M., Baj A., Giaroni C., Negrini D., Moriondo A. “Lymphatic spontaneous contractility: TRP channels-mediated modulation by temperature and osmolarity” Atti del 69° Congresso Nazionale della Società Italiana di Fisiologia, Firenze, Italy, 19-22 September 2018

Bistoletti M., Micheloni G., Baj A., Porta G., Giaroni C. “Changes in the expression of homeobox transcription factors OTX1 and OTX2 in the rat myenteric plexus after DNBS-induced colitis” (oral communication) XXI SIF seminar, Milano, Italy, 19-22 September 2018.

Caputi V., Cerantola S., Marsilio I., Bistoletti M., Gucciardini A., Mereu M., Giordano G., Giaroni C., Papaleo F., Giron MC. “Genetically-driven reduction of catechol-O-methyltransferase expression affects dopaminergic pathways in mouse small intestine” NeuroGASTRO Congress, Cork, Ireland, 29 August – 1 September 2018.

Giaroni C., Bistoletti M., Caputi V.; Fagiani F., Filpa V., Marsilio I., Cerantola S., Crema, F., Baj A., Pascale A., Giron MC. “nELAV mRNA-binding protein, HUC/D alteration in adolescent mice small intestine after sntibiotic treatment-induced dysbiosis” NeuroGASTRO Congress, Cork, Ireland, 24-26 August 2017.

Bolognese F., Bistoletti M., Orlandi VT. “Response of Pseudomonas aeruginosa transposon mutants to photodynamic induced stress” First Joint Congress of the French and Italian Photochemists and Photobiologists, Bari, Italy, 19-22 September 2016

Palombella S., Raimondi I., Cinquetti R., Taiana E., Gariboldi M., Bistoletti M., Monti E. and Campomenosi P. “Regulation of the expression of the metabolic enzyme Proline Dehydrogenase in cancer cells in response to stress”. Atti del Convegno AGI, Cortona, Italy,25-27 September 2013.